Technische Universität München
TUM School of Engineering and Design

Structural Sizing Optimization of Aircraft Wing Structure Coupled with Direct Aeroelastic Mission Performance Sensitivity Analysis

Stephan Rechtik

Vollständiger Abdruck der von der TUM School of Engineering and Design der Technischen Universität München zur Erlangung eines Doktors der Ingenieurwissenschaften (Dr. -Ing) genehmigten Dissertation.

Vorsitz: apl. Prof. Dr. -Ing. Christian W. M. Breitsamter

Prüfer*innen der Dissertation:

1. Prof. Dr. -Ing. Fernaß Daoud
2. Prof. Dr. -Ing. Kai-Uwe Bletzinger

Die Dissertation wurde am 06.06.2023 bei der Technischen Universität München eingereicht und durch die TUM School of Engineering and Design am 20.11.2023 angenommen.

Contents

List of figures

List of tables

List of Symbols

a acceleration.

b trimming variable(s).

b_α angle of attack.

B trimming analysis.

b_β sideslip angle.

$b_{\delta,i}$ control surface deflection.

$\mathcal{L}_b$ set of all operational conditions.

b_T thrust as a operational condition.

c_D drag coefficient.

c_{D0} parasitic drag coefficient.

c_{Di} lift induced drag coefficient.

c_F force coefficient.

c_p pressure coefficient.

c_{TSFC} thrust specific fuel consumption.

d boundary condition.

D drag.

F aerodynamics analysis residual function.

f volume force per unit mass.

f_{F2S} mapping function from fluid to structural domain.

r_f reserve fuel factor.

F forces.

F_a aerodynamic forces.

F_e engine force.

F_g force due to gravity acceleration.

F_ω force due to a angular velocity.

F_s forces due to structural weight, thermal expansion and so on.

F_{tot} total force.

g gravitational acceleration.

g inequality constraint function.

G set of constraint functions.

g constraint function.

g acceleration due to gravity.

γ flight path angle.

h equality constraint function.

h specific enthalpy.

h flight altitude.

h width.

$\dot{h}$ flight climb rate.

k thermal conductivity.

l length.

l flight state parameter.

$\mathcal{L}_l$ set of all flight variables.

L lift.

$\frac{L}{D}$ lift to drag ration.

m mass.

m_{elem} mass of a single element of an finite element model.

m_f fuel mass.

$\dot{m}_f$ fuel mass change rate.

m_{fem} mass the finite element model.

m_{fin} final mass.

m_{init} initial mass.

m_o other masses.

m_p payload mass.

m_s structural mass.

m_{tot} total mass.

Ma Mach number.

M moments of force.

M_a aerodynamic moments of force.

M_s structural moment of force.

M_{tot} total moment of force.

n normal.

$\mathbf{n}$ normal vector.

p pressure.

p_a aerodynamic load.

ψ_f functional at an end of a mission.

p_g load due to gravity acceleration.

p_i load due to a acceleration.

P point/location.

p_T net thrust load.

ψ_t functional in global time frame.

ψ_τ functional in local time frame.

p_{tot} total loads.

q dynamic pressure.

R residual of a governing equations of an analysis.

r radius.

R range.

r reserve factor.

$\mathbf{r}$ radius vector.

S structural analysis residual function.

s distance.

s flight path distance.

S_p panel area.

S_{ref} reference area.

S surface.

T temperature.

T thrust.

τ_B local time variable at a time step B.

τ local time variable.

t time variable.

t_0 time at take-off.

t_A starting time of a mission segment.

t_B final time of a mission segment.

t_f final time (landing, running out of fuel, reaching reserves).

η_T thrust setting.

v_T thrust vector.

u response of a structural analysis (deformation).

v speed.

v_{CAS} calibrated air speed.

v_{GS} ground speed.

v_∞ free stream velocity magnitude.

v_{Ma} mach number.

$\boldsymbol{v}$ speed vector.

w response of a aerodynamic analysis (velocities and pressures).

w_{el} contribution to aerodynamic state variables due to elasticity.

w_{rg} aerodynamic state variables representing a rigid state.

x longitudinal axis in body axis system.

$\mathcal{X}$ design variables set.

x design variable.

x_0 longitudinal axis in aircraft-carried earth axis system.

y_0 lateral axis in aircraft-carried earth axis system.

x_a longitudinal axis in air-path axis system (axis in direction of a flight velocity vector).

x_b trimming design variables.

x_s longitudinal structural axis.

$\mathcal{X}_f$ design variables shape set.

$\mathcal{X}_s$ design variables sizing set.

$\mathcal{X}_t$ design variables topology set.

y lateral axis in body axis system.

y state variables of a multidisciplinary system.

y_a lateral axis in air-path axis system (cross stream axis).

$\mathcal{Y}$ set of state variables in a multidisciplinary system.

$\dot{y}$ time derivative of a state variables of a multidisciplinary system.

y_s lateral structural axis.

z normal axis in body axis system.

z_0 normal axis in aircraft-carried earth axis system.

z_a normal axis in air-path axis system.

z_s normal structural axis.

α angle of attack.

β sideslip angle.

Γ vortex strength.

$\mathbf{\Gamma}$ vortex strength vector.

κ weighting coefficient.

μ doublet.

Ω transient condition.

Ω_A transient condition at the beginning of a segment.

Ω_B transient condition at the end of a segment.

ψ_0 functional at a beginning of a mission.

Φ dissipation function.

Φ potential.

ϕ kernel of a radial basis function.

ϕ bank angle.

ψ functional.

ψ yaw angle.

Ψ objective function.

ρ density.

σ source.

σ stress.

σ_{crit} critical normal stress.

τ shear stress.

τ state variable of an engine analysis (temperatures/pressures).

τ_{crit} critical shear stress.

θ pitch angle.

$\mathbf{A}$ matrix of aerodynamic influence coefficients.

$\mathbf{A}_{c_p}$ matrix of aerodynamic pressure coefficients.

$\mathbf{J}$ Jacobian matrix.

K stiffness matrix of a linear structural system.

N matrix of surface normals.

$\mathbf{Q}$ selection matrix.

${}^{0b}T$ transformation matrix from body to aircraft-carried ground frame.

T_α rotation matrix about angle of attack axis.

${}^{ba}T$ transformation matrix from air-path to body frame.

T_β rotation matrix about side slip axis.

${}^{bs}T$ transformation matrix from structure frame to body frame.

T_θ rotation matrix about pitch axis.

T_ϕ rotation matrix about bank axis.

${}^{s0}T$ transformation matrix from aircraft carried ground system to structural frame.

${}^{sa}T$ transformation matrix from air-path frame to structure frame.

T_ψ rotation matrix about yaw axis.

Part I.
Introduction

1. Motivation

The fuel efficiency of today's aircraft has improved by about 80% per passenger seat, according to the Global Market Forecast by Airbus [6] from 2019. Although due to an overall increase in aviation traffic the total amount of CO_2 being released is on a steady rise, offsetting net benefits that the improvement in flight efficiency has brought, as shown in the fig. 1.1.

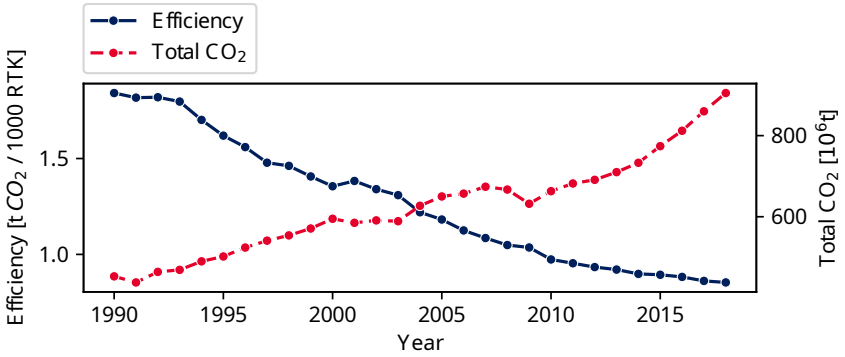

Figure 1.1: History of aircraft efficiency based on data from IATA published in [1]

Achieving a carbon neutral growth from 2020 onward together with a reduction of net aviation emissions by 50% till 2050 compared to 2005, those are two of the goals stated in the International Civil Aviation Organization (ICAO) technical report from 2010 [7]. Such a commitment represents significant challenges for the world of aviation and the industry hopes to achieve this goal with continuous improvements in four key areas. These being a technology and sustainable alternative fuels, operations, an infrastructure and market-based measures.

Even though fuel efficiency has improved significantly, fuel costs still represented above 20% of all operating costs of airlines in the years between 2015 and 2019, as documented by the International Air Transport Association (IATA) in their Airline Industry Economic Performance report [3] from June of 2020. The reported profitability development is presented in the fig. 1.2. At the same time, ever-changing jet fuel prices have a direct impact on an airline's profitability, only magnifying the portion of operating costs that the fuel represents. The current situation drives a demand for fuel efficient aircraft and presents a strong motivator for manufactures to keep improving their technological solutions.

An aircraft design process, testing and certification procedures represent a very long and expensive endeavour, keeping the rate at which completely new aircraft configurations are introduced to a minimum. A more common choice taken by aircraft manufacturers is to redesign an already existing configuration. A large amount of engineering time is spent on reiterating various designs, trying to satisfy a set of updated requirements while attempting to achieve an optimal flight efficiency.

An additional source of unexpected costs, that can occur at any phase of a design

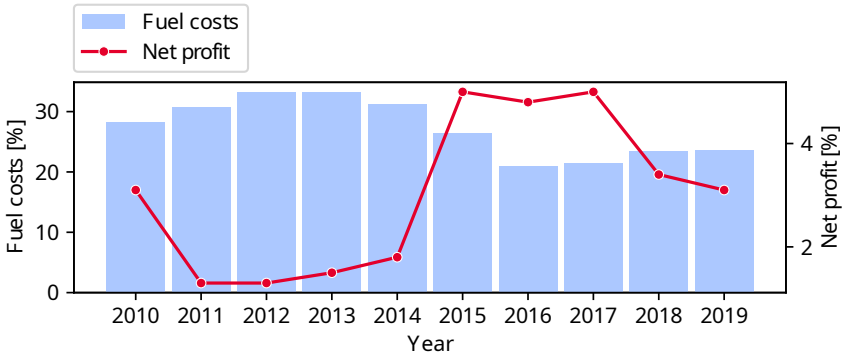

Figure 1.2: Airlines costs based on data from IATA ([2, 3])

process, is hidden in the possibility of a non-feasible design passing through to later development stages. As such, the wish to keep the expenses connected to a complex aircraft design process in check and to reduce the time investment drives the research and industry to employ more integrated and flexible design tool chains. These efforts resulted in a push towards an inclusion of a Multi-Disciplinary Analysis and Optimization (MDAO) methodology across multiple design stages in order to exploit any possible beneficial interactions between various disciplines. An example of common disciplines involved in an aircraft design is characterized in the fig. 1.3.

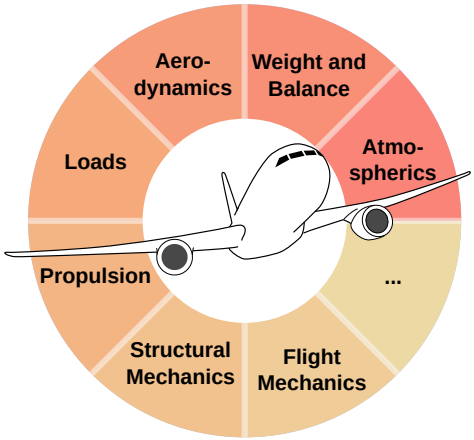

Figure 1.3: Various disciplines involved in an aircraft design

Any design process with the goal of developing a new aircraft from scratch can be split to three parts according to Raymer [8]. These being a conceptual, a preliminary and a detail design phase. But even before starting a conceptual part of a design process can be initiated, a design board together with a customer has to establish clear aircraft requirements. The output of a conceptual design phase should be a thoroughly examined aircraft concept with a clearly specified configuration, chosen after a trade-off

investigation of various aircraft configurations. In this phase the requirements can still change, as various initial design concept are examined and first cost estimations are provided and new technologies are considered. Due to the iterative nature of this design phase, tools with fast computational turn-over are preferable. As a development process progresses through the preliminary design stage, increasingly accurate methods are utilized to evaluate the responses of aerodynamics, structural mechanics and dynamics, propulsion and others. The enhanced accuracy of employed methods should lead to a more realistic estimation of costs and time, that an aircraft would incur, should it be put into production. As the name suggests, a detailed design phase is about designing and constructing specific aircraft parts ready for certification and manufacturing. It is assumed that a configuration won't change any more and therefore the detailed parts like spars, ribs, engine pylons, landing gears and others can be properly designed, with a minimal risk of having to redesign those parts because of a change to the aircraft configuration. During a detailed phase high-fidelity analysis tools are employed, leading to actual fabrication an testing of all the considered parts. The main part of this design phase ends with the manufacturing of the first aircraft. Overview of the aircraft development stages is provided in the fig. 1.4, highlighting the trade-off between knowledge and design freedom, as presented by Mavris [9].

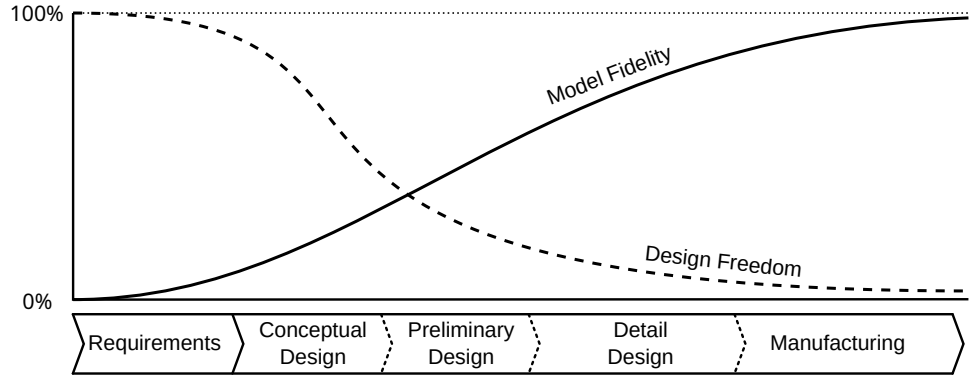

Figure 1.4: Aircraft design phases over time

2. State of research

As one of the first attempts to showcase the importance of a multi-disciplinary approach to an aircraft design can be considered a paper by Ludwig Prandtl from the year of 1933 [10]. A minimization of an induced drag was targeted as an objective function together with applying equality constraints for specific values of a total lift and a moment of inertia resulting from a lift distribution across a wing. The intention behind including a moment of inertia in one of the equality constraints was for it to represent a maximum allowed structural bending moment, which could be considered as a cross disciplinary constraint connecting an aerodynamic analysis to a structural design. Since a span was considered as a design variable, such a criteria model served to limit an otherwise unbounded increase of a wing length, witch results in a more favourable lift to drag ratio, through punishing such a design through an increase of an inertia moment at a wing's root. The results showed that in a case where a wing span is not fixed, and can therefore be freely optimized, a lift distribution across a wing producing the least amount of induced drag is not that of an elliptic shape, but more closely resembles a distribution for a tapered wing. Even though his work was purely analytical using only empirical mathematical expressions based on Kutta-Joukowski theorem as his aerodynamic model, he managed to display the impact of considering more than a single discipline when optimizing an aircraft design. Robert T. Jones later on in 1950 [11] expanded on this Prandtl's, keeping the conversation about MDO's importance alive.

Further research progress into an aeroelastic optimization was achieved by Raphael T. Haftka in 1976 [12], looking for an efficient modal flutter analysis approach for the use in a structural design. His work emphasized the importance of an automated design procedures, for which had interest just started to rise at the time. Only one year later in 1977, Haftka [13] continued on the topic of an aerostructural optimization. This time looking for an optimal in-flight wing shape in an effort to investigate the trade-off between structural weight savings and a drag reduction. Another study looking at a lift distribution coupling aerodynamic analysis with coupled to a structural response was that of M. Barhelemy from 1988 [14]. That study has presented a proof of concept for a viable methodology to perform a shape sensitivity analysis for high level geometrical parameters like a wing area, an aspect ratio, a sweep angle and similar while considering a trimming analysis to assure that only feasible flight states are being evaluated. Notwithstanding the mathematical models used were not as advanced as they are now, three decades later, the importance of using an MDO model was exhibited, which coupled aerodynamics, structural mechanics and a trimming.

With a steady rise in computational capabilities, aeroelastic MDO models started to integrate more complex aerodynamic and structural simulations. In 1995, P.J. Röhl [15] presented a multi-disciplinary procedure for a jig shape determination based on an in-flight shape. The study has coupled an optimal cruise wing shape determination based on a mission analysis, an engine cycle analysis and a structural weight estimation, which was in turn coming from a structural optimization problem with the task of minimizing the model's mass while undergoing aeroelastic deformations. At the same time the MDO

model has included strength and buckling constraints to assure the design's structural feasibility. The aeroelastic response has been simulated by using an aerodynamic analysis based on a potential flow theory for a zero-thickness lifting surface which was in turned coupled to a FEM solver, which modelled a wingbox by using a combination of 2D and 1D elements. The published work showed the feasibility of more complex MDO models by linking an aerodynamic and structural optimization procedures into one single problem.

A common aspect of many of various research works was the inclusion of only a single flight condition when evaluation a flight performance [16, 17, 18]. Although such a concrete focus does indeed achieve a high improvement in performance, it is possible that a slight deviation from the flight state, which was the target of the optimization, might lead to a quick performance degradation. In regard to this potential limitation, M. Drela in 1998 [19] has set up a simple optimization problem to investigate the impact of multi-point objective functions on an airfoil design. Even though the study was considering aerodynamics as the only discipline, by using a large set of shape design parameters M. Drela was able to show a large discrepancy between designs coming from a single-point and multi-point optimization problems. The performed work was used to establish a proposal for the choice of sampling points, at which flight performance should be evaluated in order to compute an objective function. Similar examination was made by S.E. Cliff later on in 2001 [20] in an investigation of an aerodynamic optimization of a high speed civil transport. Such results have motivated an increased use of multi-objective functions in an aircraft design optimization [21, 22, 23].

Regardless of the strides a computational technology has achieved since the first appearance of an MDO concept in an aircraft design, the demand for a higher accuracy and more complex systems has kept a simulation efficiency an essential aspect when designing any MDO tool chain. In the year 2000, K. Maute [24] has presented global sensitivity equations of a fluid-structure interaction problem with the goal to make an optimization involving complex coupled models more attractive, mainly by making the staggered procedures used to solve such systems more efficient. The proposed global sensitivity analysis approach was consequently utilized in an optimization problem involving an aerodynamic analysis by the Euler method coupled to an idealized structural model of a composite wing. Both a direct and an adjoint sensitivity approach was utilized in a wing shape and structural optimization task for a single non-trimmed flight condition using the SQP algorithm [25].

In the dissertation of J.F. Gundlach from 2004 [26] a combination of disciplines including a mission analysis, weights, avionics, structures, aerodynamics and subsystems at a level of a conceptual design stage has been utilized with a target of enhancing an UAV design. A Trefftz plane analysis [27] have been utilized to obtain an aerodynamic response and a piecewise linear beam model has been used as a structural representation of a wingbox, but both were left decoupled. The framework has integrated a general wing shape, a power to weight ratio and weight fractions as design variables using a genetic algorithm by D. Carrol [28] in order to obtain an improved UAV design.

An another study was performed by R. Perez in 2008 [29], who used an augmented Lagrangian particle swarm algorithm to look for optimal non-planar lifting surfaces.

To model a coupled aeroelastic behaviour the study applied an equivalent beam FEM model to obtain a structural response and a panel method to obtain aerodynamic effects. Sizing design variables were considered together with shape variables like wing area, wing span and twist, sweep and dihedral. The study has shown a large shift in solution when including only aerodynamic effects in an optimization problem, resulting in a C-wing configuration, in comparison to an optimization problem including aeroelastic effects, showing a winglet and raked tip configuration with and without span constraint respectively.

In 2010, G. J. Kennedy [30] presented a comparison of methods commonly used for an aeroelastic analysis and optimization. To exemplify the importance of coupling between an aerodynamic and a structural solver the study has employed an aerodynamic panel method and a shell based FEM model. During the study, four aeroelastic solution methods were evaluated. The non-linear block Gauss-Seidel, non-linear block Jacobi, Newton-Krylov and the approximate Newton-Krylov methods. The study has applied the chosen algorithm together with an adjoint sensitivity analysis to an aerostructural optimization of a non-swept wing with a target of drag minimization. Viable flight state was assured by using a lift constraint whose value was obtained based on a wing weight. The optimization has included structural thickness of elements and span-wise twist as design variables and has shown a minimal difference between an aerostructural and a pure aerodynamic optimization for the investigated configuration, while minimizing drag at only a single flight state.

An extended investigation into a multi-point shape and sizing optimization of a long-range aircraft configuration was performed by R. P. Liem et al. in 2012 [31], whose integral task was to design a fuel efficient long range aircraft while avoiding a possible optimum degradation that could be caused by considering only a single-point performance. The study has included hundreds of missions based on historical statistical data which were used to define actual flight conditions, while employing Kriging surrogate models based on high-fidelity aerostructural analysis to handle thousands of flight analyses to offset some of the computational demands. Only the fuel burned during cruise segments was computed using numerical integration, while the take-off, climb, descent and landing were estimated using fuel fractions. Additionally to a fuel burn consumption, the mission analysis had to assure prescribed mission payload and range. The utilized kriging models were built w.r.t to the Mach number, an altitude, an angle of attack and a tail angle at selected sample points, which were selected based on the historical data. High-fidelity aerostructural analysis has been performed for each of these points to obtain sample pressure drag coefficient. These sampled performance indicators were then used to build a Kriging models used to obtain values needed to assemble weighted multi-point objective function. Finally a gradient-based optimization algorithm SNOPT [32] supported by an adjoint sensitivity analysis was utilized, showing an impact of the inclusion of a large number of sample points in an objective function on an aircraft design. The optimization problem has included critical loads assessment by using two additional load cases, a 2.5g pull up manoeuvre and 1.3g gust approximation while using Kreisselmeier-Steinhauser constraints aggregation [33, 34] to include stress and fatigue

structural constraints.

Int the year 2013, J.R.R.A. Martins together with A.B. Lambe [35] assembled a review of up to the time existing discrete methods intended for an evaluation of derivatives applicable to MDO models. The overview was based on a newly derived unifying Chain Rule equation that could be used as a starting point for all the considered approaches. Computation methods for an evaluation of total derivatives which use a direct or an adjoint approach were acknowledged, while considering finite differences, the complex-step method and a symbolic differentiation for the purposes of a partial derivatives computation. The derived general methodology was largely theoretical and was expanded upon later in a study by J. T. Hwang et al. in 2013 [36], who applied it to a small satellite design problem. Another survey of at that time current research state by J. R. R. A. Martins [37] was done in regards to existing MDO architectures. It serves as a reference by discussing the benefits and drawbacks of the various established frameworks.

In a dissertation by T. Wunderlich from 2013 [38], an MDO framework was established which was intended for a wing planform shape and sizing optimization of a transport aircraft with a focus on high fidelity simulation models. These were represented by a RANS aerodynamic model coupled to a structural FEM model, providing a complex aerostructural response. Three objective functions were investigated for the purposes of planform and twist optimization, these being a lift to drag ratio, a range and a fuel consumption, where the last two were evaluated using the Breguet equation. The optimization framework has included structural failure criteria in the form of stress constraints for three critical load cases, including cruise, 2.5g pull-up and landing manoeuvre. As an optimization algorithm a deterministic method of order zero was chosen, this being the Subplex algorithm by T. H. Rowan [39]. The results have shown a fuel consumption relative to a carried payload and a range as a well suited objective function for the purposes of a wing planform optimization.

G.K.W. Kenway [40] has presented a large scale application of a multi-point optimization of a transport aircraft configuration in 2014. The work has employed a large scale Euler based CFD model coupled to an FEM based structural model. For an objective function two options were considered and subsequently compared. These being a take-off gross weight and a fuel burn, both of which were estimated by using the Breguet range equation. The investigated flight conditions consisted of five cruise states, intended for an objective function evaluation, and 2 manoeuvre states representing critical load cases. It has been shown that both of the objectives have led to an improved design resulting in a reduced fuel burn. Although the objective function integrating a fuel burn was able to provide an overall more efficient flight performance in comparison to the objective function based on a gross take-off weight. The improved efficiency was achieved by significantly increasing the wing span, showing the viability of the proposed framework, though the computational efforts were still considerable due to the high-fidelity models used.

An another work looking into a fuel burn minimization was a dissertation of F. Gallard [41] from the same year. A part of the study has formulated an aircraft performance optimization as a robust mathematical problem with manageable computational costs.

The dissertation introduced a so called Gradient Span Algorithm that could be utilized to automatically choose a set of operating conditions to be included in a multi-point optimization problem to ensure minimal computational cost for a given process. The established framework was subsequently used for an outer shape optimization with CAD based shape design variables including curvatures, tangent angles and an airfoil camber. A CFD analysis using a RANS formulation was used to model aerodynamic responses, neglecting any structural behaviour influence.

T. Lukaczyk et al. [42] has presented an aircraft design suite intended for conceptual design stages called SUAVE, with an intention to allow for a flight performance evaluation based on various underlying physical models with differing fidelities. It has allowed an inclusion of various mission profiles, propulsion networks and flexible interchangeability of integrated physical models and has been used to investigate various unconventional aircraft configurations, laying a groundwork for further research. One year later in 2016 E. Botero [43] has added support for aircraft noise computation and low fidelity panel aerodynamic solver AVL and in 2017 T. MacDonald [44] has utilized geometry generation, meshing and higher fidelity CFD solver in the SUAVE framework. Finally in 2019 M. Clarke [45] has shown conceptual level optimization for an electrical VTOL UAV using design variables like wing area, aspect ratio, various rotor radii, cruise and ascent/descent speed, showing a direct impact of performance optimization on optimal mission profiles.

In the year 2016, a dissertation by S. Deinert [46] has developed a framework for a simultaneous shape and sizing optimization, while fully integrating a coupled aerostructural analysis. The shape parametrization was achieved on a CAD level with mapping to a high-fidelity structural FEM and an aerodynamic panel model, while providing a way to perform a direct sensitivity analysis. The presented framework has targeted optimization problems of industrial complexity with a large number of structural constraints to assure design's feasibility. The dissertation has utilized a gradient based optimization algorithm NLPQL by K. Schittkowski [47], to evaluate single- and multi-discipline objective functions together with various single- and multi-disciplinary formulations including a mission performance estimation based on the Breguet range equation. In the end the proposed framework was applied to an industrial scale passenger transport aircraft configuration with the results reiterating that only multi-disciplinary objective function formulation can achieve a true performance improvement.

Even though a use of various singular disciplines without any considerations for their mutual interactions when evaluating an aircraft's performance leads to an improved design, it has been discussed in the works of E.S. Hendricks at al. [48] and Falck et al. [49], both from 2017, that neglecting the coupling does have a profound impact on a precision of those estimates and on a final design provided by a respective optimization process. They have shown the viability of a fully coupled mission trajectory analysis and an expensive propulsion or aerodynamic analysis into a single optimization problem. Falck et al. [49] has performed an additional investigation into an influence of thermal constraints on a trajectory of an electric aircraft, showing a strong coupling effect between design constraints and a flight profile.

Expanding on the work of D.A. Burdette from 2016 [50], J.P. Jasa in 2018 [51] has performed gradient based aerostructural optimization with a goal of investigating possible benefits of morphing wing technology and its impact on a mission fuel burn. The optimization process has targeted the nominal design, morphing twist across a mission and an altitude profile. Because of high computational demands of a fully coupled mission analysis when dealing with a high-fidelity CFD solver, the choice was made to reduce the fidelity of the included aerodynamic solver in the form of using a VLM method coupled to a 6-DOF 1D structural FEM model. A fixed-design, static-design and direct morphing optimization problems were compared. These were defined as a pure mission profile optimization and structural stiffness with mission profile optimization in the first two cases. The third case expanded on the static-design by including morphing design variables, allowing for the twist distribution to actively change during a mission. Though the addition of a morphing into the optimization problem has yielded very limited benefits it has exemplified the importance and possible impact of a fully integrated mission analysis for highly coupled systems or path-dependent optimization problems.

Adler [52] has performed an optimization in order to investigate the impact of a mission choice on an aircraft design. Aerostructural simulation was performed using a VLM model together with a 1D FEM model. The mission path itself was not part of the optimization. A short mission of 3000 nmi was used to obtain aircraft performance for the objective function of the optimization. It has been shown, that when the climb part of a flight part presents a significant contribution to the overall fuel burn, a design obtained through optimization with a coupled mission analysis yield better results that a design obtained through multi-point or Breguet range approximation.

The existing research closely relating to the topic of this thesis is summarized in the table 2.1. It shows a high interest in the continuous improvement of an aircraft performance using various methodological approaches and diverse combinations of considered disciplines. MDO processes have become a common sight in the area of aircraft design at any stage of their development, increasing accuracy of optimization processes by considering the interaction between various disciplines. Although, due to the still prevailing high computational demands connected to such complex interactive systems it is a common approach to focus on a subset of disciplines. At the same time, the choice of a design variable is of an equal importance, since it has a major impact on efforts connected to the related model parametrization and hence on computational demands as well. As such, the choice is often done with respect to the design stage for which a given aircraft configuration is being optimized or by considering the simulation tools that are planned to be integrated. The later relates to a concept of a model fidelity that presents a direct relation between a model accuracy and corresponding computational efforts, which is the reason why so many different aerodynamic, structural and other related solution methods are present across the existing research spectrum. Hence there is no single specific MDO definition, but based on the current state of the research and an industrial knowledge a MDO framework has to appropriately consider and integrate an optimization algorithm, an objective function, a criteria model, a parametrization model and underlying simulation models.

Even though a methodological development in the field of aircraft design spans many topics and disciplines, this thesis stays focused on those related to its application range. As such, the presented work spotlights an MDO with special considerations for a structural optimization under aeroelastic loads, a construction feasibility assurance through the use of structural constraints, a flight performance optimization and a mission analysis.

Article	Year	Objective	Design freedom	Physical models
[10, 11]	1933	drag	planform wing shape	empirical equations
[12, 13]	1976, 1977	drag	planform wing shape	empirical equations
[15]	1995	weight	planform wing shape	potential flow model, FEM, engine model
[19]	1998	drag	airfoil shape	Euler CFD
[24]	2000	lift to drag	planform wing shape, structural variables	Euler MDO, idealized structure
[29]	2008	Breguet equation	wing shape, structural parameters	potential flow model, structural beam model
[31]	2012	mission performance	wing shape, structural parameters	surrogate hi-fi aerodynamics data, structural FEM, integrated mission analysis
[38, 40]	2013, 2014	Breguet equation	wing shape, structural parameters	hi-fi CFD, FEM
[51]	2018	mission performance	wing twist morphing, structural parameters, mission path	1D FEM, VLM model
[52]	2022	mission performance	wing shape, structural parameters	1D FEM, VLM model

Table 2.1: Overview of closely related research articles

3. Intent of this thesis

Based on the industry's push towards improving cross-functional involvement during an aircraft development, an international drive for more environment friendly aviation and a current state of research, this thesis tries to develop and propose an MDAO framework for a structural design while simultaneously evaluating aeroelastic behaviour and a fully integrated mission analysis. The software tool called Lagrange [53] was used in the proposed framework to perform the task of an aeroelastic solver. The tool provides this functionality by combining a FEM solver while integrating a low fidelity potential flow aerodynamic solver. At the same time it provides all related sensitivities necessary for a structural feasibility study and a set of gradient based optimization algorithms. In addition to the existing feature set, additional functionality including a database based aeroelastic analysis and a mission simulation was added during the work on this thesis.

A valid mission analysis and a subsequent optimization require a more accurate source of aerodynamic data than a low fidelity potential flow solver can provide, mainly due to the reliability of a drag estimation. A common approach for aircraft manufactures to deal with a mission analysis is to use databases containing aerodynamic polars. These are usually generated by responsible aerodynamic departments and can consist of simulation data obtained by CFD analyses, wind tunnel or flight test data. Such databases start to be generated already in early design stages, either for an in-flight or jig shape, and their quality only improves together with progressing aircraft development. Due to this they lend themselves well for the purposes of flight performance optimization.

Whereas the trimming procedure for a critical loads analysis was an already existing part of the Lagrange tool chain, the same approach to a trimmed aeroelastic analysis was not suitable for a mission simulation and a related sensitivity analysis. This was due to the fact that a number of various flight states had to be evaluated, where each of these states was dependent on results of a previous one. Further complexity that a new trimming analysis had to handle when deployed in a mission performance tool was the need for the ability to deal with various flight parameters as trimming variables. For these reasons an additional trimming algorithm that could appropriately include the influence of a thrust on a steady flight performance while dealing with an aeroelastic behaviour was integrated into the framework.

The database based aeroelastic analysis together with the corresponding trimming approach was consequently utilized in the mission analysis tool. Since investigated mission tools, commercial and non-commercial, hadn't lent themselves well for the purposes of a direct fully coupled aeroelastic trimmed analysis at the time of their evaluation, it has been decided to develop a light weight in-house solution. The main requirements did consist of the ability to be able to perform a mission analysis with both aerodynamic polars and a fully coupled FSI solver, to define a mission profile by the use of segments, to terminate these segments using various flight parameters as boundary conditions and finally to provide analytically or semi-analytically derived gradients of flight parameters over time w.r.t. design variables of interest. The scope of this thesis was limited to direct sensitivity method being utilized, as the current state of the backbone framework

represented by the Lagrange tool didn't allow for an effective exploitation of an adjoint approach and as it allowed for a greater flexibility in formulating various objective functions, since all required derivatives were automatically provided without any need for additional implementation.

Finally, all the developed tools and methodologies had been assembled into an MDO framework allowing for a structural design and a mission performance to be merged into a single optimization problem. Afterwards this scheme was tested and evaluated by applying it to an industrial scenario, in which an aircraft of a civilian mid range passenger configuration was target of an optimization. The considered optimization problem focused on an internal wing structure design which would improve a mission performance, while leaving an outer shape intact. Such an optimization problem represented a case in which the jig shape of a wing is not allowed to change to avoid costs connected with retooling but a performance improvement is required to boost a marketability. Various objective functions were considered and employed with the resulting designs being compared to each other in order to evaluate their suitability for a flight performance optimization. This included a classical single-point, multi-point and a full mission analysis based performance values and weighed their disadvantages and benefits against each other. Based on the findings a conclusion could be made in regards to a reasonable choice of a performance measure for similar optimization problems. Additionally, further required development was proposed to boost the applicability of the proposed framework and its ability to further exploit an aircraft performance.

Part II.
Theory

4. Aircraft optimization

An aircraft design optimization can be approached in various ways, as exemplified by [54, 55, 56, 41, 40, 46, 57] and others, with differences spanning all the related aspects like a methodology, a choice of algorithms, a set of design variables or a targeted performance measure. In all the cases the choice of an underlying physical representations has a noticeable impact on obtained solutions, which can be observed when looking at tasks considering a pure aerodynamic performance optimization in earlier design phases with the target of defining an in-flight shape of a wing [58, 59, 60] and comparing those to optimization problem integrating internal structures as well [46, 61, 62, 30]. Additionally, a decision in regard to the way a performance measure is evaluated and what criteria are included are of utmost interest. A pure aerodynamic optimization might not satisfy structure related constraints like maximum stress and deformation, resulting in a structurally unsafe design. At the same time even though a coupled aeroelastic analysis is included in an optimization process to appropriately model an in-flight shape, a design algorithm might lead to results which cannot satisfy mission performance demands that were set up for an aircraft by its requirements. This leads to an idea of including a mission analysis in an optimization process, as considered by [54, 63, 64, 41]. In an ideal scenario a single aircraft optimization problem would include all of the above mentioned disciplines and many more. In reality this would lead to MDO compositions of an infinite complexity that currently established methods are not able to handle. As such, it is important to define targets and requirements of an intended optimization process right at the beginning.

4.1. Optimization model

In the scope of this thesis the concept of an optimization model is considered as encompassing all the necessary components required to successfully solve an optimization problem. A general idea about what is needed to set up a task involving a MDO optimization is provided for example by [65, 66] and in the scope of this thesis a model consisting of five major components is considered. These being an objective function, a constraints model, a parametrization model, a simulation model and finally an optimization algorithm. The interaction between the various parts is illustrated in the fig. 4.1.

Each of the components provides an essential functionality to the overall problem and even though they have their own set of requirements, it is of a critical importance to consider the mutual interaction between the five components, as the requirements of one of them can enforce demands on another. This can be exemplified by imagining a computational case in which a structural feasibility of an optimized design has to be ensured Such a case calls for the inclusion of a robust structural representation model which is able to provide adequate data like stress and strain to a criteria model. Another illustrative situation is a case where an objective model should include various flight performance indicators, as this would require an accurate aerodynamic model.

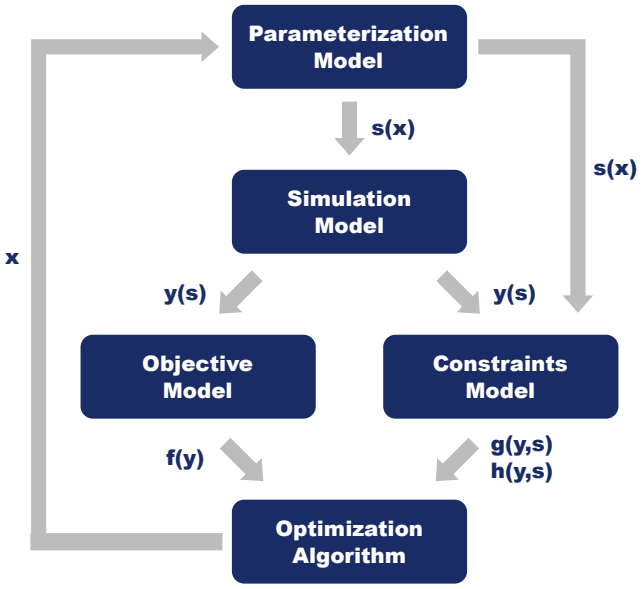

Figure 4.1: Design variable propagation in an optimization model

4.1.1. Parametrization model

A parametrization model defines so called design variables x and serve as an input for an optimization algorithm to exact changes upon.

$$x \in \mathcal{X} = \{\mathcal{X}_t, \mathcal{X}_s, \mathcal{X}_f\} \tag{4.1}$$

Design variables are considered by an optimization algorithm as purely mathematical and have to be therefore linked to their representation in a simulation model. Hence, the main limiting factor for any parametrization model is the underlying simulation model, which defines all available model variables $s \in \mathcal{S}$ that a design variable can be linked to. Depending on the linked model variable, three types of parametrization are usually acknowledged, these being sizing, shape and topology, all included in the set of possible design variables in eq. (4.1). Illustrative examples are shown in the fig. 4.2. Although these are not necessarily mutually exclusive, it is common for them to be considered separately, as each of them carries different model mapping requirements, since they have a distinct impact on a simulation model.

Shape parametrization $\mathcal{X}_f$ is applied in the cases where the outer form of a domain is allowed to change. If this is related to a shape optimization of an aircraft wing then changes can be done on a high level to its span, chord, sweep or on a low level where a wing's surface can be a subject to a free form morphing.

Sizing parametrization $\mathcal{X}_s$ is the most common as it acts upon an existing geometry and physical structure. When considering a FEM structural model a sizing design variable could be linked for example to a thickness of a specific set of elements, size of a flange

or a cross sectional shape of beam elements.

A goal of topology optimization is to acquire a superior material layout within a given space. In comparison to a sizing design variables, a topology parametrization $\mathcal{X}_t$ doesn't have a straight forward linking to a simulation model [67, 68]. A rough description can be provided by stating that a material distribution inside of a fixed domain is its parametrization. Even though it is possible to solve an optimization problem which includes a sizing and a topology parametrization at once, both cannot be acting upon the same domain.

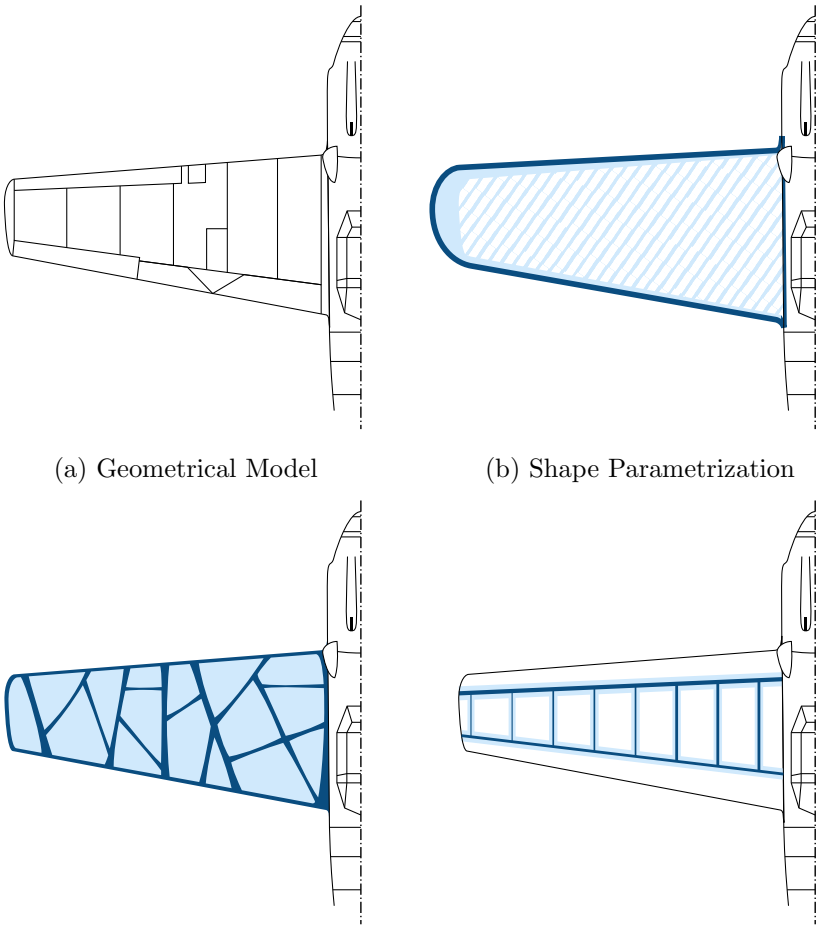

(a) Geometrical Model (b) Shape Parametrization

(c) Topology Parametrization (d) Sizing Parametrization

Figure 4.2: Example of parametrization categorization shown for a wing optimization

As such, what state variables are available for linking by a parametrization model depends on the used simulation model. If one wants to effectively exploit an optimization model it is necessary to extend a parametrization model across as many disciplines involved in a single simulation model as possible.

4.1.2. Simulation model

A simulation model forms the backbone of an MDO process and serves as a mapping function between model variables s and an objective or a constraints model by simulating system responses. In the context of an optimization process, a simulation model maps state variables s to responses y, shown by eq. (4.2).

$$R : \mathcal{S} \rightarrow \mathcal{Y} \tag{4.2}$$

Since this thesis is dealing with the topic of an aircraft design and performance optimization, the simulation model has to be able to appropriately approximate a real in-flight behaviour. Depending on requirements, such a simulation model can consist of a single discipline [69, 54] or multiple ones [46, 41]. Since this thesis intends to investigate the impact of a structural design on a flight performance, several various disciplines have to be coupled in the simulation model, summarized by the fig. 4.3.

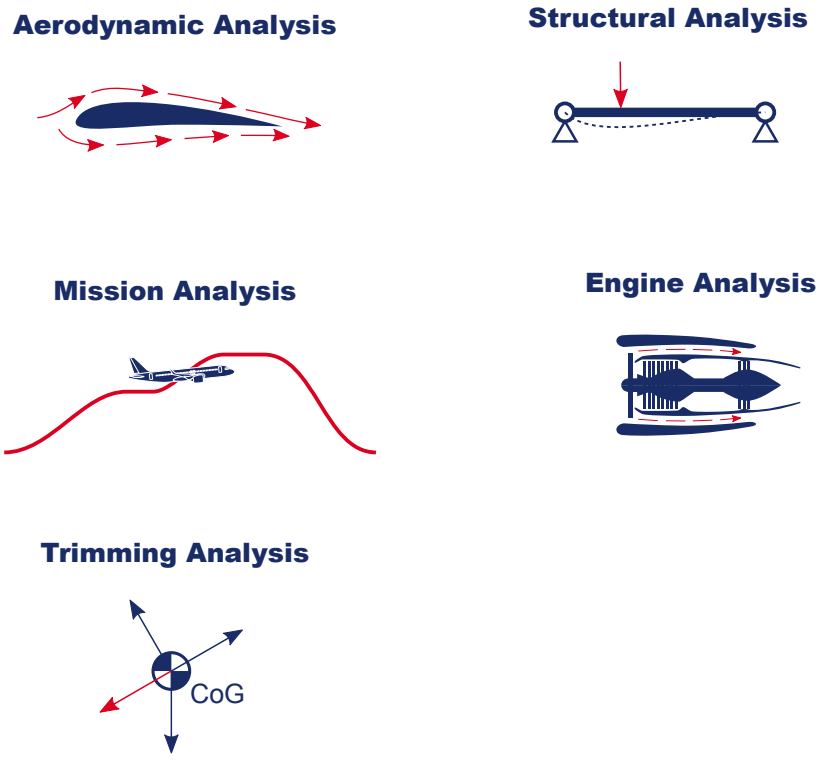

Figure 4.3: An example of disciplines involved in MDAO model intended for an aircraft design optimization

It is assumed that each of the included disciplines, or sub-models, follows its own governing equations which uniquely define that discipline's equilibrium state. Since each of the sub-systems is used to describe a different aspect of the whole system, they bring their own state variables $y \in \mathcal{Y}$ into the overall system. In general, the residual

eq. (4.3) describes a system where all involved disciplines are fully or at least partially interdependent.

$$R_i = R_i\left(y_0, \ldots, y_i, \ldots, y_n\right) = 0 \tag{4.3}$$

A multi-disciplinary system doesn't have to necessarily include only mutually interactive sub-systems, but it is often the case that at least a few of the related disciplines include responses of other sub-systems in their governing equations. A full interaction simulation can provide more realistic results, which are paid for by increased computational demands. Hence, it is common to neglect some of the interactions that are deemed to be of a limited impact, especially in practical application.

4.1.3. Objective function

An objective function, or the so called performance measure, extracts a value from a simulation model which should be minimized by the optimization process. It could be a single measure obtained from a response of an underlying simulation model, or it could compound several response values together. In the context of an aircraft design, common objective functions include a structural mass of an aircraft, a maximum range, an endurance or noise generated during aircraft operation. In the scope of this thesis, a mathematical representation of an objective function which is a target for a minimization is defined by the notation in the eq. (4.4).

$$\Psi\left(x\right) \rightarrow min \tag{4.4}$$

In general, it is possible to optimize only a single objective function at a time. If more than one performance indicator should be a target of an optimization, there are several possibilities how to deal with such a requirement. Firstly, a representative weighted functional could be defined that compounds all the required performance measures. Secondly, a trade-off study could be performed to build up the so called Pareto front, which provides a visual representation of various optimal designs obtained by varying weights combination. Thirdly, a physics based compound functional could be assembled, which blends the various performance measures of interest into a single value. An example of such a functional in the area of an aircraft design is the Breguet range equation [70] which combined a lift to drag ratio as a representation of an aerodynamic performance, an aircraft's mass, and a thrust specific fuel consumption related to an engine performance. As neither of the approaches changes the proposed optimization procedure, no particular importance is laid on optimization problems with multiple objective functions in the scope of this thesis. When choosing an objective function in the context of an aircraft optimization many options are available [46].

Drag

A common choice for a flight performance indicator is a drag value, as it is directly proportional to a thrust required to flight a specific manoeuvre and hence is linked to a fuel efficiency. Even though a drag value is an output of an aerodynamics analysis,

it has been shown, that it is important to consider an interdependent influence of a structural behaviour [15] as well. This is a result of a change of a wing form mid flight, where the wing undergoes deformations due to aerodynamic loads [61]. Dependent on an underlying simulation model it is possible to consider only a specific component of an overall drag. The eq. (4.5) shows the overall drag coefficient being composed of an induced drag and a parasitic drag.

$$c_D = c_{Di} + c_{D0} \tag{4.5}$$

For example, in the cases where a lower fidelity method like vortex-lattice based solver is applied, it is possible to obtain only a lift induced drag term directly. Since the data available to build an objective function is dependent on the responses of a simulation model, it is important to consider the targeted objective function from the start of an optimization model preparation, so that all sub-systems of a simulation model can be adequately chosen.

Structural mass

A structural mass represents an important indicator of the quality of an aircraft design, since it has a direct impact on a flight performance. The eq. (4.6) defines the overall mass of an aircraft as a sum of a structural, a payload and a fuel mass together with other sources of weight, like furnishings or an auxiliary power unit.

$$m_{tot} = m_s + m_f + m_p + m_o \tag{4.6}$$

Even though the maximum allowable weight of an aircraft is commonly fixed by design requirements, an optimization problem targeting a structural mass still have its merits. By reducing a weight of an aircraft's loads carrying structure it is possible to improve a flight efficiency by reducing the amount of fuel burned during a specific mission or to increase an aircraft's profitability by extending an mission's payload limit. In the case a FEM analysis is a part of the underlying simulation model a structural mass can be accurately evaluated as a mass sum of all contributing elements, as defined by the eq. (4.7).

$$m_s(x) \approx m_{fem}(x) = \sum_{i=1}^{n_{elem}} m_{elem_i}(x) \tag{4.7}$$

The mass evaluated using the eq. (4.7) represents only a loads carrying structure without all the necessary wiring, piping, furnishings and other installations. Even though that is the case, a structural mass remains the dominating feature of an aircraft's empty mass and can be therefore taken as a valuable indicator of design quality.

Mission performance

Even though both a structural mass and a drag coefficient can be used for the purposes of an optimization, building an objective function based on only one of them without the

consideration for their interdependency can lead to a design, which doesn't adequately represent the best performance improvement [29, 46]. A possible way to alleviate this problem is to merge a structural mass and a drag coefficient into a single compound objective function, with a practical example being the Breguet range [70], shown in the eq. (4.8). The Breguet range equation has already been used for a mission performance estimation in various research studies [71, 29, 38, 46].

$$R = \frac{v}{g\ c_{TSFC}} \frac{L}{D} \ln\left(\frac{m_{init}}{m_{fin}}\right) \tag{4.8}$$

The Breguet equation estimates an achievable range by merging an aerodynamic performance, an engine efficiency and an aircraft's mass in a single function under the assumption, that a velocity v is assumed to be constant together with Thrust Specific Fuel Consumption (TSFC), L and D. The inclusion of an engine performance is represented by the term of Thrust Specific Fuel Consumption (TSFC) c_{TSFC}, which describes the amount of fuel burned per single second for a unit of thrust. Since the drag to lift ratio is assumed to be constant, the Breguet formula describes a flight with a steady increase of altitude over time, which comes as a result of a reduction of a required lift over time due to a weight reduction from a continuous fuel burn. In an ideal scenario this would happen gradually, but for reasons of air traffic safety a continuous change of altitude is generally not allowed. Hence, mission profiles with a large target range do instead incorporate climb steps to achieve altitudes with a more beneficial lift to drag ratio. An available option to mitigate the inaccuracies connected to the assumption of a constant aerodynamic performance is possible to evaluate the Breguet equation for smaller time ranges, in which the $\frac{L}{D}$ ratio could be considered close to constant.

Expanding on the idea of a finer discretization is a concept of a fully coupled mission analysis, which can be used as a source of optimization data representing aircraft performance [63, 41, 40]. Even though this thesis targets a trip fuel minimization as the main performance measure there are various options how to integrate a trip fuel in an objective function. Firstly, a minimization of a trip fuel and minimization of a required initial fuel offer a seemingly equivalent definition, but even though they are very similar, a critical difference exists in their gradient computation with respect to considered design variables. In the case of a gradient of a trip fuel its value changes after each optimization iteration, as it is computed based on values obtained from a mission analysis. In comparison, when considering an initial fuel as an objective function, its gradient remains the same for the whole optimization procedure, as it is independent on the mission computation. An another option of interest would be payload maximization for a specific mission. While not directly improving an aircraft efficiency it has a potential to increase profitability.

4.1.4. Constraints model

Since any design change coming from an optimization process leads automatically to a different response of the underlying simulation model, it is necessary to assure that such

a change doesn't compromise design feasibility or viability. Hence, to achieve a valid design, which satisfies all limitations set by physical properties or design requirements, integration of a constraints model into any optimization task is necessary. In the scope of an MDO for an aircraft design constraints introduce e.g. maximum allowable stresses, buckling/stability restrictions or manufacturing limitations. A constraints model is generally built using two types of constraint functions. An equality constraint $h(x)$ which requires that a tracked value stays constant during an optimization process. The other one is an inequality constraint $g(x)$, which represents a one sided limit for a tracked value. Both of these are commonly defined in a residual form shown in the eq. (4.10).

$$h(x) = 0 \tag{4.9}$$

$$g(x) \leq 0 \tag{4.10}$$

Strength constraints

An elementary design check in regard to a structural safety is a criterion of maximum stress, which validates that no material failure occurs due to critical loads. This is achieved by evaluating stresses and strains resulting from a response analysis of an underlying simulation model. As it is necessary that the feasibility check is performed continuously during an optimization process, strength constraints are introduced to the overall optimization model. Formulation of such constraints varies depending on involved material models [72, 73, 74]. A general implementation of these constraints is represented by a definition provided by the eq. (4.11), which would be evaluated for each element of an FEM model. The value σ_{crit} represents the highest allowable stress given by material specifications.

$$g(x) = \frac{\sigma(x)}{\sigma_{crit}} - 1 \leq 0 \tag{4.11}$$

Structural stability constraints

A structural failure due to stresses and strains exceeding material limitations represents only a part of all possible failure modes that have to be investigated to assure a safe structural design. A possibility of a local loss of stability has to be evaluated as well when sizing a loads carrying structure of an aircraft, as it consists of many slender components like spars, ribs, stringers or a wing-box skin. Integration of buckling constraints in an optimization avoids the danger of obtaining a design which would fail due loss of stability. Based on the relationships by [75] a concept of a reserve factor r is used to define stability constraints. In the eq. (4.12), the actual normal and shear stresses on a component are compared to a critical normal and shear stress values, which are determined from a loading type, a geometrical shape, material properties and structural supports of a local structural patch. The actual implementation as constraint functions and their evaluation is handled by the software suite Lagrange [53], which was utilized for the purposes of a structural analysis in the scope of this thesis.

$$\frac{1}{r} = \left(\frac{\sigma(x)}{\sigma_{crit}}\right) + \left(\frac{\tau(x)}{\tau_{crit}}\right)^2 \tag{4.12}$$

Trimming constraints

An aerostructural analysis can be deemed valid only if all simulated flight states represent realistic flight conditions, meaning that a flight equilibrium has to be achieved for all of them. A quasi steady manoeuvre can be incorporated into an optimization procedure either in the form of an extended coupled analysis introducing additional governing equations describing a flight equilibrium or by reformulating the same formula into constraint functions. The eq. (4.13) and eq. (4.14) represent forces and moments in all six DOFs at an equilibrium respectively. The forces and moments have various sources on an aircraft, as shown in the fig. 4.4.

$$h_F(x) = F_a(x) + F_s(x) = 0 \tag{4.13}$$
$$h_M(x) = M_a(x) + M_s(x) = 0 \tag{4.14}$$

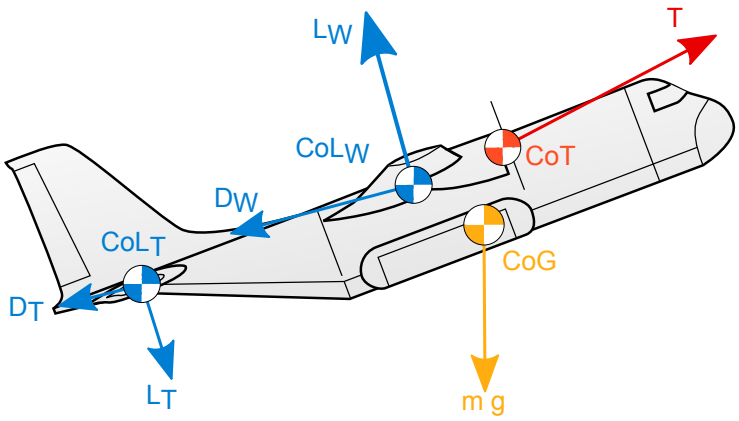

Figure 4.4: Major forces contributing to a flight equilibrium

In both approaches, additional unknowns, with an explicit influence on a flight equilibrium have to be introduced. These unknowns are called trimming variables b in the scope of this thesis. The trimming variables are usually linked an angle of attack of an aircraft and to control surface deflections of elevators, stabilizer, rudders, flaps and others. Depending on the type of a manoeuvre that is to be simulated, not all DOFs have to be constrained or all control surfaces have to be linked to trimming variables. This simplification can be for example allowed in those cases where a symmetric aircraft

is being investigated while being subject to symmetrical loading conditions. In such a case, only three Degree of Freedom (DOF)s, representing the forces and moments in a symmetry plane, have to be considered and hence only three trimming variables have to be designated. An additional simplification, either in order to reduce the number of DOFs even further or because of a lack of appropriate data, is represented by a possibility of removing a drag and and thrust force from the trimming equation system. This would mean that in a fully symmetrical flight state only forces in a lift direction and moments around a pitching axis would have to be in equilibrium. Especially in the cases of critical loads evaluation and wing sizing at early design stages can this complexity reduction be of benefit, especially since the forces in the direction of an longitudinal axis don't significantly contribute to stress and strain values when compared to the impact of lift forces when considering traditional civilian aircraft configurations [46]. If the main purpose of the trimming analysis is to obtain a valid drag force estimate, such a simplification cannot be utilized.

Mission performance constraints

An optimized design has to fulfill performance requirements like a take-off distance, an MTOW, a fuel efficiency, a loiter endurance, an achievable range, or an admissible payload. A possible aggregation encompassing many of these requirements can be represented by a mission performance analysis. Hence, a set of design mission profiles is evaluated for the purposes of obtaining a complex response representative of an intended application case for an aircraft design. When considering a mission analysis inside of an MDO model it is important to include two sets of constraints. Firstly, it is necessary to assure that only viable flight states are considered, limiting parameters like a maximum engine thrust setting, a highest amount of fuel allowed by on-board tanks or a peak altitude. Secondly, constraints introduced to target a flight performance. These can include indicators like a minimum range, a time to climb, a reserve fuel or noise levels. The approach utilized in this thesis implements parts of both constraint sets, although from the performance perspective only a range and a reserve fuel has been considered. Respective constraint values can be computed based on the eq. (4.16) and eq. (4.15), which have to be evaluated during each optimization step.

$$m_f(t_f) = m_f(t_0) + \int_{t_0}^{t_f} \dot{m}_f(t)\ dt \tag{4.15}$$

$$s(t_f) = \int_{t_0}^{t_f} v_{GS}(t)\ dt \tag{4.16}$$

The specific amount of fuel that has to remain in the fuel tanks at the end of a mission is defined by aircraft certification agencies like the EASA. According to EASA, the reserve fuel is split into a contingency fuel, an alternate fuel, a final reserve and an additional fuel. The intention is to guarantee a safe flight trip even in such cases, when having to loiter because of a heavy traffic at an airport, or due to a sudden change

of a destination airport. Based on the situations considered for which the reserve fuel has to be estimated, the amount required is defined as dependent on an aircraft's flight performance. To avoid having to simulate loiter segments of a mission or a full alternative profiles for a redirected flight, a simplification for the amount of reserve fuel needed was chosen for the purposes of an MDO process introduced in this thesis. Constraint defined by the eq. (4.17) uses a fuel reserve factor r_f to set the amount of fuel left at the end of a mission as a relative of the trip fuel value.

$$g(x) = 1 - \frac{m_f(t_f)}{r_f\left(m_f(t_f) - m_f(t_0)\right)} \leq 0 \tag{4.17}$$

4.1.5. Optimization algorithm

All of the up to now introduced sub-model of an overarching MDO model are used as the source data to be fed into an optimization algorithm, which is responsible for finding a design improvement under applied constraints. In the context of optimization, there are many established algorithm families as discussed for example by G.N. Vanderplaats [66] or H. Baier [65]. Choosing a suitable optimization algorithm is a task that has to be performed while investigating analysis aspects and features of utilized simulation and parametrization models. A first consideration is commonly done in regards to an availability of a gradients of the objective and constraints models. If no gradient computation is available or cannot be implemented in a case of a too complex simulation model, or if a system displays very noisy responses, a stochastic optimization algorithm might be chosen as a reasonable choice. Otherwise gradient based algorithms might prove more suitable. Since optimization deals with repeated MDA model evaluations, it is essential to include an algorithm's computational performance into the decision making. From a perspective of a time efficiency, accuracy and implementation intricacy a choice of an appropriate algorithm has to be based on following criteria.

- Complexity of an underlying MDA model
- Number of design variables defined by a parametrization model
- Type of design variables
- Number of constraints in a constraints model
- Continuity and non-linearity of objective and constraint functions
- Noisiness of design space
- Computational efficiency

Since the optimization problem considered in the scope of this thesis deals with an optimal sizing of loads carrying structural components, a large number of constraints is to be expected in order to guarantee a final design's structural integrity. As these constraints are applied at all design relevant elements of an FEM model per considered

critical load case, the number of all relevant constraints can reach up to several hundred thousands. In general, the number of design variables that would be included in an aircraft structural design MDO problem on an industrial scale could reach thousands as well. In the scope of this thesis their number will be kept under one hundred to save on a computational time. Motivated by the fact, that an existing aerostructural solver Lagrange [53] already exposes many of the required gradients and since for an integrated mission analysis a sensitivity analysis was implemented as well, the NLPQL algorithm introduced by K. Schittkowski [47] will be utilized to solve the targeted MDO problem.

4.2. Model selection

Based on a design phase and related targets for which an optimization task should be incorporated, it is possible to derive a large number of different optimization models. An ideal all encompassing scenario that has a high potential of achieving a true global optimum needs to integrate many disciplines, which would have to be represented by high-fidelity simulation models together with their mutual interactions. Unfortunately, such a case is currently still out of a reach for current technological capabilities in the area of an aircraft design. As such it is important to provide examples of practical models that can be utilized in a current environment, with an overview being given in the table 4.1.

This thesis tries to establish a viable approach to deploy an optimization model during early or mid preliminary design phases where an outer wing shape is already fixed and engines are chosen. At that point in time, internal structure of wings is still not necessarily final and as such provides an opportunity for an optimization process to be applied. What remains is to develop an internal structure that satisfies given design requirements and doesn't compromise an aircraft performance. A structural sizing optimization problem deals with a trade-off between a structural safety and a weight, where an optimization process should find the best possible value of a performance measure while still satisfying all constraints set by a constraints model. In situations where a mission performance should be considered, it is of benefit to consider two analysis types with regard to their application. An ultimate loads analysis, which deals with critical loads and deformations that an internal structure of an aircraft has to withstand. Secondly, a mission analysis used to measure a flight performance over a longer time span. By dealing with both of these models in a separate manner it is possible to apply physical representations of varying fidelity, which are more fit for their respective purpose, while keeping computational demands under control.

Target	in-flight aerodynamic performance
Design phase	early conceptual
Physics	low fidelity aerodynamics
Constraints	wing planform size
Parametrization	outer wing shape
Target	mission performance
Design phase	late conceptual
Physics	medium/high fidelity CFD, low fidelity CSM, mission analysis
Constraints	structural safety, mission feasibility
Parametrization	components sizing, outer wing shape, mission planing, engine sizing
Target	mission performance
Design phase	mid/late preliminary
Physics	medium/high fidelity CFD, high fidelity CSM, mission analysis
Constraints	structural safety, mission feasibility
Parametrization	components sizing, mission planing
Target	structural weight
Design phase	early/mid preliminary
Physics	low/medium fidelity CFD, high fidelity CSM
Constraints	structural safety
Parametrization	components sizing

Table 4.1: Examples of optimization models for aircraft design in early and mid development phases

5. Mission Analysis

In general, a mission analysis merges an aerodynamic performance, a structural weight, a trimming analysis, a propulsion performance and others. Hence, its results can be considered as a robust source for a flight efficiency evaluation. A widely acknowledged mission performance estimator compounding otherwise single-disciplinary measures like a lift to drag ratio, a thrust specific fuel consumption or a weight is the Breguet range equation [46]. Some of the limitations inherent to the Breguet equation could be alleviated by applying a discretization to a considered cruise segment, updating the flight behaviour parameters in the equation at each segment. A mission analysis represents a step further by discretizing the whole mission profile. In this case, the flight behaviour es evaluated continuously over all segments of a given flight trip, while continuously updating a fuel mass state and flight other performance indicators. A mission analysis requires a well defined mission profile that an aircraft follows over time. There are few options available when defining a flight profile, for which the choice very often depends on an intended application. A continuous definition of a flight path can be obtained using basis splines [40], which provide a formulation with well defined path derivatives. An another often adopted approach is based on a segment-wise discretization of the whole mission profile [76]. Such a case can be more often found in an industrial setting as it provides more realistic representation of flight schedules, that are controlled by air traffic control authorities. The mission response and sensitivity analysis implemented in this thesis's framework utilizes the segment-wise approach. A basic nomenclature for a mission profile definition that this thesis follows is presented in the fig. 5.1.

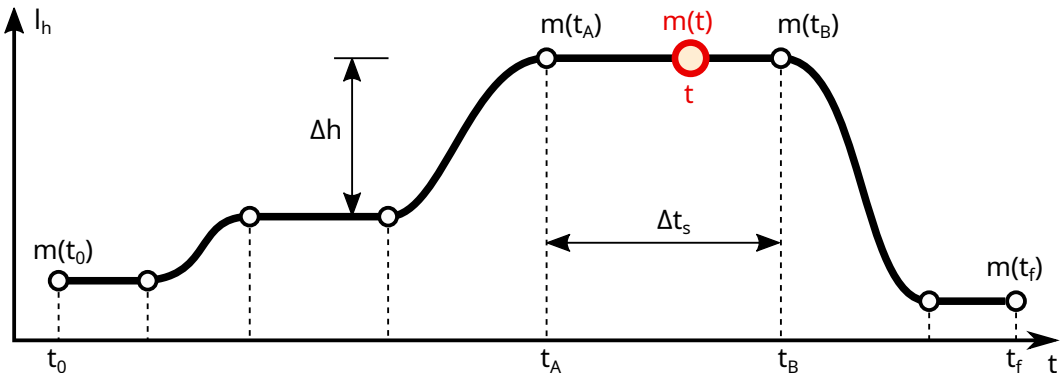

Figure 5.1: A general mission description with nomenclature

A mission profile is defined between a initial time at the start of a trip t_0 and a final time after landing t_f, whereas the number and type of internal segments is dependent on a mission type and an airport's local conditions. Some examples of mission types are characterized in the fig. 5.2. For example, a standard passenger aircraft mission would consist of a taxi-in, an initial take-off, several climb and acceleration segments, main cruise segments with possibly one or more climb steps, descent and deceleration segments, an airport approach, landing and an taxi-out. There is a large number of

mission state variables that change during a flight while an aircraft is performing a mission, be it a system temperature, an amount of power consumed, a level of noise generated or a fuel mass consumed during the flight. It is the amount of fuel that has been burnt during a flight that is of high interest when evaluating a mission efficiency, be it for a pure aerodynamic or an aeroelastic performance analysis. Especially in the cases dealing with MDO problems including coupled aerodynamic and structural response, change in mass is of an elevated relevance, since the mass doesn't only explicitly impact a trimming solution but implicitly through its influence on deformation distribution as well. Assuming a segment-wise profile description, a general relationship defining a fuel state at an end of a mission is shown in the eq. (5.1).

$$m_f(t_f) = \int_{t_0}^{t_f} \dot{m}_f(t)\, dt \approx \sum_{i=1}^{n_{seg}} \left(m_f(t_{A_i}) + \int_{t_{A_i}}^{t_{B_i}} \dot{m}_f(t)\, dt. \right) \tag{5.1}$$

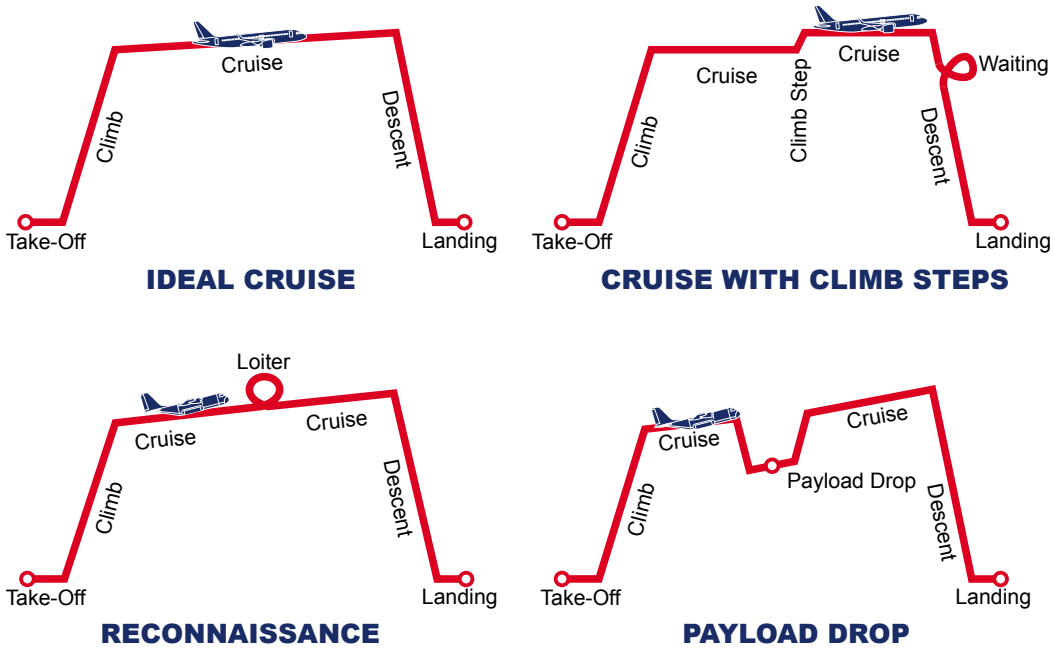

Figure 5.2: Examples of common mission profiles using a segment-wise definition

When using the segment-wise approach to a mission profile definition, it is possible to consider different flight modes for each of the segments. Each of the flight modes listed below uniquely identifies a set of trimming variables and constants.

- Cruise at a constant Mach number and altitude

- Cruise at a constant Mach number and rate of climb
- Climb at a constant CAS and thrust setting
- Climb at a constant Mach number and thrust setting
- Acceleration at a constant rate of climb and thrust setting

The fig. 5.3 exposes essential interactions of a mission analysis within an overarching optimization problem and an underlying aircraft computational model. The mission analysis itself is a part of a simulation model from the fig. 4.1 and can expose additional state variables that can be used in an optimization. At the same time it introduces its own set of constraints to ensure a flight profile validity. The main contribution of a mission analysis is to provide a source of reliable flight performance indicators summarizing a long time behaviour instead of considering only a single or a few discrete flight conditions.

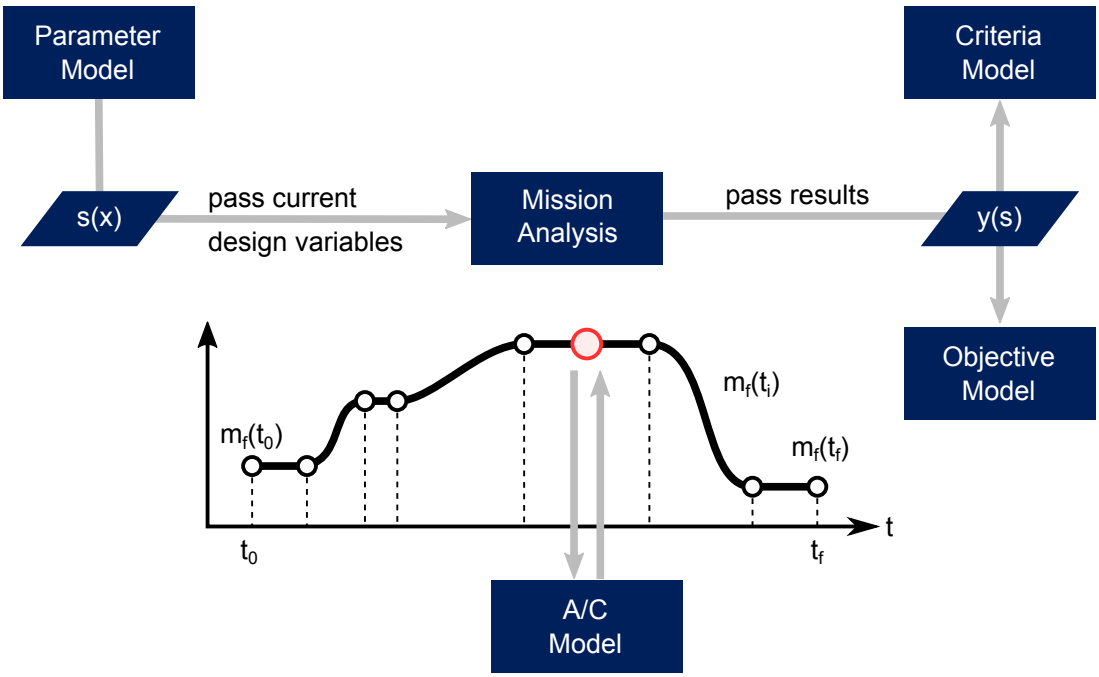

Figure 5.3: Mission analysis in an overall optimization process

5.1. State Analysis

As a subsystem of the overall simulation model, the mission analysis introduces its own state variables and governing equations. Their choice is not strictly unique and is dependent on an intended application together with a flight profile definition. In the

scope of this thesis a fuel mass is selected as a basis state variable, which is always included in a mission analysis, as it presents an immediate influence on a total weight of an aircraft and concurrently impacts a structural deformation and therefore an in-flight shape of a wing. The previous eq. (5.1) evaluates the final fuel as a function of a fuel burn rate over a mission. To be able to use the equation, it is necessary to first obtain the continuous fuel burn rate over the flight time. Independent of a type of a segment, for which the fuel flow $\dot{m}_f$ is computed, it can be expressed as a function of an underlying MDA model responsible for an aircraft flight response, for which the current total mass m_{tot} represents an input, and is therefore dependent on a current fuel mass m_f as well. This dependency is characterized in the fig. 5.4 and represents an ODE in the eq. (5.2).

$$\dot{m}_f(t) = f(m_f(t), \dots) \tag{5.2}$$

Since a flight profile is supposed to be segmented, a single mission analysis solves a sequence of serially dependent ODEs, whose continuity relation is given by the eq. (5.3). This condition enforces only a C^0 continuity. This simplification allows the time derivatives of mission state variables, like a fuel burn $\dot{m}_f(t)$, to be discontinuous between segments. An enforcement of a C^1 continuity would probably not bring a major benefit that would offset a related increase in implementation and computational complexity.

$$m_f(t_{A_i}) = m_f(t_{B_{i-1}}) \tag{5.3}$$

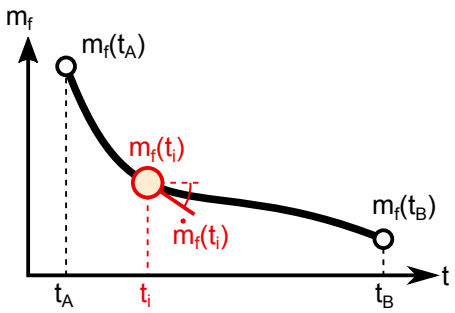

Figure 5.4: An arbitrary mission segment

Since the mission analysis deals with solving an ODE problem, any established numerical algorithm can be applied. All of the segments that are considered in a long range mission analysis represent quasi-steady flight states. Additionally there is no dynamic analysis involved in the underlying simulation model, which means that there are no significant oscillations expected in the resulting $m_f\,(t)$ function. This assumption motivates a selection of a very simple numerical integration algorithm such as Forward Euler defined in the eq. (5.4).

$$m_f(t_{i+1}) = m_f(t_i) + \dot{m}_f(t_i)\,\Delta t \tag{5.4}$$

A single segment is discretized into a number of time points t_i at which the underlying simulation model is evaluated and a fuel flow $\dot{m}_f(t_i)$ is obtained. A critical requirement for a solution algorithm used in a segmented mission analysis is the ability to terminate at a predefined condition. In the context of ODEs these conditions identifying a discrete behaviour are called events and make the mission analysis a hybrid ODE system. As an example, event can be defined for a primary variable of fuel mass m_f in the case of a cruise segment or a Mach number v_{Ma} in the case of a climb at a constant calibrated air speed v_{CAS} that has to be terminated at a crossover altitude. Due to the relative steadiness of time derivatives of the mission state variables, the ability to handle events is considered more important than n inclusion of a more complex numerical integration algorithm.

The eq. (5.2) for a fuel mass is not the only ODE that has to be evaluated. Mission state variables like an altitude $h(t)$ or a distance $s(t)$ might have to be evaluated by an ODE as well, depending on a segment type. A segment with a prescribed flight path angle γ and a Mach number v_{Ma} has a fixed flight path $h(t)$. In the case of a segment like a climb at a constant v_{Ma} and a thrust setting η_T the rate of climb $\dot{h}$ will depend on the aircraft's performance. As such a second ODE has to be introduced into the mission analysis together with the eq. (5.2).

$$\dot{h}(t) = f(m_f(t), h(t), \dots) \tag{5.5}$$

As exposed by the fig. 5.5, the mission analysis computation relies on other parts of a simulation model through a so called aircraft model. This model is responsible for evaluating point performance values like a fuel flow $\dot{m}_f(t_i)$ or a rate of climb $\dot{h}(t_i)$.

Algorithm 1 A mission evaluation algorithm

1: $t_1 \leftarrow t_0$ ▷ Set initial values
2: $m_f(t_1) \leftarrow m_f(t_0)$
3: $l(t_1) \leftarrow l(t_0)$
4: $n \leftarrow$ number of segments
5: **for** $j \leftarrow 1, n$ **do** ▷ Loop over segments
6: $\quad t_{j+1}, m_f(t_{j+1}), l(t_{j+1}) \leftarrow \text{SEGMENT}(j).\text{SOLVE}(t_j, m_f(t_j), l(t_j))$
7: **end for**
8: **return** $t_{j+1}, m_f(t_{j+1}), l(t_{j+1})$ ▷ Return end of segment state

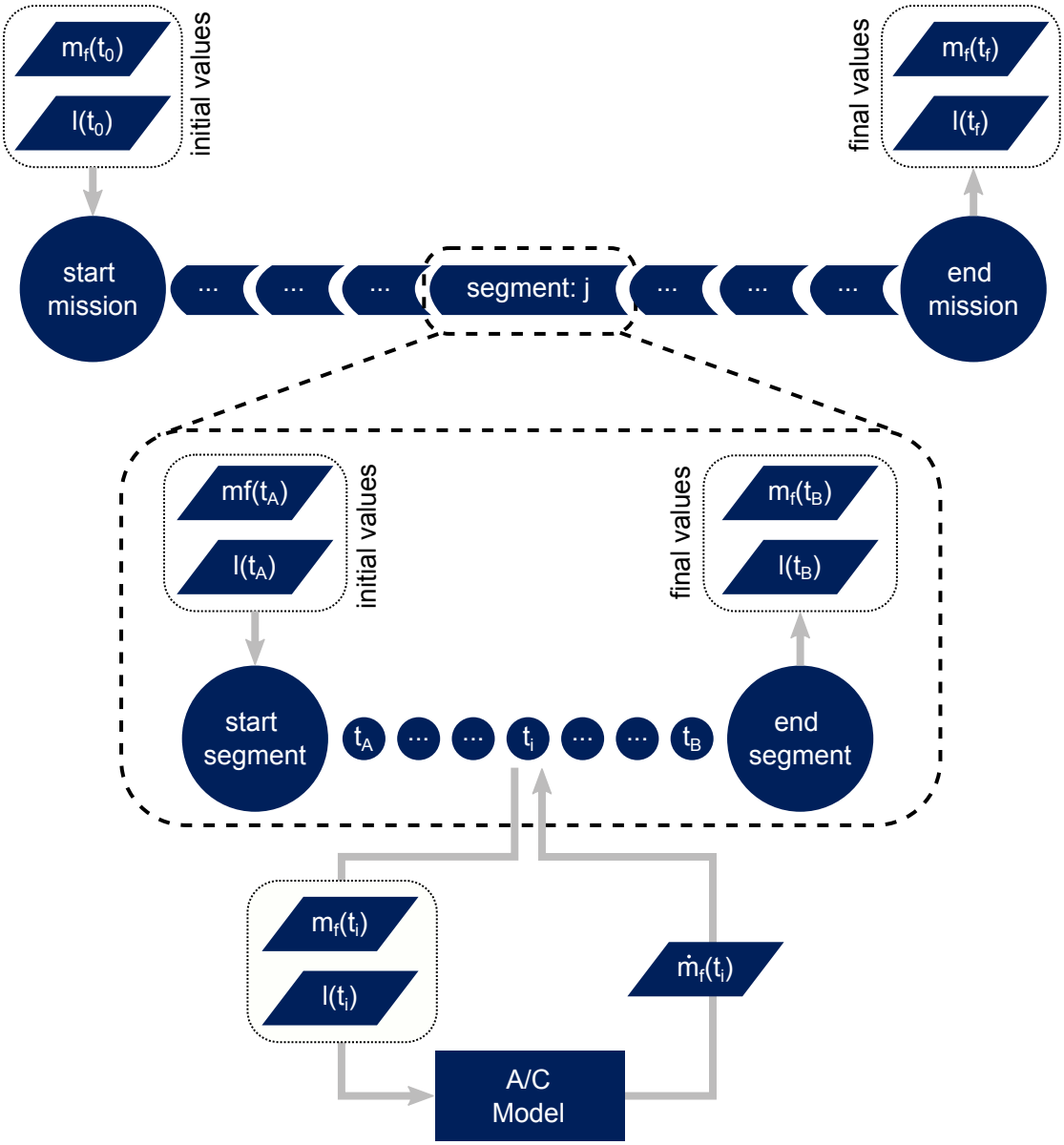

Figure 5.5: Mission computation composition diagram

Algorithm 2 A segment evaluation algorithm: Euler Forward Integration

$t_i \leftarrow t_A$
$m_f(t_i) \leftarrow m_f(t_A)$
while $conv \leftarrow False$ **do** ▷ Step through time
    $l(t_i) \leftarrow$ GET_CONDITIONS$(t_i, l(t_A))$
    $\dot{m}_f(t_i) \leftarrow$ COMPUTE_FUEL_FLOW$(t_i, m_f(t_i), l(t_i))$
    $m_f(t_{i+1}) \leftarrow m_f(t_i) + \dot{m}_f(t_i) \cdot \Delta t_i$
    $conv \leftarrow$ CHECK_TERMINAL_EVENT$(t_{i+1}, m_f(t_{i+1}), l(t_{i+1}))$
    if $conv \leftarrow True$ **then**
        $\Delta t_i \leftarrow$ COMPUTE_FINAL_STEP$(t_i, m_f(t_i), \dot{m}_f(t_i), l(t_i))$
        $m_f(t_{i+1}) \leftarrow m_f(t_i) + \dot{m}_f(t_i) \cdot \Delta t_i$
    end if
    $i \leftarrow i + 1$
end while
return $t_i, m_f(t_i), l(t_i)$

In general, an aircraft simulation model can integrate various disciplines coupled in an arbitrary manner. From the point of view of a mission analysis, the aircraft model can be considered a black box system with a predefined interface. A common approach is to represent an aircraft model by a single mass point [77], usually defined at the aircraft's center of gravity, with an aerodynamic performance being precomputed in a form of lift and drag polars. Alternatively, a more complex CFD analysis can be used to obtain a flight performance directly for given flight conditions [41]. In any case, a trimming analysis is an essential requirement of a mission analysis and will be expanded upon in the section 6. Its responsibility is to assure that all flight conditions, at which a performance is evaluated, describe viable flight states for an aircraft. The main task of a mission analysis in the presented approach is to evaluate a performance measure or a constraint that has to be integrated either in an objective model or a constraints model of the overarching MDO model. Both, an objective and a constraint function can be written in general as is presented in the eq. (5.6), in which the state variable y can represent any response of any system involved in an underlying MDA model.

$$\Psi = \psi_0\left(y,\, t_0,\, x\right) + \psi_f\left(y, t_f, x\right) + \int_{t_0}^{t_f} \psi_t\left(y,\, \dot{y},\, t,\, x\right) dt \tag{5.6}$$

For some objective functions of interest the general form allows for a dual interpretation. A fuel mass consumed during a trip $\Delta m_f(t_f)$ is one of them, as it has two possible equivalent formulation that can be used to track it.

$$\Delta m_f(t_f) = m_f(t_0) - m_f(t_f) = \int_{t_0}^{t_f} \dot{m}_f(t) dt \tag{5.7}$$

Another measure of interest considered in the presented approach is the initial total

weight of an aircraft, which follows a straightforward evaluation given by the eq. (5.8).

$$m_{tot}(t_0) = m_f(t_0) + m_s \tag{5.8}$$

Since the mission profile is discretized into a number of segments that are solved consecutively, the integral part of the eq. (5.6) is evaluated as a sum over all involved segments. Hence, it is convenient for evaluation and further explanation to move from a global time t frame to a local time τ, frame resulting in the eq. (5.9).

$$\Psi = \psi_0\left(y,\, t_0,\, x\right) + \psi_f\left(y,\, t_f,\, x\right) + \sum_{i=1}^{N_{seg}} \int_0^{\tau_B} \psi_\tau\left(y,\, \dot{y},\, \tau,\, x\right) d\tau \tag{5.9}$$

5.1.1. Cruise Segment at Constant Speed and Flight Path Angle

Since the aircraft spends the most time of its trip in a cruise, a segment that simulates the corresponding flight conditions is an essential part of the mission analysis. In this thesis, the cruise flight profile is given by the constant Mach number v_{Ma} and the constant flight path angle γ.

$$\gamma\left(t\right) = \text{const} \tag{5.10}$$
$$v_{Ma}\left(t\right) = \text{const} \tag{5.11}$$

This formulation describes a flight profile that is independent on an aircraft performance by prescribing an altitude $h\left(t\right)$ as a function of the flight path angle γ and the Mach number v_{Ma}. In this form, all related atmospheric and flight conditions can be evaluated for the whole segment beforehand.

$$h(t) = h(t_A) + \dot{h}(t) \cdot (t - t_A) \tag{5.12}$$
$$s(t) = s(t_A) + v_{GS}(t) \cdot (t - t_A) \tag{5.13}$$
$$\dot{h}(t) = v_{GS}(t) \cdot \sin\left(\gamma\right) \tag{5.14}$$

Since all the flight conditions are already given at each time step of the cruise segment, the only remaining unknown state variable is the fuel flow $\dot{m}_f(t_i)$, that corresponds to the thrust needed to balance out a generated drag. The table 5.1 summarizes which variables are provided by the cruise segment analysis as an input to an aircraft model with a corresponding output.

Input	Unknown	Output
$m_f(t_i)$, $l(t_i)$	$T(t_i)$	$\dot{m}_f(t_i)$

Table 5.1: Input/output of the aircraft model for the CRMG type of segment

5.1.2. Initial and Terminal Conditions

To define an ODE system, that uniquely describes a flight segment, it is necessary to add initial and terminal conditions. An initial condition can be either fixed or can be dependent on a final state of a previous segment. A terminal condition is used to terminate a segment when a value of interest reaches a specific value. This condition is called an event in this scope of this thesis. The initial and the terminal conditions is written in a residual form in the eq. (5.15) and the eq. (5.16).

$$\Omega_A\,(y,\,t_A,\,x) = 0 \tag{5.15}$$

$$\Omega_B\,(y,\,t_B,\,t_A,\,x) = 0 \tag{5.16}$$

The ODE event can be defined for any of the flight conditions that are tracked by the mission analysis. As an example could serve a cruise segment that is terminated after reaching a predefined distance, or a climb segment that should bring an aircraft up to a given altitude. A typical condition used in mission profiles is reaching a crossover altitude, meaning that a climb segment performed with a constant CAS ends after achieving a prescribed Mach number, after which the aircraft would transition into a climb with that Mach number being constant. The fig. 5.6 shows a cruise segment at a constant speed and a constant climb rate and the impact of a change in a terminal altitude. The change results in a completely different flight state at the end of the segment. Hence, the final flight state variables related to a mission profile cannot be determined without a solution of the underlying ODE system.

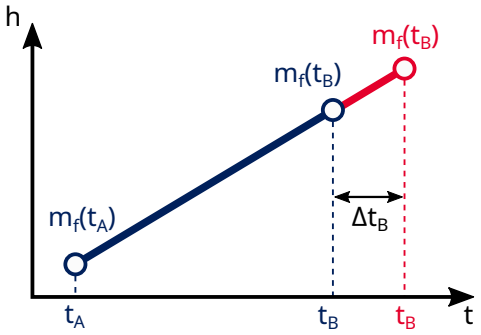

Figure 5.6: Cruise Segment at Constant Speed and Climb Rate

The fact that a length of segments depends on an aircraft's performance, exemplified by

the climb segment terminated at a specific altitude, becomes increasingly important when discussing a mission sensitivity analysis later on. Few examples of terminal conditions considered in the scope of this thesis are presented in the eq. (5.17), eq. (5.18) and eq. (5.19).

$$\text{time:} \quad \Omega\left(t_B\right) = t_B - t = 0 \tag{5.17}$$

$$\text{fuel mass:} \quad \Omega\left(t_B\right) = m_f\left(t_B\right) - m_{f,c} = 0 \tag{5.18}$$

$$\text{distance:} \quad \Omega\left(t_B\right) = s\left(t_B\right) - s_c = 0 \tag{5.19}$$

5.2. Sensitivity Analysis

To properly embed a fully coupled mission performance analysis as a part of the overarching MDO process, the analysis is required to perform a sensitivity analysis in order to generate derivatives usable by a gradient based optimization algorithm. As the first step towards developing said functionality, the governing eq. (5.2) of the mission analysis is derived.

$$\frac{d}{d\,x}\dot{m}_f(t) = f\left(\frac{d}{d\,x}m_f(t), \dots\right) \tag{5.20}$$

The obtained eq. (5.20) represents an additional ODE that has to be solved together with the one describing the system response. In general, the same solution procedure used when dealing with the response analysis can be applied to the gradient eq. (5.21), which is formulated for the utilized Forward Euler Integration solution method.

$$\frac{d}{d\,x}m_f(t_{i+1}) = \frac{d}{d\,x}m_f(t_i) + f\left(\frac{d}{d\,x}m_f(t), \dots\right) \cdot \Delta t \tag{5.21}$$

The two available methods for the definition of a sensitivity analysis, that being the direct and the adjoint method, lead to significantly differing methodologies, when dealing with a gradient computation intended for an ODE system in the scope of an aircraft optimization. In this thesis only the direct approach was considered, as it can be used to investigate the targeted MDO problem in a more flexible manner, even though in some cases it is computationally less efficient than the adjoint based computation would be. The direct approach deals with the eq. (5.21) in a straightforward way. The sensitivity ODE solved for each involved design variable x separately. The major driver of computational costs is in this case the efficiency with which all the necessary partial derivatives can be obtained. Even though the eq. (5.20) doesn't present high simulation demands in itself, it is connected to a multi-disciplinary system which is responsible for the simulation of an aircraft behaviour. Hence the computational costs accumulate over the whole mission and a good care has to be take when selecting the fidelity of the multi-disciplinary system. The direct sensitivity analysis follows the same workflow as was the case with the response analysis shown in fig. 5.5. The only difference is the need for a propagation of derivatives w.r.t. x along with the response variables, as shown in

the fig. 5.7.

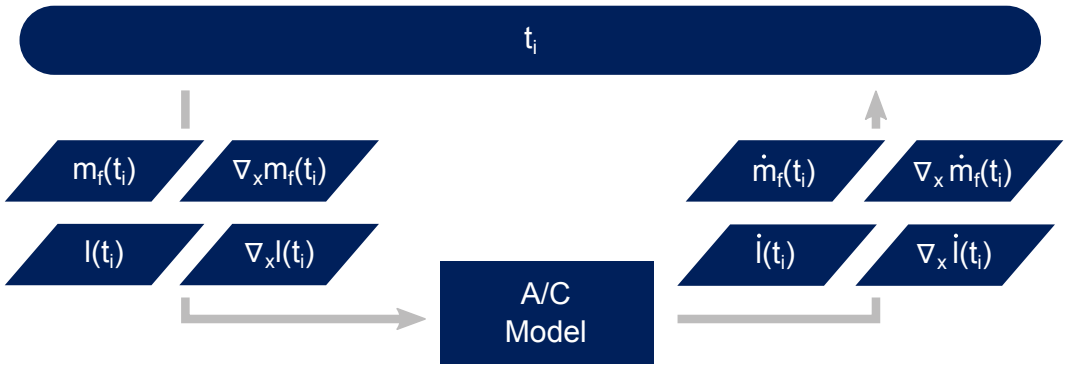

Figure 5.7: Data exchange between a mission and an aircraft sensitivity analysis during one time step t_i

The mission sensitivity analysis serves only as a source of gradients needed to obtain a sensitivity of an objective or a constraint function w.r.t. a design variable x, generally represented by the eq. (5.9). Deriving the objective function results in the eq. (5.22).

$$\frac{d\,\Psi}{d\,x} = \frac{d}{d\,x}\psi_0\,(y,\,t_0,\,x) + \frac{d}{d\,x}\psi_f\,(y,\,t_f,\,x) + \sum_{i=1}^{N_{seg}} \frac{d}{d\,x}\int_0^{\tau_B(x)} \psi_t\,(y,\,\dot{y},\,\tau,\,x)\,d\tau \tag{5.22}$$

The derivative of the objective function involving only the state at the start of a mission ψ_0 is the least demanding to compute when compared to the other parts of the equation. Since it involves only the initial conditions and is therefore already known or can be easily evaluated, as it doesn't depend on any results of the mission analysis. An example would be the total initial mass of the aircraft obtained by deriving the eq. (5.8)

$$\frac{d}{d\,x}\psi_0 = \frac{d}{d\,x}m_{tot}(t_0) = \frac{d}{d\,x}m_f(t_0) + \frac{d}{d\,x}m_s \tag{5.23}$$

where the derivatives of the fuel mass $m_f(t_0)$ and structural mass m_s are known right from the beginning. In some cases it is possible that the initial time of the mission itself is dependent either directly or indirectly on a design variable. Hence, this possibility should be considered in the gradients computation as well, resulting in the eq. (5.24).

$$\frac{d\,\psi_0}{d\,x} = \frac{\partial\,\psi_0}{\partial\,y}\frac{d\,y}{d\,x}\,(t_0) + \frac{\partial\,\psi_0}{\partial\,t_0}\frac{d\,t_0(x)}{d\,x} + \frac{\partial\,\psi_0}{\partial\,x} \tag{5.24}$$

The gradient of the part of the objective function related only to the final state requires, that the mission sensitivity analysis be computed first, and as such has in the case of the direct approach similar computational requirements as the part with an integral over the whole mission time. Based on the various termination conditions used to define an end

of a segment, it is unavoidable to have a terminal time t_f that is dependent on a design variable x. Due to this possibility the derivative of the terminal part of the objective function should be written as in the eq. (5.25).

$$\frac{d\,\psi_f}{d\,x} = \frac{\partial\,\psi_f}{\partial\,y}\frac{d\,y}{d\,x}\,(t_f) + \frac{\partial\,\psi_f}{\partial\,t_f}\frac{d\,t_f(x)}{d\,x} + \frac{\partial\,\psi_f}{\partial\,x} \tag{5.25}$$

In the case that the direct sensitivity analysis approach is chosen, the derivatives of the state variables $y(t_f)$ have to be evaluated first. In the case that the solution would be obtained in a global time frame, the total derivative could be obtained from the eq. (5.26).

$$\frac{d\,y}{d\,x}\,(t_B) = \underbrace{\frac{\partial\,y}{\partial\,t_A}\,(t_B)}_{-\dot{y}(t_B)}\frac{d\,t_A}{d\,x} + \underbrace{\frac{\partial\,y}{\partial\,t_B}\,(t_B)}_{\dot{y}(t_B)}\frac{d\,t_B}{d\,x} + \frac{\partial\,y}{\partial\,x}\,(t_B) \tag{5.26}$$

When using the mission segmentation approach together with the direct sensitivity analysis method, the derivatives of responses are primarily obtained in the local time τ and as such the eq. (5.26) is not explicitly used. Instead of it the derivative computation from the eq. (5.27) is used.

$$\frac{d\,y}{d\,x}\,(\tau_B) = \underbrace{\frac{\partial\,y}{\partial\,\tau_B}\,(\tau_B)}_{\dot{y}(\tau_B)}\frac{d\,\tau_B}{d\,x} + \frac{\partial\,y}{\partial\,x}\,(\tau_B) \tag{5.27}$$

The gradients computed in the local time frames are consequently transformed into the global time frame to be used in further computations. The functional ψ under the integral in the eq. (5.22) can be derived using the Leibnitz integration rule.

$$\begin{aligned}\frac{d}{d\,x}\int_0^{\tau_B(x)} \psi_t\,(y,\dot{y},\tau,x)\,d\tau =& \psi_t\,(y,\dot{y},\tau_B,x)\,\frac{d\,\tau_B}{d\,x} \\ &+ \int_0^{\tau_B(x)} \left(\frac{\partial\,\psi_t}{\partial\,x} + \frac{\partial\,\psi_t}{\partial\,y}\frac{\partial\,y}{\partial\,x} + \frac{\partial\,\psi_t}{\partial\,\dot{y}}\frac{\partial\,\dot{y}}{\partial\,x}\right) d\tau\end{aligned} \tag{5.28}$$

The derivative of the terminal time $\tau_B(x)$ has to be obtained separately from the main sensitivity ODE solution. This term can be computed by deriving the terminal condition represented by the eq. (5.16) transformed into the local time frame.

$$\frac{d\,\Omega_B}{d\,x} = \frac{\partial\Omega_B}{\partial y}(\tau_B)\frac{dy}{dx}(\tau_B) + \frac{\partial\Omega_B}{\partial\tau_B}(\tau_B)\frac{d\tau_B}{dx} + \frac{\partial\Omega_B}{\partial x} = 0 \tag{5.29}$$

By substituting the eq. (5.27), which defines the total derivative of the response variable $y(\tau_B)$, into the eq. (5.29), the resulting derivative of the terminal time $y(\tau_B)$ w.r.t. the design variable x is obtained as the solution to the resulting equation. The overall segment solution procedure is visualized in the fig. 5.8. The resulting mission response

variables and their total derivatives become the initial conditions of an ODE system defining the following segment.

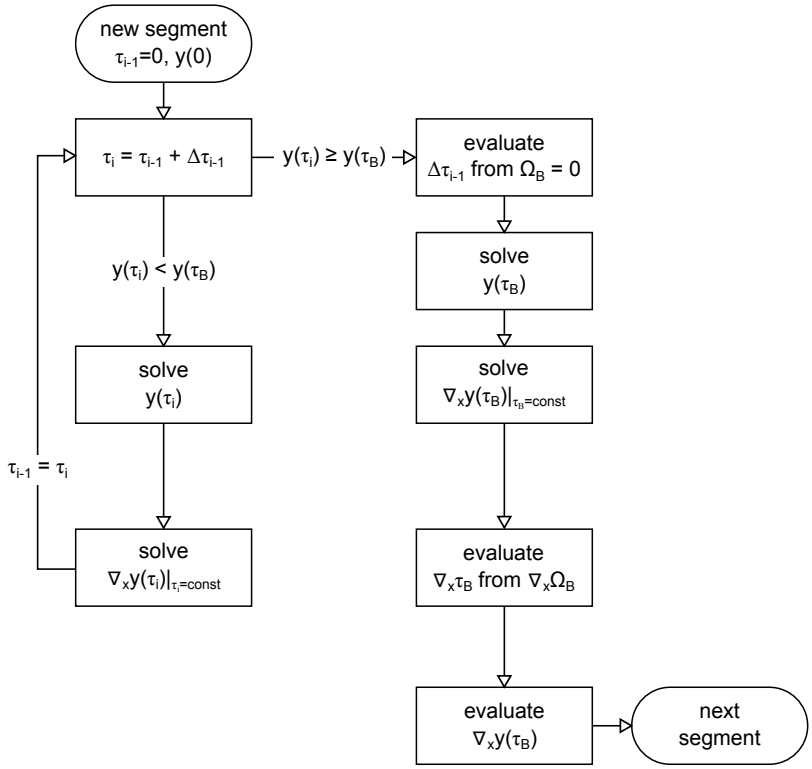

Figure 5.8: Segment solution procedure

6. Trimming Analysis

Only viable flight states, that an aircraft would in reality experience, can provide valid data for the purposes of an aeroelastic analysis and to measure an aircraft performance. This can be achieved by the addition of a trimming analysis in the aircraft model. Although the term trimming analysis is used only for steady flight states, the lack of consideration of any dynamic effects should have a negligible impact on the mission performance analysis, as it doesn't simulate any critical manoeuvres. The governing equation defining the trimmed state can be defined as an equilibrium of forces acting upon the aircraft.

$$B = B\left(y, b\right) = 0 \tag{6.1}$$

The response variables of the trimming governing equations are represented by a vector of variables b, which is a subset of a set of all flight variables $\mathcal{L}_l$. Hence, the vector b represent the unknowns that are the solution to the trimming equilibrium residual B. In the scope of the aircraft design, a basic set of available trimming variables b consists of an angle of attack and a side-slip angle. The set can be extended by various control surfaces available on aircraft like elevators, ailerons or rudders.

$$b \in \mathcal{L}_b,\ \mathcal{L}_b = \{b_\alpha,\ b_\beta,\ b_{\delta,i},\ b_T,\ \dots\} \tag{6.2}$$

In general the residual eq. (6.1) represents a vector with six DOFs, with three describing total forces at a reference point and the remaining three being a yaw, pitching and roll moment. The goal of the trimming analysis is to find such a combination of the operational conditions b that enforce equilibrium in all six DOFs.

$$\text{3 DoFs force} \quad = \underbrace{\int_\Gamma p \cdot \mathbf{n}\ d\Gamma}_{\text{surface force}} + \underbrace{\int_\Omega \rho \cdot \mathbf{g}\ d\Omega}_{\text{body force}} \tag{6.3}$$

$$\text{3 DoFs moment} \quad = \int_\Gamma p \cdot \mathbf{n} \times \mathbf{r}\ d\Gamma + \int_\Omega \rho \cdot \mathbf{g} \times \mathbf{r}\ d\Omega \tag{6.4}$$

The forces contributing to the overall residual come from various sources, such as aerodynamics, inertia or propulsion. The number of DOFs for which the residual equations $\mathcal{L}_b$ have to be defined can be reduced based on the expected flight manoeuvres. This is achieved by applying assumptions stemming from the knowledge of specific manoeuvres for which the trimming analysis should be performed. In the simplest form of the residual equations $\mathcal{L}_b$, only a two-dimensional manoeuvre can be considered, such as a level cruise, and at the same time the contribution of a thrust force to an overall lift can be neglected. This results in the trimming equation set $\mathcal{L}_b$ with only two DOFs, these being a sum of forces in the lift direction and a sum of moments around the pitching axis. For such a manoeuvre only two trimming variables b have to be defined, with a common choice being the angle of attack and the stabilizer deflection. An abstract formulation of

a more general two-dimensional manoeuvre is presented in the fig. 6.1, showing various coordinate systems in which the disciplinary forces can be defined.

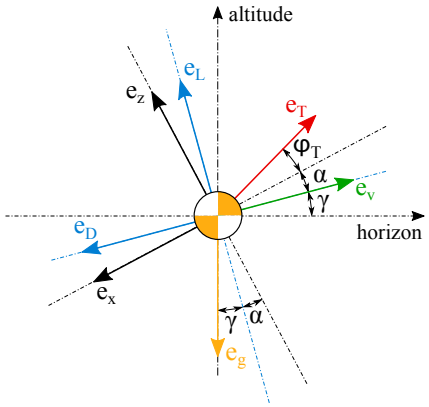

Figure 6.1: Trimming concept for a 2d manoeuvre.

In general, a solution of the trimming governing equation system 6.1 can be approached in two distinct ways. Firstly, a traditional non-linear equation methodology can be utilized, where the residual is solved together with all incorporated disciplines as an enclosed system, ensuring that the flight equilibrium is achieved at each optimization iteration of the overall MDO process. This approach is used in the mission analysis, since sequential flight conditions have to be evaluated before feeding the results of the mission analysis to an optimization algorithm. The Newton-Raphson solution algorithm can be used to solve the trimming analysis as an enclosed system, where the Jacobian of the trimming residual equations is used for the non-linear solution of the trimming analysis and for a consequential sensitivity analysis. The second methodology consists of enforcing the equilibrium equations 6.1 through optimization constraints added to the constraints model of the MDO process. This assures that the flight equilibrium is achieved at the final optimization iteration by adding a set of trimming constraints for each critical load case considered in the optimization. At the same time, the parametrization model is extended by a set of design variables x_b linked to the trimming variables b. The second approach is utilized for the solution of critical load cases to achieve a structural feasible design, since each of the considered load cases can be evaluated independently on each other. In the case, that a gradient based optimization algorithm is deployed, both of these techniques present similar requirements on the underlying aircraft simulation model, which is responsible for the evaluation of total forces, in the form of a trimming Jacobian $\nabla_b B$. The only difference is, that in the case of a closed trimming analysis loop, the gradient of the residual equations B with respect to trimming variables b is used only in the scope of the trimming analysis itself, whereas in the case of an integration of the trimming analysis into the constraints model, the Jacobian is merged into the overall gradient matrix of the optimization problem. For the trimming variables that are used in the load case analysis, the relation in the eq. (6.5) applies.

$$b \in \Omega,\ \Omega = \{b \in \mathbb{R}^n | h_j(b) = 0, j = 1, \ldots, k\} \tag{6.5}$$

A possible advantage of integrating the trimming analysis as an addition to the constraints model is the fact, that it doesn't limit the number of trimming variable b that could be used to deal with the trimming constraints. If a higher number of trimming design variables is present in the parametrization model than is the number of free DOFs specified by the equilibrium system B, the optimization algorithm can probably find the best possible combination of values for an optimized aircraft design.

6.1. Trimmed State Analysis

In general, the trimming equations system B is expressed as a force and moment equilibrium, which results in 6 DOFs for a three dimensional model.

$$B = p_{tot}\,(b, y) = \left\{ \begin{array}{l} F_{tot}\,(b, y) \\ M_{tot}\,(b, y) \end{array} \right\} = 0 \tag{6.6}$$

There are several sources of forces and moments that act upon the aircraft whose contributions to the trimming residual B can be included, with the major ones being aerodynamic, gravity, inertia and engine forces, as considered in the eq. (6.7). A functional dependency of a resulting residual is fully dependent on the underlying simulation model.

$$F_{tot}(b, y) = \sum_i F_{a_i}(b, y) + \sum_j F_{e_j}(b, y) + \sum_k F_{g_k}(b, y) + \sum_l F_{\omega_l}(b, y) \tag{6.7}$$

It is common, that each of the forces and moments coming from the various disciplines are defined in their respective coordinate systems. A properly set up trimming equation system should fulfill the equilibrium conditions in each of the coordinate systems, as expressed by the eq. (6.8) and eq. (6.9).

$$F_{tot} = {}^{s}F_{tot} = {}^{b}F_{tot} = {}^{a}F_{tot} = 0 \tag{6.8}$$

$$M_{tot} = {}^{s}M_{tot} = {}^{b}M_{tot} = {}^{a}M_{tot} = 0 \tag{6.9}$$

The residual equation system in the eq. (6.6) is in general non-linear. The Newton-Raphson method is deployed for solving the trimming problem inside of the mission analysis. Therefore, the underlying simulation model has to provide the trimming Jacobian $\nabla_b B$, which is represented in the eq. (6.10) as a first derivative of the eq. (6.6).

$$\frac{d}{d\,b}B = \frac{d}{d\,b}p_{tot}\,(b,y) = \left\{ \begin{array}{l} \frac{d}{d\,b}F_{tot}\,(b,y) \\ \frac{d}{d\,b}M_{tot}\,(b,y) \end{array} \right\} = 0 \tag{6.10}$$

The solution procedure of the chosen Newton-Raphson algorithm is defined as

$$\frac{d\,B(b_k)}{d\,b} \cdot \Delta b_{k+1} + B(b_k) = 0 \tag{6.11}$$

$$b_{k+1} = b_k + \Delta b_{k+1} \tag{6.12}$$

The figure 6.2 presents an XDSM diagram [78] describing a general trimming procedure where the element R represents an internal discipline responsible for the evaluation of total forces acting upon the aircraft. In the usual context of an aircraft optimization the system R is modeled by a coupled aerodynamic and structural analysis.

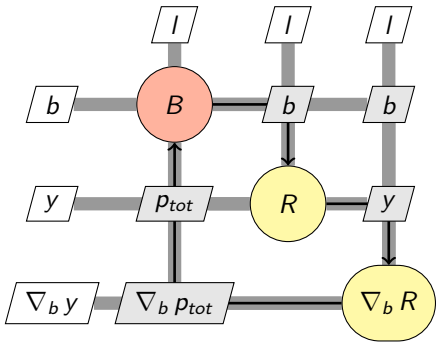

Figure 6.2: A workflow for a trimming analysis using the Newton-Raphson method

6.2. Trimmed Sensitivity Analysis

To successfully embed the trimming analysis in the gradient based MDO process it is necessary to be able to obtain derivatives of the trimming analysis with respect to the design variable x. These sensitivities have to satisfy a relationship analogous to the equation 6.10 used in the trimming state analysis, but instead of deriving w.r.t. the trimming variable b, the derivation is performed w.r.t. the design variable x.

$$\frac{d}{d\,x}B = \frac{d}{d\,x}p_{tot}\,(b,y) = \left\{ \begin{array}{l} \frac{d}{d\,x}F_{tot}\,(b,y) \\ \frac{d}{d\,x}M_{tot}\,(b,y) \end{array} \right\} = 0 \tag{6.13}$$

Firstly, if the trimming analysis is implemented in a form of an extension to the constraints model of the overarching MDO model, the trimming variable b is declared as independent to the design variable x. In such a case, the derivative eq. (6.10) and the eq. (6.13) are utilized in the same manner to obtain their respective contributions to the overall Jacobian of the constraints model, as presented by the eq. (6.14).

$$\nabla g = \begin{bmatrix} \nabla_x G & \nabla_b G \\ \nabla_x B & \nabla_b B \end{bmatrix} \tag{6.14}$$

The fig. 6.3 represents this approach in the form of an XDSM diagram, in which the element O stands for an optimizer, which is fed the gradients by two the independent sensitivity analyses $\nabla_b R$ and $\nabla_x R$. The approach using independent trimming variables is utilized for the critical load case part of the aircraft optimization model. The possible drawback of this approach is the introduction of additional design variables and constraints into the overall optimization problem, although this doesn't have to necessarily translate into a loss of computational efficiency in comparison to alternative approaches.

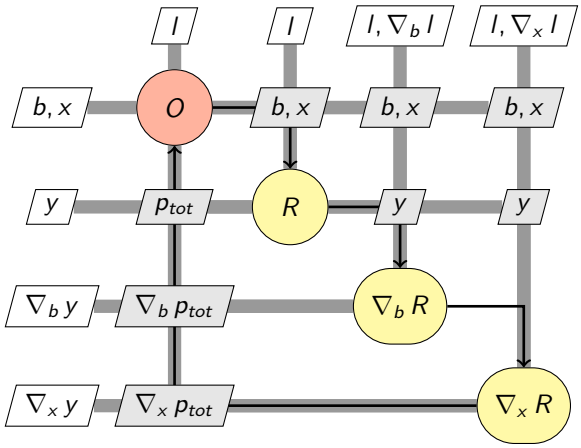

Figure 6.3: A workflow of a trimming sensitivity analysis with independent trim variables

In the scope of this thesis, the mission analysis was developed with the encapsulated trimming analysis, hence the corresponding sensitivity analysis has to be approached in a different manner, than is the case for the critical loads analysis. The need for the alternative method is based on the sequential dependency of flight states inside of the mission analysis, where the results of one trimming analysis translate to an input of the one performed in the next time step. The main difference lies in the fact that the trimming variable b is considered to be dependent on the design variable x. An XDSM diagram representing this alternative approach is shown in the fig. 6.4, which presents a flow for a problem involving the trimming analysis only, without the integrated mission analysis, for simplicity. Here, the trimming analysis is considered as an internal

part of the overall aircraft model, which then provides any required sensitivities to the optimization model. As such, an optimization algorithm is provided with the response and gradient values already representing the trimmed state.

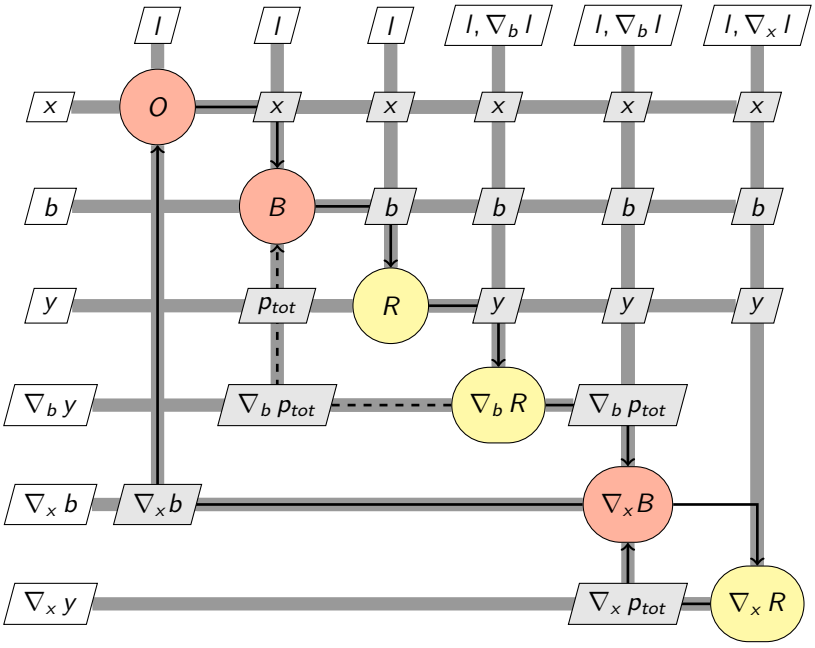

Figure 6.4: A workflow of a trimming sensitivity analysis with dependent trim variables

The Jacobian of the constraint model is defined by the equation 6.15, which expresses the trim variable b as a function of the design variable x, hence the chain rule.

$$\nabla g = \frac{\partial g}{\partial x} + \frac{\partial g}{\partial b}\frac{d b}{d x} \tag{6.15}$$

If the direct sensitivity analysis method is used to deal with the gradient computation, the required output of the trimming sensitivity analysis is the derivative of the trimming variable w.r.t. the design variable. To obtain a relationship that would allow to compute the necessary terms, the eq. (6.6) is derived by the design variable x, resulting in the eq. (6.16).

$$\frac{d B}{d x} = \frac{\partial B}{\partial x} + \frac{\partial B}{\partial b}\frac{d b}{d x} = 0 \tag{6.16}$$

Since the Newton-Raphson solver is employed in the trimming response analysis, its Jacobian from the eq. (6.10) can be reused in the eq. (6.16). As such, the only remaining unknown, before the equation 6.16 can be solved, is a partial derivative of the residual B w.r.t. the design variable x.

7. Aero-structural model

In the scope of the overall MDO configuration, an aircraft simulation model is responsible for feeding the system with results of physics based analyses like aerodynamics, structural mechanics, propulsion, thermodynamics, atmospherics and others. A range of disciplines and their possible combinations, which can be used to assemble the simulation model, is almost limitless. Not only can the included disciplines differ between various MDO models, but significant variations can be found in regard to the fidelity of those disciplines. A specific set of disciplines and their computation methods in the MDO model has to be chosen based on the intended application case, since an inclusion of disciplines that might not significantly impact optimization results can still lead to a significant rise in modelling complexity and computational demands. Generally, low-fidelity models are able to describe only a fraction of all the physical phenomena that can occur, while high-fidelity models can provide results that are very close to an actual behaviour. Ideally, only high-fidelity models would be used in all situations, as they provide the highest accuracy. Unfortunately the high-fidelity numerical models come with high computational costs which makes them close to prohibitive in some cases, especially when a large number of repeated simulations has to be performed. In such situations, the lower-fidelity models gain on appeal, mainly thanks to their much shorter simulation times, as long as they provide satisfactory approximation. Since one of the main goals of this thesis is to investigate an impact of aeroelastics on the mission performance, representations of structural mechanics and aerodynamics is to be included in the aircraft simulation model.

In this thesis, the structural responses are simulated using the Finite Element Method (FEM). FEM models are a common sight in the industry and academia, but significant differences can be seen in the concrete modeling of structural features across various applications, even though they are based on the same theory. On the side of aerodynamics, a larger diversity of simulation methods with various governing equation formulations can be seen. In both disciplines, the main trade-off between the different levels of fidelity lies in the computational speed and the accuracy. Additionally, the high-fidelity prediction models often require an expensive modeling process as well. For example, when computing aerodynamics using vortex-lattice methods, only a flat two dimensional mesh of an aircraft has to be prepared. Such a modeling process is rather cheap. On the other hand, the Navier-Stokes methods provides very accurate results, but the modeling requirements are very significant when compared to the efforts needed for the low-fidelity methods. Not only a surface mesh of a simulated object has to be modeled, but a volumetric solid mesh spanning several times the largest dimension of the aircraft model has to be generated. Due to this reasons, various fidelity levels are used in the industry parallel to each other and across design stages. For this reason, it is important to be able to switch between the different fidelities in a single design process.

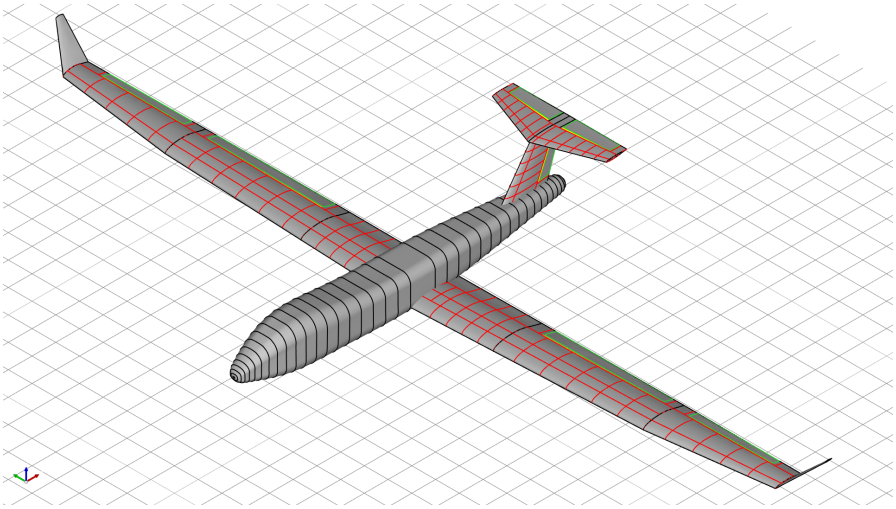

(a) Geometrical Model

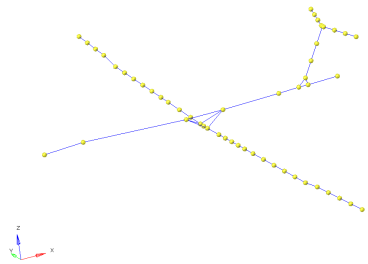

(b) Beam Model

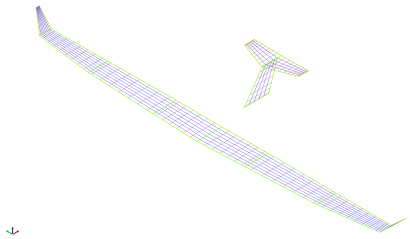

(c) AVL Model

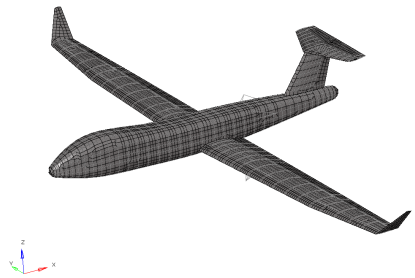

(d) Shell Model

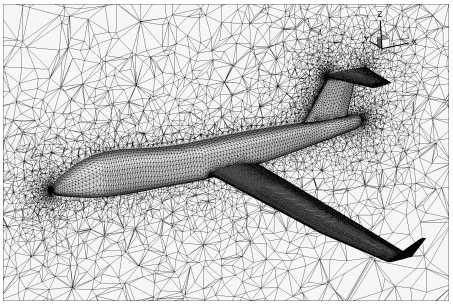

(e) Euler Model

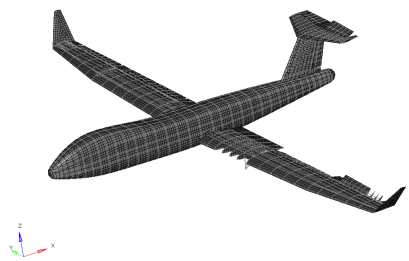

(f) Shell Model with Control Surfaces

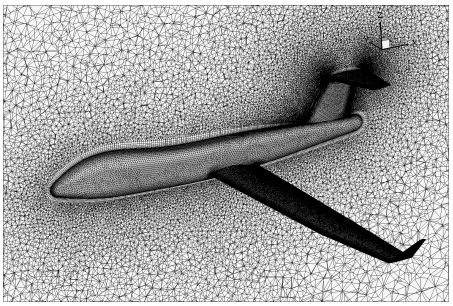

(g) RANS Model

Figure 7.1: Examples of various simulation models for the purposes of an aeroelastic analysis

7.1. Aerodynamics

The aerodynamic analysis is the main source of loads on the structure during a flight and are strongly influenced by an in-flight wing shape. In the area of a numerical simulation, a large range of solution methods is available [79, 80, 81], which can approximate the aerodynamic behaviour with various levels of accuracy and computational efficiency. In general, every fluid simulation has to satisfy conservation of mass, energy and momentum while obeying a continuity assumption in a fluid domain. These laws are collected into the so called Navier-Stokes equations [79].

$$\frac{\partial \rho}{\partial t} + \nabla \cdot (\rho \, \mathbf{v}) = 0 \tag{7.1}$$

$$\frac{\partial \rho \, \mathbf{v}}{\partial t} + \nabla \cdot \left(\rho \, \mathbf{v} \cdot \mathbf{v}^T\right) = \rho \, \mathbf{f} - \nabla p + \nabla \cdot \tau \tag{7.2}$$

$$\frac{\partial \rho \, h}{\partial t} - \frac{\partial p}{\partial t} = \Phi + \nabla \cdot (k \nabla T) \tag{7.3}$$

For practical problems, for which the Navier-Stokes equations cannot be solved analytically, a numerical analysis is commonly deployed. Still, solving an aerodynamic problem defined by the full set of Navier-Stokes equations can prove computationally prohibitive. In order to alleviate some of the computational demands, simplified fluid flow definitions have been introduced in the form of inviscid and irrotational flow, resulting in reduced modeling requirements and decreased computational time. But the said decrement of complexity in the underlying governing equations results in a decline of accuracy as well, presenting a trade-off between the computational speed and the veracity of the simulated fluid behaviour. The fig. 7.2 shows this trade-off in qualitative manner for some of the most commonly used solution approaches to the aerodynamic simulation.

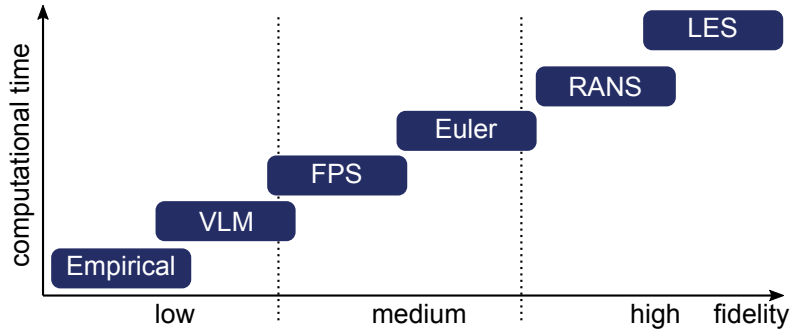

Figure 7.2: A qualitative fidelity trade-off of aerodynamic solvers

The computational cost of the truly high-fidelity physical representations can make them prohibitive for some application fields, e.g. early aircraft design stages, where a large number of evaluations needs to be performed. At such stages, it is beneficial to employ a low or a medium fidelity solver, even though a behaviour simulated by these

solvers is of a lower credibility. It is possible to address this drawback by deploying said solvers for problems, where a fluid's behaviour is expected to satisfy assumptions made by a specific solution method. For example, a low fidelity solver based on a potential flow can provide viable results for a low speed flight with negligible boundary layer and insignificant vorticity. Even some simple elementary equations can be effectively used for performance estimation in early design stages. In the scope of this thesis a fluid analysis is represented by a residual equation 7.4, which is defined independent on an actual solution method, where any of the specific system variables are substituted by a variable of fluid state variables w.

$$F = F(w) \tag{7.4}$$

Proper selection of the aerodynamic computation model is of an utmost importance when considering its deployment for the mission performance analysis, which requires an evaluation of a large number of interdependent flight states. The difficulty of this decision is tied to the importance of an adequate drag estimation, since it has a major impact on the mission analysis. Lower fidelity methods based on a potential flow assumption provide a drag estimate of only a limited viability [82], mainly due to the lack of a viscous drag component and a limited true wetted surfaces representation. An Euler based analysis provides a better induced drag approximation, but due to the lack of a viscous layer, its application for the mission analysis has to be well argued. A RANS based solver can represent an aerodynamic behaviour with a properly estimated viscous drag, but at the cost of very high computational demands. It is a common sight in the industry to utilize aerodynamic polars or surrogate functions that approximate a fully integrated high-fidelity aerodynamic analysis based on a precomputed set of sample points. Such an approach is well suited for a pure mission performance evaluation in those cases, in which the aircraft configuration is already fixed. But the deployment in an MDO setting with a target of modifying the in-flight shape, representing the aerodynamic performance using a polar has to be carefully considered, since sample points of the polar are usually computed for a specific in-flight shape. Even though the outer design form of the wing would be fixed, the in-flight shape can still change due to a shift in mass distribution from a fuel burn or due to modifications in the internal loads carrying structure. For that reason, an approach using a computation on demand of the flight behaviour is utilized in the mission analysis considered by this thesis. In this case, the accuracy of the responses and sensitivities is limited only by the accuracy of the involved solvers and their interactions. A drawback this methodology carries is that the number of simulations that will have to be performed to evaluate the mission sensitivity analysis can become a significant driver of the computation costs.

In the scope of this thesis, the aerodynamic analysis is represented by a residual equation 7.5 independently of the type of a solver used. The equation expresses the analysis as a function of the aerodynamic state variables w, which can differ depending on the formulation of the underlying method, be it vortex strengths for a VLM based method or velocities and pressures for high-fidelity representations. Additional functional dependency is linked to the trimming variables b, which mostly impact boundary conditions of

the aerodynamic problem like the angle of attack, the free stream velocity or the various control surface deflections. To allow for a consideration of the impact of a structural behaviour on the aerodynamic analysis, the structural response variables u are included as well.

$$F = F(u, w, b) \tag{7.5}$$

In their simplest form, many of aerodynamic quantities can be estimated by empirical equations, which provide main benefit during the very early aircraft design stages. Well established empirical relations that can be used to evaluate the lift and the induced drag are summarized for example by Raymer [8]. Due to their low accuracy and their limited coupling potential to the structural response, such equations are not considered in the scope of this thesis. On the other hand, high-fidelity solvers like those based on the RANS method are avoided as well, mainly due to their high computational demands. These become especially prohibitive in a setting that requires a high number of flight state evaluations like the mission analysis. For those reasons, a low-fidelity potential based solution and a database based mid-fidelity approach are considered for the use in the critical loads analysis and the mission analysis respectively.

7.1.1. Vortex-Lattice method

To provide the aerodynamic response for purposes of the constraints model intended to assure design feasibility, a low-fidelity model based on the VLM is integrated into the aircraft simulation model. This choice is based on the assumption of an deployment in the early and mid aircraft development stages. VLM based models can provide a reasonable level of accuracy when estimating the lift and the pitch moment [81], which are the main drivers of the structural deformation of the wing. The VLM belongs to a family of potential flow methods [80], all sharing the common assumption of isentropic and irrotational flow. Isentropic flow describes airflow of constant entropy, which can be assumed in flows where viscous effects are negligible. This is mostly the case outside the boundary layer. Additionally, potential flow simplifies airflow by assuming it to be irrotational, which is once again often the case outside the boundary layer or wake. Assuming the flow to be irrotational automatically presumes isentropic behaviour as well and results in a flow where the free flow velocity $\boldsymbol{v}$ that can be expressed as a gradient of potential Φ [80], characterized in the eq. (7.6).

$$\boldsymbol{v} = \nabla\Phi \tag{7.6}$$

When applied to the differential form of the conservation of mass, assuming steady and incompressible flow, the governing equation of potential flow can be formulated as the so called Laplace's equation.

$$\nabla^2\Phi = 0 \tag{7.7}$$

Additionally to the Laplace's eq. (7.7), a specification of boundary conditions is re-

quired to define a unique potential state. This is for the VLM the impermeability condition 7.8, defined in a direction of a surface normal $\mathbf{n}$ over a wetted surface.

$$\nabla\Phi \cdot \mathbf{n} = 0, \tag{7.8}$$

By this definition, the VLM belongs to a family of Boundary Element Method (BEM) [83]. In general, a solution can be obtained by using source and doublet elements, σ and μ respectively. By combining both their influence, the total potential at a specific location P can be expressed by the eq. (7.9), where S is the wetted surface at which the doublets and sources would be defined. The influence of the source σ and the doublet μ elements is proportional to the distance r to the point P.

$$\Phi(\mathbf{P}) = -\frac{1}{4\pi}\int_S \left[\sigma\left(\frac{1}{r}\right) - \mu\frac{\partial}{\partial n}\left(\frac{1}{r}\right)\right] dS\mu \tag{7.9}$$

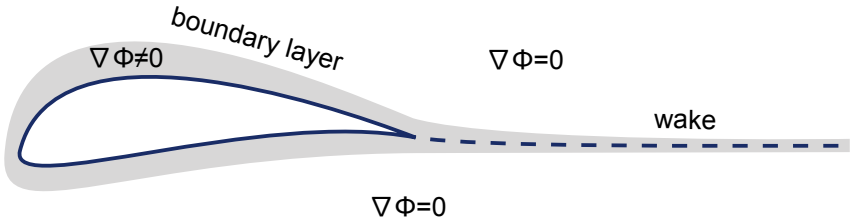

Figure 7.3: A qualitative visualization of a domain with an applicable potential flow assumption.

For simple geometries, it is possible to obtain analytical solution to the Laplace's eq. (7.7). For an actual realistic application cases this becomes infeasible. Hence, a number of numerical methods have been developed in the past to solve the potential flow formulation. The most common are the Lifting Line Theory [84], Vortex Lattice Method [85] and the 3D Panel Method [80]. In the scope of this thesis the response variables of the aerodynamic system are represented by the symbol w. These together with the matrix of aerodynamic influence coefficients $\mathbf{A}$, the surface normals N and the free flow velocity v_∞ define the potential flow governing equation 7.10.

$$F = \mathbf{A} \cdot w + N\,(u, b) \cdot v_\infty = 0. \tag{7.10}$$

The VLM method can provide valid results only for geometries that are close to that of a thin, lifting and finite wings moving at a constant speed through an undisturbed, inviscid, incompressible and irrotational flow under a small angle of attack. These assumptions usually limit the utilization of the VLM to low speed subsonic flows.

Numerical solvers that are based on the VLM discretize a wetted surface into many singularity elements, also called panels [80]. These singularity elements provide an ele-

mentary solution to the Laplace's equation 7.7. One of these elements is the so-called 'horseshoe vortex element', which automatically satisfies the dissipation condition 7.11.

$$\lim_{r\to\infty} \nabla\Phi = 0, \tag{7.11}$$

The "horseshoe" element consists of a bound vortex and two trailing vortices which are shed into a wake, as visualized in the fig. 7.4. The element's contribution to the velocity field can be computed by summing up the vortex segment specific contributions given by the eq. (7.12).

$$\Delta\mathbf{v} = \frac{\Gamma}{4\pi}\frac{d\mathbf{l}\times\mathbf{r}}{r^3} \tag{7.12}$$

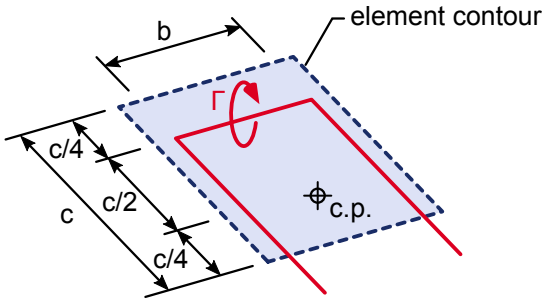

Figure 7.4: Vortex development on and behind a wing with wake.

The linearity of the Laplace's eq. (7.7) and the principle of superposition allows to discretize the surface into a set of elements, where each of the elements provides an elementary solution to the Laplace's equation. Enforcing the impermeability condition 7.8 at these elements results in the eq. (7.13) where j means the j-th point at which the boundary condition has to be satisfied and the sum over i is the sum over all elements contributing to the disturbed flow.

$$\sum_i a_{ij}\Gamma_i = -\mathbf{v}_\infty \cdot \mathbf{n}_j \tag{7.13}$$

For the purpose of simplification, the equation 7.13 is expressed in a vector form in the eq. (7.14) and will be used from this point on as the governing equation of a VLM based aerodynamic solver.

$$\mathbf{A}\,\boldsymbol{\Gamma} = \mathbf{d} \tag{7.14}$$

After solving the governing eq. (7.14) of the VLM system for a given set of boundary conditions and obtaining a corresponding vortex strength distribution $\boldsymbol{\Gamma}$, it is possible to obtain aerodynamic forces by the use of a Kutta-Joukowski theorem [80], expressed

in the eq. (7.15).

$$F = \rho \Gamma \mathbf{v}_\infty \times \mathbf{h} \tag{7.15}$$

Alternatively it is possible and even beneficial to avoid an explicit solution to the equation 7.14 and express a surface pressure as a direct function of the boundary conditions [86, 87]. This approach is based on solving the governing equation for a normalized free stream velocity and assembling a pressure coefficient matrix $\mathbf{A}_{c_p}$ which can be used to directly obtain panel pressure distribution using the eq. (7.16). The main advantage of this formulation is that the pressure coefficient matrix depends only on the geometry and the Mach number related to the free stream, allowing for a fast evaluation of the surface forces, which provides a significant reduction of computational efforts when dealing with the aeroelastic analysis.

$$\Delta \mathbf{c_p} = \mathbf{A}_{c_p} \mathbf{d} \tag{7.16}$$

7.1.2. Database approach

Having to solve a large number of aeroelastic problems, as is the case when a mission analysis is involved, still presents a computationally demanding prospect. The fact that the mission analysis requires a higher quality aerodynamic data which can be used to accurately model drag across large set of flight states only exasperate the requirements. A common approach to alleviate some of the calculation demands is to prepare a set of aerodynamic polars beforehand, which consist of a set of sample flight states, for which the aerodynamic analysis is performed. Consequently, aerodynamic coefficients required by the mission can be obtained by interpolating between the sample points. This approach allows for an effective evaluation of a mission performance [88, 77], but provides a limited viability when dealing with an optimization tasks, since such a database is commonly built for an already fixed aircraft configuration. To be able to still deal with a large number of flight states, for which the aerodynamic response is required, while allowing for a design optimization to be viable, a concept of surrogate surfaces was utilized by some [40, 76, 63] for the purposes of a mission performance optimization.

The approach adopted in this thesis was chosen based on the requirements of an airframe sizing design while integrating the mission performance optimization. This requires a medium to a high fidelity aerodynamic data together with the need to evaluate a large number of consequent interdependent flight states. By concentrating only on an airframe sizing, together with the intention of storing only aerodynamic data excluding any influence of structural stiffness, it is possible to avoid the need to regenerate the aerodynamic database after each design update stemming from an optimization step. This is achieved by performing the aerodynamic analysis using a CFD solver of choice, in the scope of this thesis it was the SU2 solver [89], at a predetermined set of sample points defined. Since in the scope of this thesis the database should be deployed in the mission performance analysis, only quasi-steady flight manoeuvres are assumed and as such the parametrization is performed with the angle of attack, Mach number and a

stabilizer deflection. An example of a distribution of the sample points is presented in the fig. 7.5, showing a non-uniform spread. It has to be expected, that a full factorial parametrization will not be achieved, as it is possible that for some extreme operational conditions the CFD solver of choice might not be able to converge. At the same time it may be of interest to refine the spread around operational conditions, in which the aircraft spends most time, likely increasing the accuracy in those areas.

When aerodynamic forces are requested during the mission analysis for a specific flight state, they will be evaluated by an interpolating between operational conditions. This introduces a potential source of inaccuracy which is brought by a chosen interpolation method and an overall precision is limited by a density of the precomputed data points. On the other hand, it allows for a much faster evaluation of the mission analysis, which is a critical argument when having to perform a large number of aeroelastic simulations.

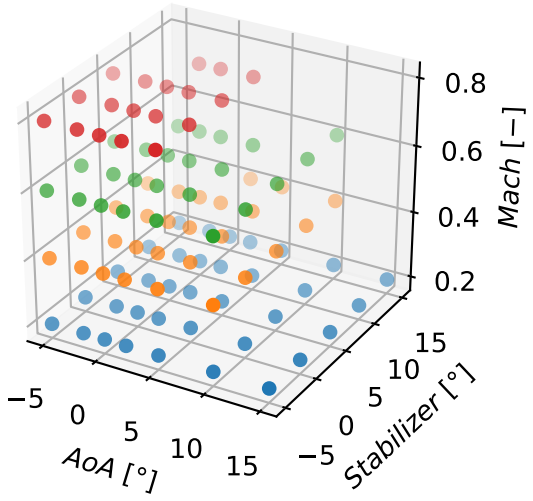

Figure 7.5: Example of parameter space discretization

To reduce the amount of data that has to be stored and evaluated during the optimization task, the original surface pressure distribution, like that shown in fig. 7.6, is reduced to forces and moments at integration points spread throughout the investigated geometry, as exemplified in the figure 7.7. The actual integration point distribution and corresponding zoning is dependent on the type of aircraft configuration, the internal loads carrying structure and the intended application. A careful consideration has to be taken when deciding the number of points that should be used to build up the database, since this presents a trade-off between computational speed and method accuracy.

The zones and their corresponding integration points can be defined with regard to specific aircraft parts for an increased accuracy, as conceptualized in figure 7.8. Though in those cases, where the underlying FEM model doesn't include control surfaces, or is not a target the optimization task, this increase in database complexity might prove detrimental to computational performance without a significant impact on the final

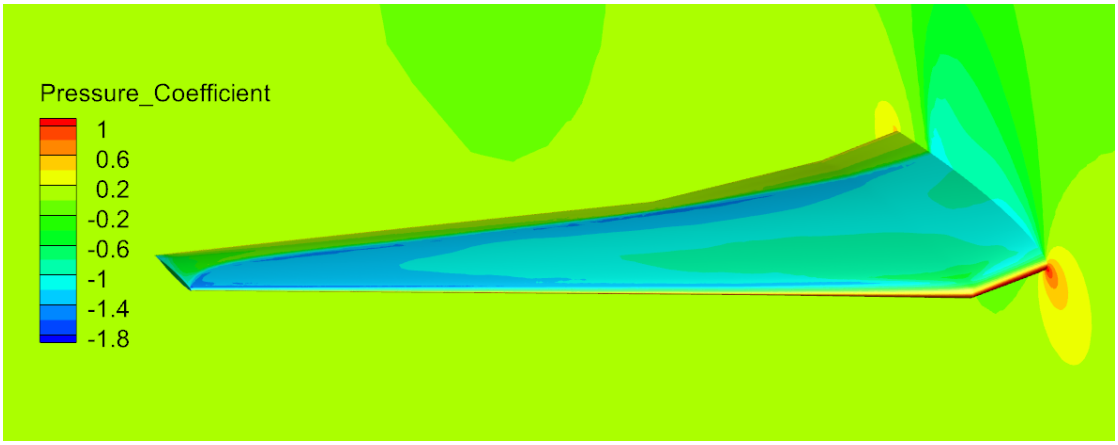

Figure 7.6: Example of surface pressure distribution

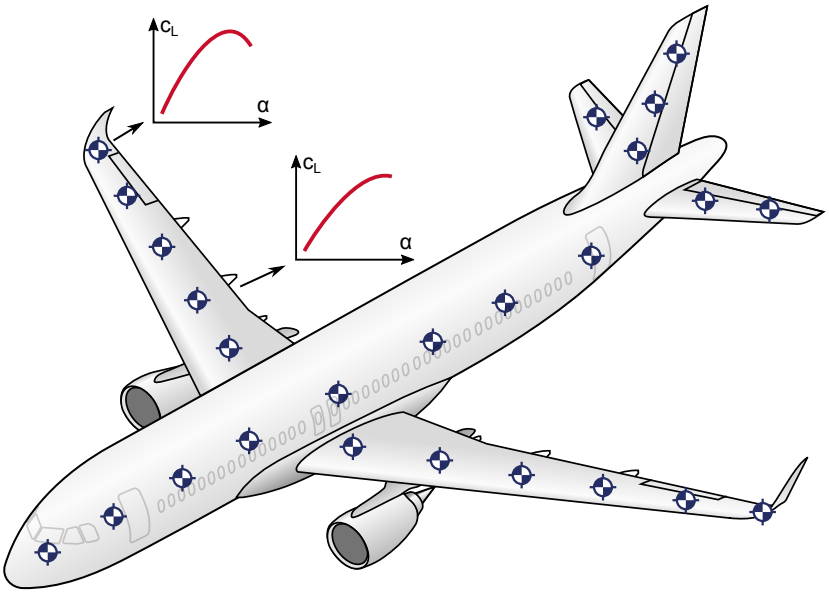

Figure 7.7: Example of integration points distribution

design.

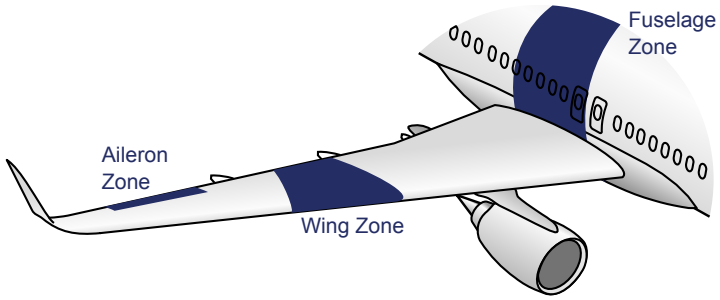

Figure 7.8: Zoning concept for an aerodynamic database

To generate the forces and moments, the surface mesh is cut according to a chosen zoning, example of which is shown in the figure 7.9, and is integrated over to obtain forces and moments at the assigned integration point using the eq. (7.17) and eq. (7.18).

$$F = \int_S p \cdot \mathbf{n}\, dS \tag{7.17}$$

$$M = \int_S p \cdot (\mathbf{r} \times \mathbf{n})\ dS \tag{7.18}$$

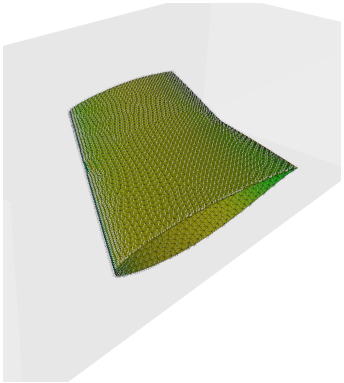

Figure 7.9: Example of a cut through a wing surface

The integration points are connected to the surrounding loads carrying structure by suitable loads distributing elements, as conceptualized in the fig. 7.10. Only those points of the underlying structure should be connected that can be deemed to be structurally strong enough to distribute the loads while not suffering from local deformations due to excessive concentrated loads.

For the purposes of loads evaluation, the governing equation of the database approach can be formulated as the eq. (7.19), where the selection matrix $\mathbf{Q}$ serves for linking of the trimming variables $\mathbf{b}$ and the flight path variables $\mathbf{l}$ to the database parameters $\mathbf{w}$.

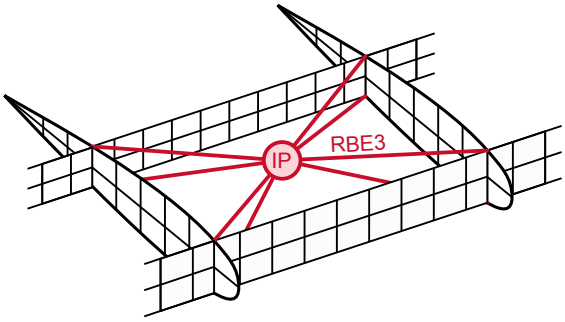

Figure 7.10: Connection concept between integration points and FEM model

$$F = \mathbf{w} - \underbrace{\mathbf{Q} \cdot \begin{Bmatrix} \mathbf{b} \\ \mathbf{l} \end{Bmatrix}}_{\mathbf{w_{rg}}} - \mathbf{w_{el}}\left(\mathbf{u}\right) = 0 \tag{7.19}$$

When evaluating the aerodynamic loads from the precomputed database, the loads are directly interpolated from the database using the operational conditions consisting of the results of the trimming analysis b and flight path parameters l. To keep the later evaluation and processing consistent with the computation on demand approach of the aerodynamic analysis, the form of the governing equation 7.4 will be kept the same with the use of equation 7.19 to describe the aerodynamic analysis using the precomputed database. Since one of the goals of this thesis is to investigate the importance of elasticity in the aircraft performance optimization with an integrated mission analysis, the influence of structural deformations $\mathbf{u}$ is included in the last term of the eq. (7.19). As such the eq. (7.19) expresses that the database parameters used to represent the aerodynamic state variables $\mathbf{w}$ can be split into a part describing the aerodynamic response of an undeformed structure $\mathbf{w_{rg}}$ and a part purely describing the influence of the deformation $\mathbf{w_{el}}$. The impact of deformations $\mathbf{w_{el}}$ on the evaluation of aerodynamic forces follows the method introduced by Barriety [90] which uses a coupled VLM model to obtain a local effective angle of attack and side-slip angle based on the structural deformations and uses the new angle of attack value to obtain the corresponding force and moment values.

After the aerodynamic state variables are known, the forces and the moments can be obtained by interpolation at each of the stored integration points. Since the data saved in the database is present only for a discrete and limited set of of flight conditions, it is necessary to include an interpolation model to obtain values for flight states in between. The dimensionality of the dataset is mainly dependent on the targeted application, in which the aerodynamic database should be deployed. In many industrial situations, a common approach is to reduce the dimensionality of the dataset by storing aerodynamic coefficients instead of the explicit forces and moments, and that only

for already trimmed flight states. If during a sample points evaluation the trimming analysis is already included, it is possible to remove several dimensions related to the control surfaces, leaving only the angle of attack and the Mach number as the only two dimensions. Storing the dimensionless aerodynamic coefficients together with the reference area and the the Mach number used for the normalization can be used to evaluate flight states at various altitudes without having the altitude as a database parameter, which is especially helpful when performing the mission analysis. Unfortunately, some of these database dimensionality reductions cannot be as easily utilized when considering the structural deformation and its influence on flight behaviour for the purposes of the structural optimization process. This limitation comes from the dependency of the aerodynamic loads on the in-flight shape which is the result of the aerostructural analysis being dependent on a structural stiffness, which is in turn a function of sizing design variables. Since the stiffness changes between each optimization iteration step, the aerodynamic coefficients stored in the database become inaccurate, since these were computed for a specific in flight shape. A possible way to deal with this problem can be to regenerate the database after each design update or to include the design variables as an additional set of dimensions in the database parametrization set, though both of these approaches would lead to a significant loss in computational performance. Additionally, in the case of the mission analysis, the fuel mass and its distribution changes during the flight and has as such an impact on the in-flight shape as well.

Hence in a general case, an n-dimensional parametrization of the aerodynamic database is to be expected, and as such an appropriate interpolation algorithm has to be employed. For the purposes of the methodology presented in this thesis, interpolation models were built using the Radial Basis Functions (RBF) [91].

$$c_F(w) = \sum_{i=1}^{N} \kappa_i \, \phi(|w - w_i|) \tag{7.20}$$

The weight coefficients κ are evaluated during the the creation of the interpolation model from the N sample points stored in the database for a given choice of a kernel function ϕ. After such an approximation function is prepared, the coefficients can be obtained for any flight conditions w using the general formulation from the eq. (7.20). Consequently the aerodynamic forces obtained through the interpolation model are defined on integration points, as conceptualized in the figure 7.7, and are mapped to the structural model. To avoid limiting future development, a mapping method from the database points to the FEM points is assumed to be a part of the evaluation process. This allows for a possibility of varying the distribution of points between the database's integration points and the structural model points, though in the application investigated in the scope of this thesis, only the Nearest-Neighbor Interpolation (NNI) method was used, since coincidence between the integration points and their FEM representation is assured. As such a general formulation for obtaining the database force or moment at the corresponding node of the FEM model is formulated in the eq. (7.21).

$$p_a(w) = \begin{Bmatrix} F_a(w) \\ M_a(w) \end{Bmatrix} = f_{F2S}(c_F(w)) \tag{7.21}$$

7.2. Structural analysis

In the utilized framework, the structural analysis is represented by the well established FEM approach [92, 93, 94, 95], for which a general governing equation is defined in the eq. (7.22). Since the intended application is to evaluate the trimmed aero-structural analysis, a dependency of the structural residual on the structural variables u as well as on the aerodynamic and trimming variables, w and b respectively, has to be considered.

$$S = S(u, w, b) \tag{7.22}$$

In the current scope of this thesis, only a linear structural analysis is considered, resulting in the expanded governing eq. (7.23). The equation summarizes the most important sources of loads on the structure together and their dependencies.

$$S = K \cdot u - p_a(w) - p_g(b) - p_i(b) - p_T(b) = 0 \tag{7.23}$$

The structural stiffness is represented by the global stiffness matrix K, which assembles the elasticity contributions of all elements from the FEM model. In the scope of the considered aero-elastic analysis, a higher fidelity structural model should be utilized, which combines one and two dimensional elements like rods, beams and shells. Additionally, rigid type elements are be utilized in the aircraft structural model to model some connections, which can either be assumed to be structurally non-deformable or are used just to carry loads from one part of the structure to another. Such a simplification can be exploited in those parts of the model, which is not of interest or a subject to stress or strain evaluation, under the assumption that such rigid element don't change the overall stiffness characteristics. Lastly, a concentrated mass elements are be added to the structure to represent features like engines, pylons, fuel tanks and others in those cases, where their stiffness contribution to the global response can be assumed to be negligible. These elements don't contribute to the global stiffness matrix K, but instead are used to assemble inertia loads p_g.

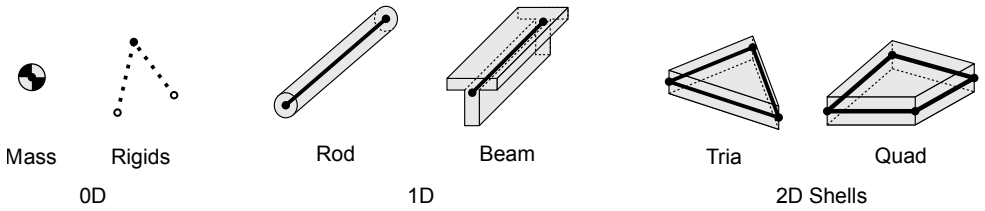

Figure 7.11: Commonly used element types in an aerostructural FEM model

For the purposes of the coupled aeroelastic analysis, it is important to determine and expand upon the interdisciplinary dependencies of the structural analysis. The major source of loads comes from the aerodynamic forces and moments $p_a(w)$, whose computation is dependent on the solution of the aerodynamic solver and the mapping between the aerodynamic and structural domains. The loads term $p_g(b)$ in the eq. (7.23) describes the forces due to gravitational acceleration, whose inclusion is necessary not only to accurately estimate the final in-flight shape for the specific set of flight conditions b, but is required if the results of the structural analysis should be used in the mission simulation as well. In general, the forces due to gravity are dependent on a current mass configuration of the aircraft and the aircraft's body orientation w.r.t. the gravity vector, making the forces due to a uniform gravitational acceleration a function of the flight conditions as well, as shown in the eq. (7.24).

$$p_g(b) = (m_s + m_p + m_f)\ {}^{s0}T(b)\ {}^{0}g \tag{7.24}$$

Additional set of inertia forces is considered in the term $p_i(b)$, which is be used to include inertia forces coming for example from an acceleration during a flight. In the case of the structural analysis for the purposes of the mission simulation, only symmetrical quasi-steady flight states are considered, for which the forces from a rotational velocity can be considered negligible. As such, only the uniform acceleration is currently included in the total force evaluation. The acceleration vector a is defined in the flight path coordinate system and it, or the resulting forces, has to be transformed into structural coordinates first. Detailed explanation of the various coordinate systems can be found in the appendix A. Also, for some specific trimming tasks, the acceleration itself can be defined as a trimming variable, resulting in the eq. (7.25).

$$p_i(b) = (m_s + m_p + m_f)\ {}^{sa}T(b)\ {}^{a}a(b) \tag{7.25}$$

The thrust forces $p_T(b)$ have to be considered especially when applying the structural model in the mission analysis. The orientation of these forces can be defined directly in the structural coordinate system, since for fixed engines the direction moves consistently with this coordinate system. The magnitude of these forces can be a function of trimming variables, depending on a type of the mission segment definition that is being trimmed for, or it can be given as a constant. This thesis considers the engine forces from the eq. (7.26) to be a function of a thrust lever setting τ, which can be a part of the trimming variables b in some cases.

$$p_T(b) = f(\tau) \tag{7.26}$$

Finally, the concept of defueling should be discussed when defining the aircraft simulation model for the use in an aero-elastic mission simulation. A defueling function describes the order and way in which the various fuel tanks on an aircraft are emptied during a flight. As such, it can have an impact on the mass distribution and hence the in-flight shape of wings. In the scope of this thesis, a uniform defueling schedule is assumed, resulting in the eq. (7.27), describing the fuel state at a point i for a fuel tank

j as a linear function of its initial fuel state.

$$m_{fj}(t_i) = \frac{\sum_{j=1}^{N} m_{fj}(t_i)}{\sum_{j=1}^{N} m_{fj}(t_0)} m_{fj}(t_0) \tag{7.27}$$

7.3. Aero-structural loop

The aerodynamic and the structural analysis have to be coupled together to be able to simulate the actual in-flight aircraft shape together with a corresponding flight behaviour. The aero-structural model, which represents the innermost analysis model in the scope of the overall mission simulation, is represented by two governing equation systems, representing the structural and the aerodynamic solution respectively. The dependency on the trimming variables b has been omitted in the eq. (7.28) and eq. (7.29), since these represent a pure input from the perspective of the inner aero-structural analysis loop.

$$\text{Aerodynamics} \quad F = F(u, w) = 0 \tag{7.28}$$

$$\text{Structural Mechanics} \quad S = S(u, w) = 0 \tag{7.29}$$

Such a task represents a multidisciplinary problem in itself, even before tying it to the overarching trimming and mission analysis. It is uncommon that this kind of system could be solved using only analytical means and is therefore handled in a numerical manner. The solution procedures can be split into two main families, these being the monolithic and the partitioned approaches [96, 97, 98]. The monolithic approach requires access to the governing equations and relations of all the subsystems. This is the main advantage and disadvantage of the monolithic approach as it allows for a more efficient evaluation algorithms to be employed and at the same time supports an easier access to relevant variables and parameters that have to be exchanged across the various systems. On the other hand, this requires that it is feasible to access the internal equations of each of the subsystems, making this of only a limited usability when using black box style subsystems that do not provide suitable access to its internal governing equations or state variables.

Alternatively, the partitioned approach evaluates all the subsystems sequentially, where each of these systems provides output for the following analysis in a predefined order. There is some freedom in how to build such a partitioned solution system, as the order in which the subprocesses have to be solved is not explicitly prescribed. Due to the fact, that the whole system has to converge to a single solution, each of the subsystems will be solved more than once, hence it represents an iterative solution process.

The solution procedure employed in the proposed framework is based on the partitioned approach. This decision was made with respect to the already existing computational tools and their capability, that were to be employed for the purposes of the aero-structural analysis. In the actual implementation, two distinct coupled aero-structural simulation models are utilized. One of them for the purposes of the stress and strain evaluation incorporated in the structural feasibility assessment for the criteria model of

the overarching optimization problem. The second one is involved in the mission simulation. Each of these models is using an identical structural model, but employs a different source of aerodynamic loads and their mapping methodology. Still, both of these models share the same partitioned staggered coupling algorithm to solve the aero-structural problem. The application of the solution algorithm in the case of a deployment in the mission analysis setting is visualized in the figure 7.12, in which case it is additionally coupled to a trimming solver B. Further on, the results are passed on to the engine model E to compute the fuel burn rate and to the encompassing mission analysis P.

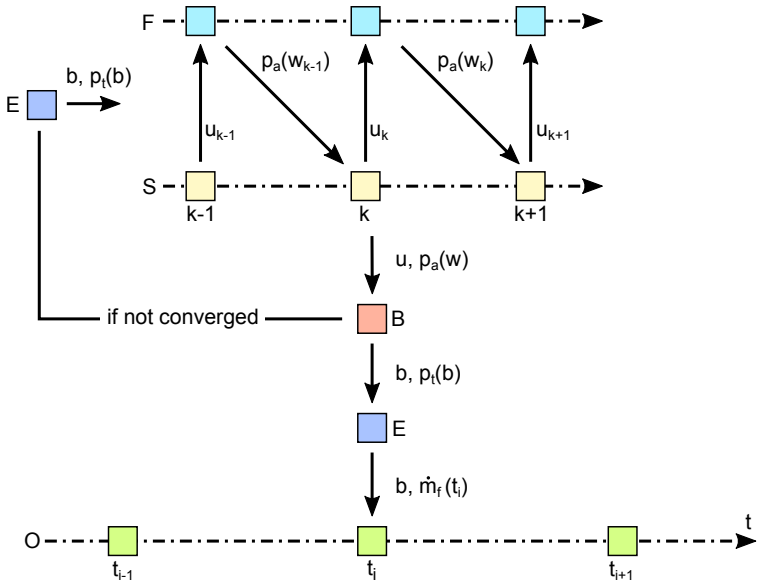

Figure 7.12: A partitioned approach for an aero-structural analysis in a mission simulation

Since the FS system constitutes a coupled multidisciplinary problem, an appropriate solution approach has to be deployed. In the scope of the developed framework, a fixed point iteration approach [99, 100] has been utilized, as visualized in the figure 7.12. This means a consequent evaluation of the aerodynamic forces based on the aerodynamic system F given a fixed in-flight shape based on the displacements obtained from the structural system S.

Algorithm 3 An example of a fixed point iteration algorithm

```
1: i ← 0
2: u_i ← 0                                          ▷ Set initial values
3: while conv == False do                           ▷ Solution loop
4:     i ← i + 1
5:     w_i ← F(u_{i−1})
6:     u_i ← S(p_a(w_i))
7:     conv ← CHECK_CONVERGENCE(u_i, u_{i−1})
8: end while
9: return u_i, w_i                                  ▷ Return converged state variables
```

7.4. Integration into a trimming analysis

An aero-structural model which is to be deployed together with the trimming analysis has to be able to express its dependency on the trimming state variables b, which have a direct influence on the aerodynamic simulation. It is possible for a trimming variable to have an explicit influence only on the structural analysis, this being the case for example for the flight-path angle, and hence only indirectly influence the aerodynamic simulation through the deformations of the structure. In most cases, the trimming variable b has an explicit influence on both, the aerodynamic and the structural analysis. Since engines are not modeled on the side of the aerodynamic model in the scope of this thesis, and hence change of the airflow around the engines is neglected, the direct impact of the thrust setting τ is considered only on the side of the structural analysis. In general, the aero-structural equilibrium equations 7.28 and 7.29 can be expanded as shown in the eq. (7.31).

$$F = F\left(u\left(b\right), w\left(b\right), b\right) = 0 \tag{7.30}$$

$$S = S\left(u\left(b\right), w\left(b\right), b\right) = 0 \tag{7.31}$$

The trimming analysis introduced in the section 6 requires a Jacobian of the trimming governing equations B w.r.t. all relevant trimming variables b, as shown in the eq. (6.10). Analogously to the response analysis itself, the required sensitivities can be obtained from the coupled equations 7.32 and 7.33. This leads to the need for the structural and aerodynamic solver to support the evaluation of partial and total derivatives of their governing equations, shown in the eq. (7.33), depending on a chosen sensitivity analysis approach.

$$\frac{d}{d\,b}F = \frac{d}{d\,b}F\left(u\left(b\right), w\left(b\right), b\right) = 0 \tag{7.32}$$

$$\frac{d}{d\,b}S = \frac{d}{d\,b}S\left(u\left(b\right), w\left(b\right), b\right) = 0 \tag{7.33}$$

In the scope of this thesis, for the purposes the evaluation of trimming sensitivities, the direct sensitivity analysis is deployed. The trimming analysis was built up in such a manner that the number of equations defining the governing set B is always the same as the number of trimming variables b, hence the computational demands of the direct and of the adjoint method are be comparable. Based on the definition of the trimmed equilibrium defined by the eq. (6.6), the dependency can be extended as shown in the eq. (7.34).

$$B = B\left(b, w(b), u(b)\right) = 0 \tag{7.34}$$

It is not a necessary requirement for the aero-structural solver to expose its state variables to a trimming algorithm directly, but it has to provide all the necessary values to evaluate the trimming residuum b. In the context of an aircraft in the quasi-steady equilibrium state, this means to sum up all relevant forces, as conceptualized by the eq. (6.7). As such it is up to the aero-structural solver how to evaluate the coupled FS system, as long as it provides all the required force components. Together with the residual value itself, an essential output of the aero-structural analysis for the proposed trimming solution approach is the Jacobian, which describes the system's sensitivities w.r.t. trimming variables.

$$\mathbf{J}_B = \begin{bmatrix} \frac{\partial B_1}{\partial b_1} & \cdots & \frac{\partial B_1}{\partial b_n} \\ \vdots & \ddots & \vdots \\ \frac{\partial B_n}{\partial b_1} & \cdots & \frac{\partial B_n}{\partial b_n} \end{bmatrix} \tag{7.35}$$

The Jacobian shown in the eq. (7.35) used to solve the non-linear trimming problem via a Newton-Raphson algorithm represented in the eq. (6.11). It can be also used as a part of the overall Jacobian w.r.t. the design variables x of the constraints model in the overall optimization problem, which is expanded upon in the eq. (6.14). The trimming residual defined in the eq. (7.34) is the sum of the forces and moments acting on the FEM model, including mapped aerodynamic forces. These forces and moments are summed up from the underlying structural model by looping over all nodes of the FEM model and summing up their contributions, resulting in a vector with residuals in DOFs. Such a vector can be directly obtained from the structural solver as long as all the forces that are acting on the aircraft are properly represented in the FEM model, as expressed by the eq. (7.23).

$$B = p_{tot}\left(p_a\left(w, u, b\right), p_g\left(b\right), p_i\left(b\right), p_T\left(b\right)\right) = 0 \tag{7.36}$$

The actual trimming residual from the eq. (7.36) is obtained from a converged aero-structural analysis defined by the eq. (7.30) and eq. (7.31), for fixed trimming variable values b. Consequently, the Jacobian 7.35 w.r.t. the trimming variables b has to be evaluated using a sensitivity analysis of the aero-structural system. This is achieved by applying a chain rule to the eq. (7.36) resulting in the eq. (7.37). Since the total force

p_{tot} is obtained by summing up all forces applied on the structural model, its derivatives becomes is obtained analogously by summing up the derivatives of those forces, if the direct sensitivity analysis approach is taken.

$$\frac{d\,B}{d\,b} = \frac{\partial\,p_{tot}}{\partial\,p_a}\frac{d\,p_a}{d\,b} + \frac{\partial\,p_{tot}}{\partial\,p_g}\frac{d\,p_g}{d\,b} + \frac{\partial\,p_{tot}}{\partial\,p_i}\frac{d\,p_i}{d\,b} + \frac{\partial\,p_{tot}}{\partial\,p_T}\frac{d\,p_T}{d\,b} = 0 \tag{7.37}$$

The total derivatives in the eq. (7.37) represent the sensitivities of the forces applied on the structural model coming from various sources. The difficulty with which they can be obtained fully depends on the model, which is used for their computation. For example the thrust forces $p_T(b)$ come from the engine model. In this thesis no thrust vectoring is allowed and as such the engine forces can be expressed as a scaled unit vector, giving the direction of the thrust in the structural coordinate system. The magnitude of the thrust depends explicitly on variables like atmospheric conditions or thrust setting. At the same time it can be implicitly dependent on the response of the aero-structural system through the trimming analysis.

$$\frac{d\,p_T}{d\,b} = v_T \cdot \frac{d\,T(b)}{d\,b} \tag{7.38}$$

The total derivative of the thrust magnitude w.r.t. to the trimming variable b in the eq. (7.38) becomes unity, if the thrust magnitude is directly declared to be a trimming variable itself. Alternatively, if the thrust setting should be the trimming variable, the derivative has to be provided by the underlying engine model. Another source of forces is the gravitational acceleration. In the case, where trimming using a trim tank is not considered, only the direction of the gravitational vector is dependent on the trimming variables, resulting in the sensitivity equation 7.39.

$$\frac{d\,p_g}{d\,b} = \frac{d\,{}^{s0}T(b)}{d\,b}\;{}^{0}g\sum_i m_i \tag{7.39}$$

Only the transformation matrix ${}^{s0}T$ from the aircraft carried ground system to the structural frame system is dependent on the trimming variables like the angle of attack. The other inertia forces acting upon the aircraft considered in this thesis are related to the uniform acceleration parallel to the flight direction. At the same time the magnitude of the acceleration can be declared to be a trimming variable as well. Hence, the sensitivity of these forces can be expressed in the eq. (7.40).

$$\frac{d\,p_i}{d\,b} = \left(\frac{d\,{}^{sa}T(b)}{d\,b}\,a(b) + {}^{sa}T(b)\frac{d\,a(b)}{d\,b}\right)\sum_i m_i \tag{7.40}$$

Finally, the aerodynamic forces coming from the aerodynamic analysis represent the major part of the trimming sensitivity evaluation. These forces are a part of the aero-elastic solution loop, as expanded upon in the section 7.3, Since the trimming responses are evaluated based on the forces acting upon the structural model, the derivatives are already a part of the sensitivity solution routine defined by the eq. (7.33) and eq. (7.32).

Depending on the approach, which is used to express the aerodynamic forces, the sensitivities of the aerodynamic forces based on the VLM can be obtained from the eq. (7.15), resulting in the eq. (7.41).

$$\frac{d\,p_a}{d\,b} = \rho\,\frac{d\,w(b)}{d\,b}\,\mathbf{v}_\infty(b) \times \mathbf{h} + \rho\,w(b)\,\frac{d\,\mathbf{v}_\infty(b)}{d\,b} \times \mathbf{h} \tag{7.41}$$

If a linearization of the aerodynamic model is applied, the eq. (7.16) can be used to avoid a direct evaluation of the derivatives of the aerodynamic variables w, analogously to the response analysis using the same approach. This reduces the coupled sensitivity analysis to a structural analysis with a non-linear RHS, where the contribution to the sensitivities coming from the aerodynamic loads is expressed using the eq. (7.42).

$$\frac{d\,p_a}{d\,b} = qS_p\mathbf{A}_{c_p}\,\frac{d\,d(b,u)}{d\,b} = qS_p\mathbf{A}_{c_p}\left(\frac{\partial\,d}{\partial\,b} + \frac{\partial\,d}{\partial\,u}\frac{d\,u}{d\,b}\right) \tag{7.42}$$

This thesis utilizes aerodynamic database for the purposes of the mission performance evaluation, which requires its own sensitivity analysis approach. Since no linearization is utilized in this case, a coupled sensitivity analysis of the modeled aero-structural system has to be performed. The structural part of the system remains the same as was the case for the VLM, but the source of the aerodynamic forces and their sensitivities changes. The interpolation eq. (7.20) used in the database approach can be rewritten to provide gradients resulting in the eq. (7.43). If only the aerodynamic coefficients are stored in the database, the values obtained from the interpolation for the sensitivities have to be additionally multiplied by the used normalization values, but since these are not dependent on the trimming variables, no additional handling is necessary.

$$\frac{d\,p_a}{d\,b} = q\,S_{ref}\,c_F\,(w) = \frac{\partial\,c_F}{\partial\,w}\,\frac{d\,w(b,u)}{d\,b} \tag{7.43}$$

The total derivative of the aerodynamic variables w, representing the database parametrization in the eq. (7.43), is computed as a part of the coupled sensitivity loop. In the current implementation, the partial derivatives, which express the dependency of the stored aerodynamic coefficients w.r.t. the database parameters, is obtained numerically by eq. (7.44).

$$\frac{\partial\,c_F}{\partial\,w} \approx \frac{\sum_{i=1}^{N}\kappa_i\,\phi\,(|w+\epsilon-w_i|) - \sum_{i=1}^{N}\kappa_i\,\phi\,(|w-w_i|)}{\epsilon} \tag{7.44}$$

7.5. Integration into a sizing optimization

Analogously to the trimming variables b, the aero-structural model has to provide full support for a set of design variables x. Since this thesis deals mainly with the optimization of the structural stiffness and its impact on flight performance, only sizing design variables are considered in this section. These design variables are commonly linked to the shell thickness of 2D elements, the cross sectional areas of 1D element or the fiber orientation of composites. In the case of the gradient based optimization, the aero-

structural solver has to be able to provide sensitivities of the relevant system responses w.r.t. such design variables. The approach for obtaining these derivatives is analogous to the methodology for the trimming variables, though with different functional dependencies, as shown in the eq. (7.45) and eq. (7.46). The sizing design variables x and the trimming variables b are considered as independent on each other when solving the aero-structural sensitivity analysis.

$$\frac{d}{dx}F = \frac{d}{dx}F\left(u\left(x\right), w\left(x\right), x\right) = 0 \tag{7.45}$$

$$\frac{d}{dx}S = \frac{d}{dx}S\left(u\left(x\right), w\left(x\right), x\right) = 0 \tag{7.46}$$

The structural sensitivity equation can be obtained by deriving the governing eq. (7.23) of the FEM w.r.t. the design variable x. The target of the direct sensitivity analysis is to evaluate the derivatives of the response variables u, this being a vector of displacements of the FEM model, by solving the eq. (7.47) analogously to the response analysis.

$$\frac{dS}{dx} = \frac{dK}{dx}u + K\frac{du}{dx} - \frac{dp_a}{dx} - \frac{dp_g}{dx} - \frac{dp_i}{dx} - \frac{dp_T}{dx} = 0 \tag{7.47}$$

It is important to carefully investigate the various dependencies coming from the different sources of forces and moments applied on the structural model. As such, the thrust force should normally be independent on any sizing variable linked to the structure, and its derivative should therefore be zero. This is indeed the case, if a single frozen time step is considered, as is the case for the simulation of discrete critical manoeuvres. When dealing with the mission analysis or other transient analyses, in which the flight state at one time step is dependent on the results of the previous time step, the derivative of the thrust force cannot be discarded as being equal to zero, hence the eq. (7.48).

$$\frac{dp_T}{dx} = v_T\frac{dT(b,x)}{dx} \tag{7.48}$$

The same has to be considered in the case of other sources of otherwise constant forces like gravity or inertia. In the frozen time step analysis, only the current mass of the aircraft would be directly dependent on the sizing design variables. In a situation, where information like the flight path angle or the flight acceleration become functionally dependent on results from the previous time steps, additional derivatives appear when defining the gradient of these forces, as defined in the eq. (7.49) and eq. (7.50)

$$\frac{dp_g}{dx} = \frac{d\,{}^{s0}T(b,x)}{dx}\,{}^{0}g\sum_i m_i(x) + {}^{s0}T(b,x)\,{}^{0}g\sum_i \frac{dm_i(x)}{dx} \tag{7.49}$$

$$\frac{dp_i}{db} = {}^{sa}T(b)\frac{da(b,x)}{dx}\sum_i m_i(x) + {}^{sa}T(b)\,a(b,x)\sum_i \frac{dm_i(x)}{dx} \tag{7.50}$$

When utilizing the VLM model as the aerodynamic solver in the aero-structural analysis, the forces can be obtained using the eq. (7.15). Consequently, the gradient w.r.t. the design variable x can be taken analogously to the derivative w.r.t. the trimming variable b. The only difference lies in the functional dependencies of the variables involved in the computation of the forces. In a case of a pure sizing optimization of a single time step, only the response variables of the aerodynamic solver would be implicitly dependent on the sizing variable x through the interaction between the aerodynamic and the structural solver. This would result in the first term of the eq. (7.51) being reduced to zero. Operational conditions like the air density can become implicitly dependent on the sizing variables x in the mission analysis, in which the flexibility of the wing has an impact on for example a climb performance.

$$\frac{d\,p_a}{d\,x} = \frac{d\,\rho(x)}{d\,x}\,w(x)\,\mathbf{v}_\infty(x)\times\mathbf{h} + \rho(x)\,\frac{d\,w(x)}{d\,x}\,\mathbf{v}_\infty(x)\times\mathbf{h} + \rho(x)\,w(x)\,\frac{d\,\mathbf{v}_\infty(x)}{d\,x}\times\mathbf{h} \tag{7.51}$$

The same dependencies can be observed in the linearized formulation for obtaining the aerodynamic forces using the eq. (7.16). Here the dependency of the operational conditions on the sizing variables is expressed through the dynamic pressure q. Since the trimming variables b are considered to be independent on the design variables x at this stage, the corresponding partial derivatives of the boundary condition d are reduced to zero when compared to the eq. (7.42).

$$\frac{d\,p_a}{d\,x} = \frac{d\,q(x)}{d\,x} S_p \mathbf{A}_{c_p}\,d(u) + q(x)\,S_p\,\mathbf{A}_{c_p}\,\frac{\partial\,d}{\partial\,u}\frac{d\,u}{d\,x} \tag{7.52}$$

The process to obtain the sensitivities when using the database approach to the aero-structural analysis is analogous to those introduced for the VLM model. A slight simplification of the gradient equation eq. (7.53) can be introduced for the first partial derivative of the database parameters w w.r.t. the design variables x in the brackets, depending on the type of the design variables x and the context of the application. If only sizing variables are involved and if the parametrization of the database is performed only across variables without any impact on the atmospheric conditions, this partial derivative can be assumed to be zero. In a situation where the database parametrization includes for example the Mach number, as would be usual in the case of the mission analysis, this partial derivative cannot be neglected and is hence kept in the eq. (7.53).

$$\frac{d\,p_a}{d\,x} = \frac{d\,q(x)}{d\,x} S_{ref}\,c_F\,(w,x) + q(x)\,S_{ref}\,\frac{\partial\,c_F}{\partial\,w}\left(\frac{\partial\,w(x,u)}{\partial\,x} + \frac{\partial\,w(x,u)}{\partial\,u}\frac{d\,u(x)}{d\,x}\right) \tag{7.53}$$

Part III.
Methodology Demonstration

8. Demonstration Example

8.1. Model

To evaluate functionality and a potential impact of the proposed approach, which is intended to solve an optimization problem, which deals with a mission performance improvement on an industrial scale, a civilian passenger aircraft configuration was chosen as a demonstration model. As a baseline has served the CSR-01 configuration, which is comparable to the Airbus A320, presented in the Central Reference Aircraft data System (CeRAS) project [4]. The considered model represents a single-aisle twin-jet airliner designed for a short to medium range missions.

Figure 8.1: A geometrical representation of the CeRAS demonstration model

The CeRAS project database provides an expansive source of data that can be well exploited for the purposes of a technology integration and assessment of methodological procedures when dealing with a commercial aircraft design. The database includes overall aircraft requirements, a geometry model, a mass breakdown, a standard mission definition, propulsion charts and other data that can be utilized to build a robust optimization model targeting a mission performance.

The main geometrical model, as shown in the figure 8.1, contained in the CeRAS database was used as a basis for both the aerodynamic and the structural models used in the MDAO process. Since the provided geometrical data consisted only of an outer surface definition, more detailed components like trailing edge devices and internal structure has been additionally defined and added to the original model. In the aerodynamic model, an adequate representation of flight control devices like elevators, ailerons and flaps is a requirement when evaluating any trimmed flight states. Additionally, appropriately mirroring these devices in the structural model provides a more realistic stiffness approximation, since considering the wing as continuous in a chord direction from a

Variable	Symbol	Value	Unit
Design range		2750	NM
Design passenger capacity		150	PAX
Maximum payload	20	t	-
Maximum take-off weight	MTOW	77	t
Maximum fuel mass	MFW	18.7	t
Operating weight empty	OWE	42.1	t
Design cruise Mach number		0.78	-
Reference wing area		122.41	m^2
Wing span		34.07	m
Mean aerodynamic cord	MAC	4.18	m

Table 8.1: Key characteristics of the demonstration model

leading edge up to a trailing edge might provide an overestimated torsional stiffness. Two linked FEM models were created, both with a different area of application. The first one, as seen in the figure 8.2, was used for the evaluation of stresses and strains caused by critical loads. The model included both left and right side as the applied load cases, that had to be evaluated to assure structural safety, might be unsymmetrical. The second model was used purely for the mission performance evaluation and thus used only the right half of the whole model, since only symmetrical loading was considered during the mission analysis. As such, this half model had additional displacement constraints applied on all nodes lying in the symmetry plane, allowing only in-plane deformations to occur. For the purposes of optimization, both of the FEM models were linked to the same design variables.

Two dimensional shell elements based on the Bischoff formulation [101] were used to assemble the wetted surfaces and webs of spars and ribs of the structural model. One dimensional Timoshenko beam elements were used to model one structural components like stringers and fuselage frames. Rod type elements were extended along the intersections of the outside skin with spars or ribs, representing caps, which are used as a part of the connection between the aircraft's outer surfaces and internal loads carrying components. Example of the various element type application is shown in the figure 8.3.

The connection between the trailing edge devices and the wingbox was realized using several pairwise stiff triangular elements connected at a two coincident nodes linked by a spring element. A series of these connections created a hinge line for each of the trailing edge devices. Additionally one or more struts, depending on the size of the connected

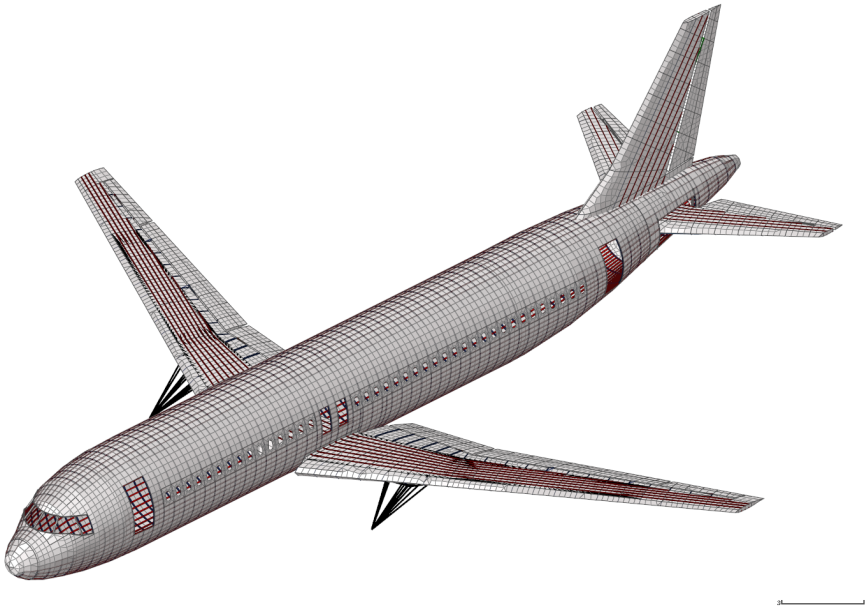

Figure 8.2: A FEM model used for a critical loads analysis

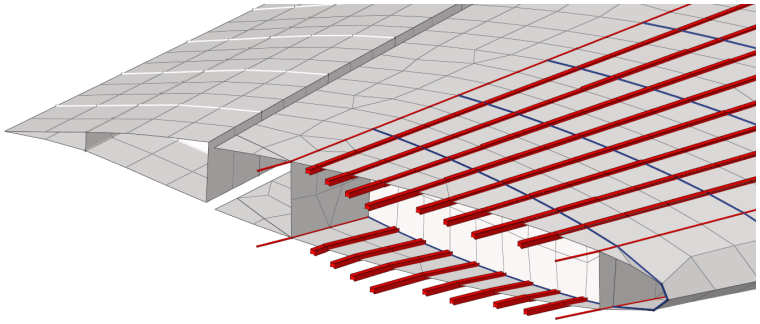

Figure 8.3: An element type utilization on a wing

trailing edge device, were used to model actuators. These did not extend or retract in the FEM model but were only present to provide a resistance against deflections caused by rotational deformations around the hinge line. Visual example for an aileron connection is provided in the figure 8.4.

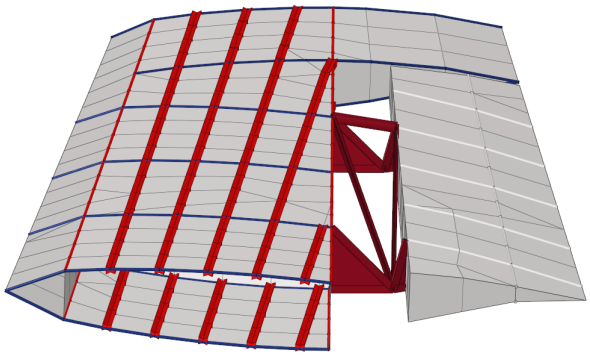

Figure 8.4: A visualization of a connection between a trailing edge device and a wing box

Two main simplifications were applied in the modeled fuselage structure. This has been done assuming that the fuselage is not a target of the optimization and as such neither stresses or strains have to be measured across the fuselage. Based on this assumption no one dimensional elements were modeled along the fuselage, which has been artificially stiffened as well, mainly to mitigate an artificial loss of stiffness due to the removal of frames and stringers from the fuselage. Since the structural elements of the FEM model only characterize load bearing structures of the aircraft model, they provide approximation of the structural part of a total weight only. Additional masses, that could not be covered by a density property of the structural elements contributing to stiffness, had to be considered as well. On one side, they have an impact on deformations through their additional loads caused by an inertia's influence and on the other side, the additional weight has a direct impact on the flight equilibrium enforced in the trimming analysis. Thus, fuel tanks, main landing gear, engines and engine's pylons have been modeled as concentrated masses and consequently connected to the surrounding structure using load distribution elements, as visualized in the fig. 8.5.

The same has been done in the area of the fuselage for masses like furnishings, payload, front landing gear and an Auxiliary Power Unit. The distribution of concentrated mass elements and their connections to the supporting structure of the FEM model is represented in the fig. 8.6.

Collectively a mass breakdown for the FEM model is summarized in the figure 8.7, except for payload and fuel mass. These are dependent on a load case or a flight state. All the masses referenced in the figure 8.7a, excluding the FEM structure, are modelled as concentrated mass points as referenced in previous figures.

For the purposes the aerodynamic simulation, two differing solvers have been utilized. Firstly, the Athena Vortex Lattice (AVL) solver with its model visualized in the figure 8.8.

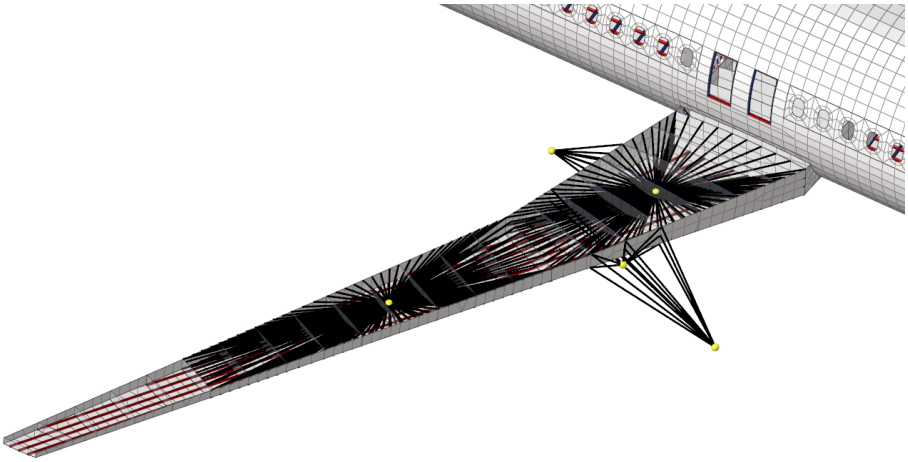

Figure 8.5: Concentrated masses in a right wing of a FEM model

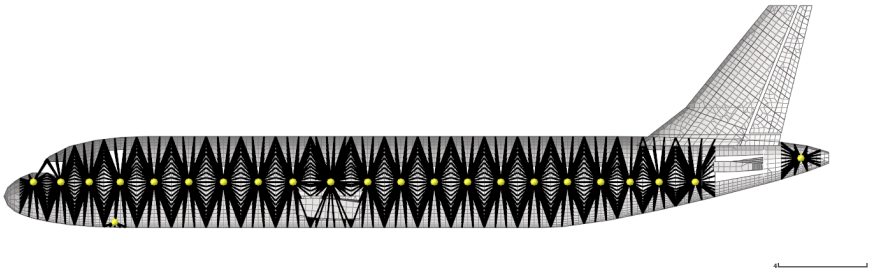

Figure 8.6: Concentrated masses in the fuselage of the FEM model

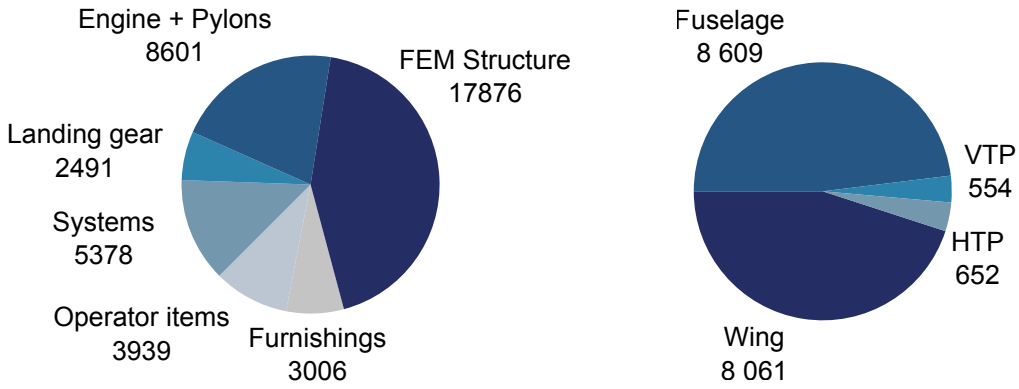

(a) An OWE breakdown in kilograms

(b) A FEM mass breakdown in kilograms

Figure 8.7: A breakdown of masses contributing to an OWE and structure carrying elements

The plate-wise representation of the lifting surfaces was discretized into 1834 panels with a cosine distribution across the chord direction. This aerodynamic model was applied for the evaluation of limit stresses and strains during the critical load case analysis. Due to the low-fidelity nature of the AVL method it wasn't used for the mission simulation, due to the lack of veracity of the drag approximation. The second aerodynamic model, that was integrated in the same framework, was intended for the use in the evaluation of the mission performance and was represented by a precomputed database, which was generated using Euler fluid simulations executed by the SU2 solver [89]. Since the medium-fidelity Euler solution was required only for the purposes of the mission analysis, which presumes purely symmetrical flight states, only one half of the aircraft was modeled and evaluated, as presented in the figure 8.9. The fuselage and the Vertical Tail Plane were neglected as to speed up the computational process and to allow for more robust morphing of the Horizontal Tail Plane mesh. This was necessary, since the database had to be parametrized for various HTP deflection angles to allow for a more accurate trimming analysis.

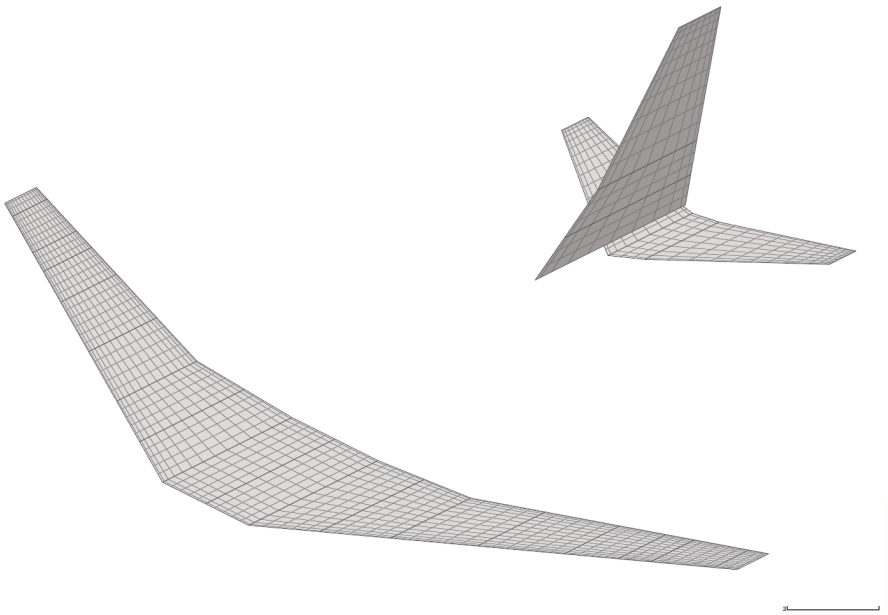

Figure 8.8: AVL model used for demonstration

The aerodynamic database was created across the angle of attack, stabilizer deflection angle and the Mach number, with the distribution of converged sample points shown in the fig. 8.10b. The surface pressure distribution, presented in the fig. 8.10a, resulting from the Euler analysis for each of the sampled datapoints, was processed and stored in the aforementioned database. This database was then used to apply the aerodynamic loads onto the FEM model during the trimmed aeroelastic analysis. The forces and moments are applied across discrete loads distribution points throughout the wing and the HTP. An example of the distribution points and their connection to the surrounding

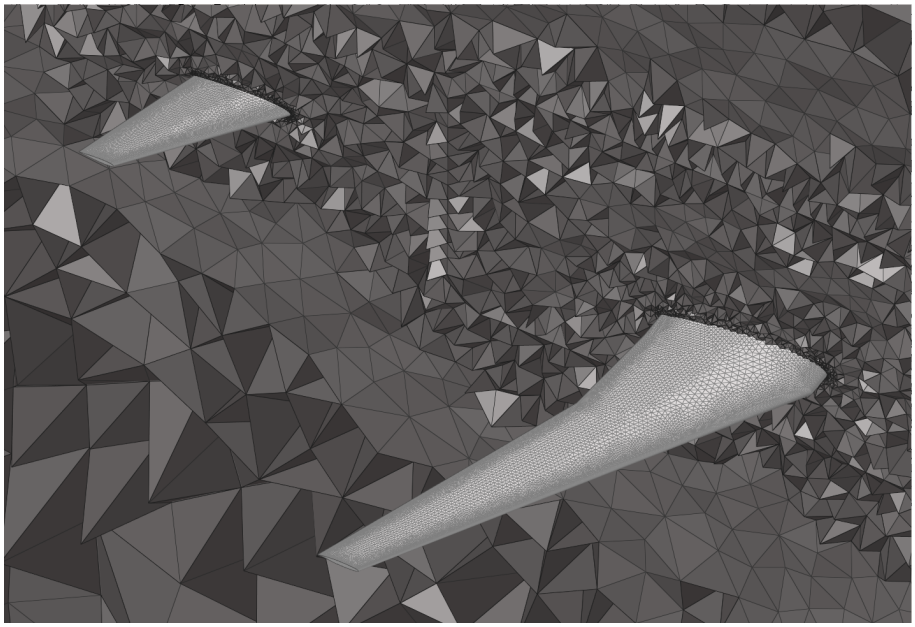

Figure 8.9: Euler model used for demonstration

structure is shown in the fig. 8.11.

8.2. Critical Load Cases

To assure the feasibility of the design resulting from the MDAO process it was crucial to include structural safety criteria in the evaluation. This was achieved by introducing critical load cases simulating the most demanding flight manoeuvres the aircraft should be able to withstand. Many of these are prescribed by certification authorities like the EASA [102] and include manoeuvres and situations like the pull-up, the push-over, the landing, the engine failure, the gust, the sudden rudder deflection and many more. Since the total number of load cases required for a full certification process would prove too computational expensive for the purposes of this methodological demonstration, only a representative subset was selected. The chosen group of flight manoeuvres consisted of load limit states defined by the v-N diagram and gust approximations obtained using the Pratt formulae [5]. The design, stall and dive speeds for the various flight levels used in the critical load case definitions were taken from a flight envelope provided by the CeRAS project [4]. Additionally a safety factor of 1.5 was applied by reducing the maximum allowable stresses that a material can withstand.

Initially a larger set of load cases was investigated than the one shown in the table 8.2 and table 8.3 and used in the optimization, but after a few initial optimization steps were performed and the preliminary results were evaluated, only a subset of the critical load cases were identified as design driving. Only the load cases generating the minimum reserve factor values across elements remained in the table 8.2 and table 8.3.

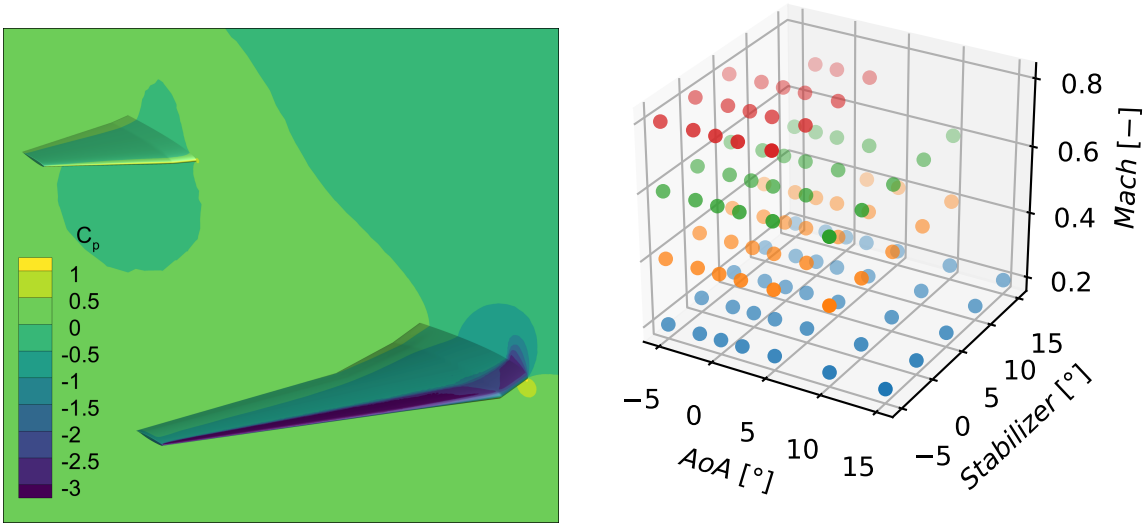

(a) An example of a pressure distribution from the SU2 solver

(b) A data point distribution of Euler based results

Figure 8.10: Data used to generate an aerodynamic database from SU2 results

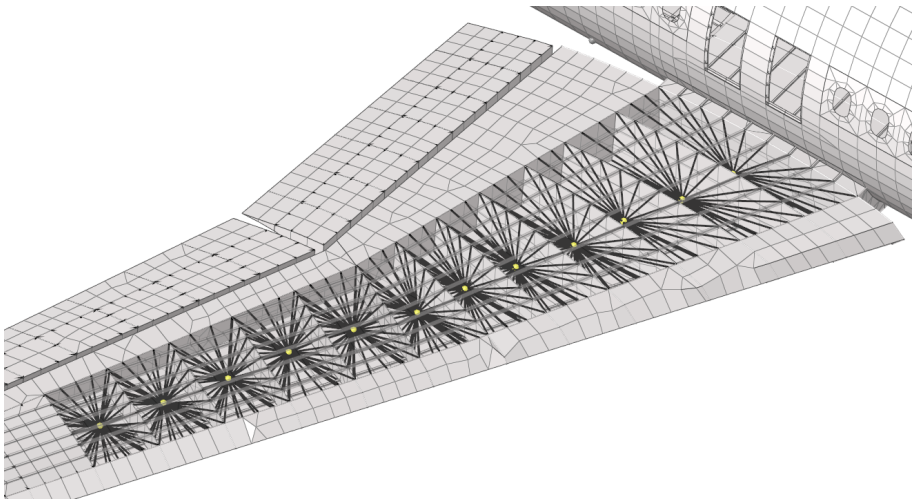

Figure 8.11: An example of integration point connections to a wing-box structure

ID	V-N Point	Speed Type	Flight Level	Mach Number	Load Factor	Mass
12103	D2	V_D	12.7	0.902	2.5	MTOW
12104	F	V_C	12.7	0.780	-1.0	MTOW
12203	D2	V_D	12.7	0.902	2.5	MZFW
12404	F	V_C	12.7	0.780	-1.0	HFMP
13101	A	V_A	37.8	0.862	2.5	MTOW
13103	D2	V_D	37.8	0.903	2.5	MTOW
13203	D2	V_D	37.8	0.903	2.5	MZFW
13401	A	V_A	37.8	0.862	2.5	HFMP

Table 8.2: Representative load cases chosen for an assurance of a structural safety based on a v-N diagram

ID	Speed Type	Flight Level	Mach Number	Load Factor	Δn_{max}	Mass
61301	V_C	12.7	0.780	1.0	2.146	MTOW
61401	V_C	12.7	0.780	1.0	1.508	HFMP

Table 8.3: Investigated load cases estimating gust influence based on the Pratt formula [5]

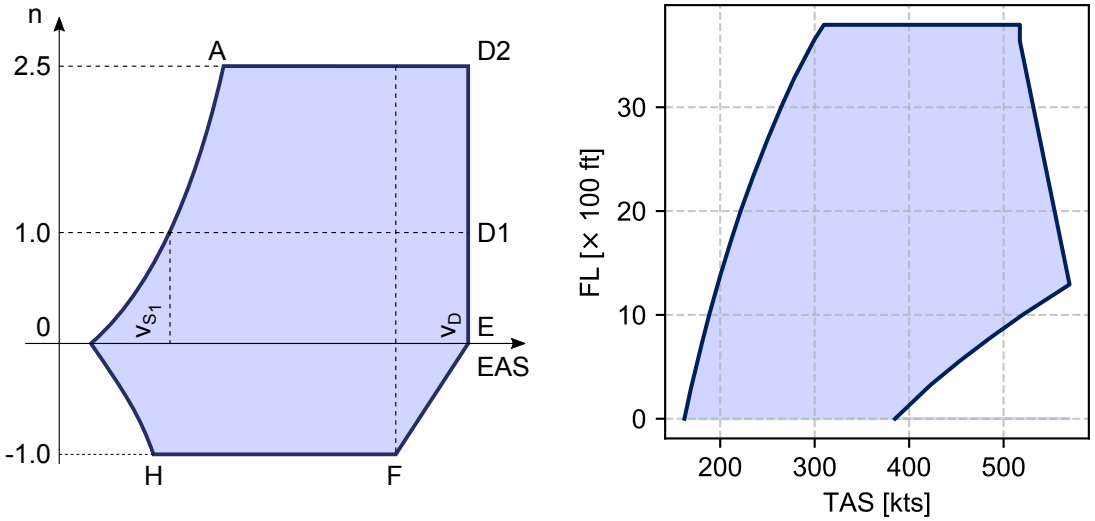

(a) A v-N diagram according to the CS-25 regulation [102]

(b) A flight envelope for the CSR-01 configuration

Figure 8.12: Figures used to establish load cases at v-N points

8.3. Propulsion Approximation

The model provided in the CeRAS database [4] used two V2527-A5 engines, which is a common type found on the Airbus A320. The engines in the used FEM model were not modeled in detail, neither during in the fluid analysis nor for the FEM analysis. Instead each of the engines was represented by a single node in the FEM model, at which a concentrated mass element was applied so that the inertia's influence of the engine might be included in the overall structural response. This simplification was done in accordance to the assumption that any local influence of the air flow around the engine is negligible during the design phase for which this demonstration was intended. Additionally, the same node, as visualized in the fig. 8.13, served as the node for introducing the thrust force that would be generated by an engine at specific operational conditions. With this, the thrust was included not only in the trimming analysis but its influence on the wing deformation was directly considered in the aeroelastic analysis as well.

Engine data stored by the CeRAS database were originally computed using the gas turbine performance software GasTurb from the GasTurb GmbH [103]. The CeRAS project made performance charts available, which consisted of discrete data points for the fuel flow and the thrust force as functions of the altitude, the Mach number and the rotational speed. A visualization of these data sheets for a single Mach number is provided in the figure 8.14. Interpolation models were generated from the accessible performance charts to provide a mapping between the thrust lever setting, the thrust and the fuel burn values. The approximation functions were built using the Radial Basis Functions interpolation algorithm based on a cubic estimation provided by the SciPy [104] library for Python.

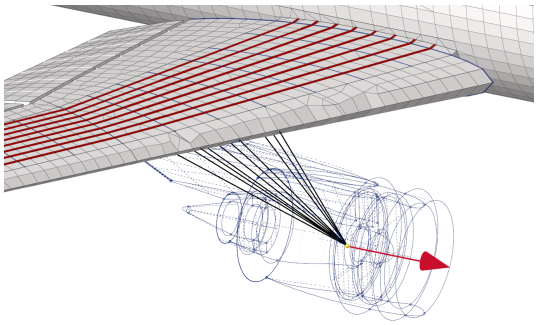

Figure 8.13: An engine representation in a FEM model

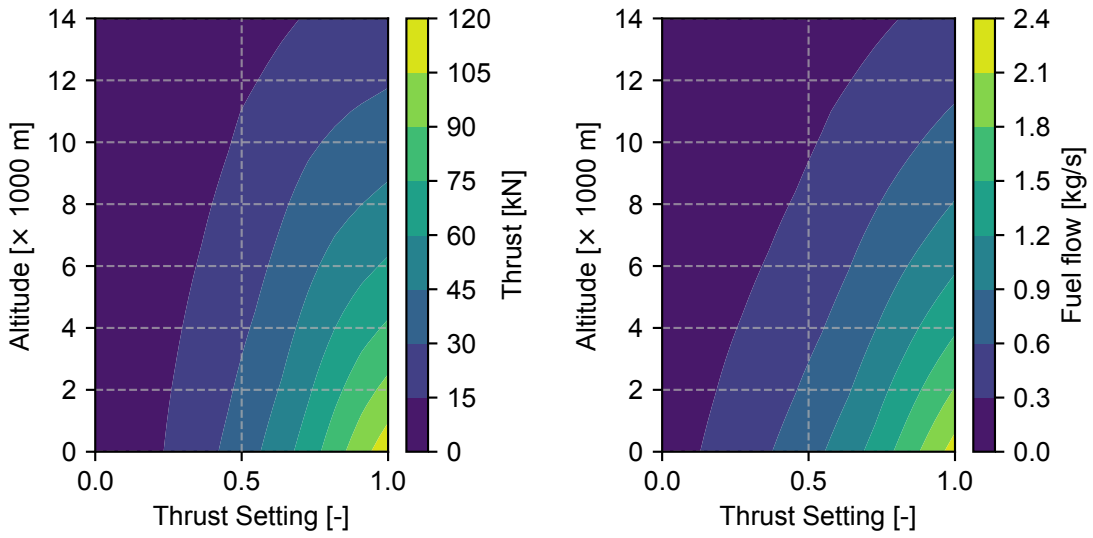

(a) A thrust force as a function of a thrust setting and an altitude

(b) A fuel flow as a function of a thrust setting and an altitude

Figure 8.14: Performance charts of a V2527-A5 engine based on data from the CeRAS project [4] for a Mach number of 0.8

8.4. Mission Definition

To be able to evaluate mission performance characteristics of the demonstration example, a single reference mission profile was chosen from the CeRAS database [4]. The selected flight profile represents a mission at the MTOW limit of the reference payload range diagram 8.15b, where the achievable range is not necessarily purely limited by the flight performance or the MTOW, but rather represents a trade-off between them.

Parameter	Value	Unit
Range		NM
Payload		kg
Cruise Mach number	0.78	-
Loaded fuel	18183.0	kg
Take-off fuel	17907.0	kg
Take-off weight	77000.0	kg

Table 8.4: Summary of the reference MTOW mission

The complete mission profile shown in the figure 8.15a, that was simulated during the CeRAS project, was simplified for the purposes of this demonstration. The simplification lied in fully simulating only the cruise segments and the climb step. This allowed for a reduction of computation demands while keeping the main mission parts contributing the most to the overall fuel burn fully simulated. Approximation using weight fractions [70] was used for those segments involving the take-off, the climb to the cruise altitude and the final descent with landing. The specific values for the weight fractions, given in the table 8.5, were evaluated using the reference simulation results provided by the CeRAS project [4].

8.5. Parametrization Model

The demonstration example represents a design update of an existing aircraft configuration, for which the outer shape is not allowed to change. As such, only the structural sizing, trimming and some mission design variables were considered in the parametrization model. An overview of the design variables is shown in the table 8.6.

Sizing variables were defined in the first place as the main input for manipulating the structural stiffness of the aircraft. More specifically, they are designated on the main load carrying components of the wing. These being the skin, spars and stringers of the wingbox. Hence, the thickness of the skin and spar elements was parametrized together with the cross-section areas of the stringers. This was done in a patch wise

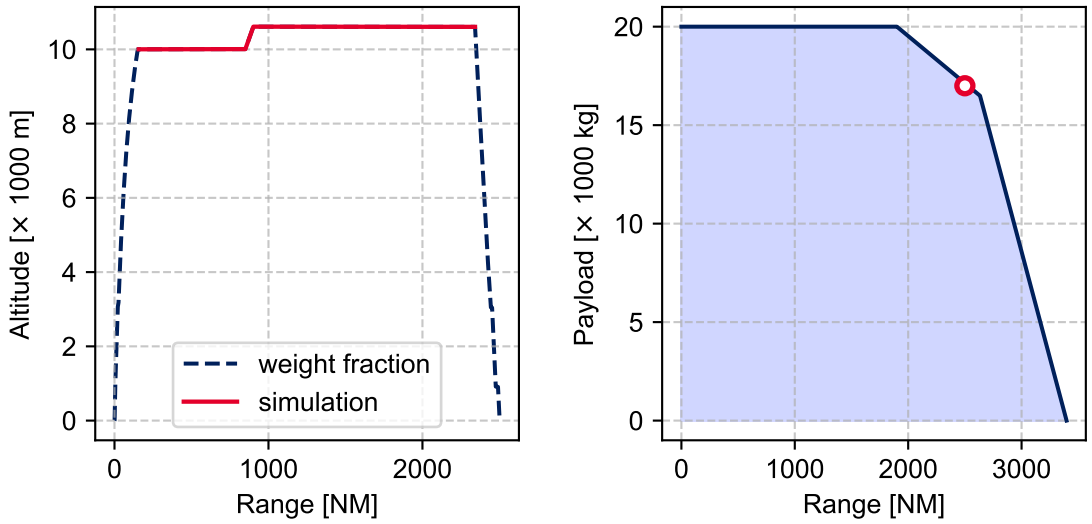

(a) Profile of a mission chosen for an optimization demonstration

(b) A payload-range diagram showing position of a demonstration mission

Figure 8.15: A mission's altitude profile and a payload-range diagram of a demonstration mission

Segment	**Type**	**Constants**
1	Take-off	$WF = 0.99849$
2	Climb	$WF = 0.97637$
3	Cruise	$\gamma = 0.0°$, $Ma = 0.78$
4	Climb step	$\gamma = 0.378°$, $Ma = 0.78$
5	Cruise	$\gamma = 0.0°$, $Ma = 0.78$
6	Descent	$WF = 0.98531$
7	Landing	$WF = 0.99882$

Table 8.5: A profile segmentation for a demonstration mission

manner, linking thickness or area of the finite elements inside a patch together into a single design variable. Example of the patch discretization is shown in the fig. 8.16 for the upper skin of the right wing. The total number of included design sizing variables came up to 48.

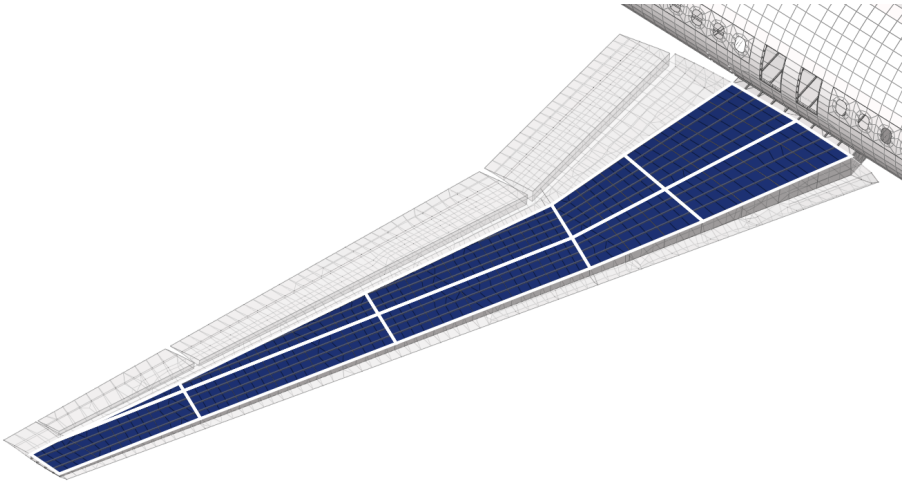

Figure 8.16: A patch-wise discretization for sizing design variables

Trimming variables were included to assure that only viable flight states were considered for the final design. This was achieved by introducing two design variables, an angle of attack and an elevator deflection, per load case, coming up to 20 trimming variables in total. The nature of both of the variable types is angular and is visualized in the fig. 8.17. The angle of attack is applied for the whole aircraft by changing the direction of the global free flow velocity vector, whereas the elevator deflection is applied locally by changing an incidence angle of the corresponding AVL panels.

Mission related variables could provide additional avenue for design exploitation. In this demonstration a single mission variable was utilized, that being the initial fuel mass state, with the main goal being to perform a specific mission with only the exact amount fuel necessary for that mission. It was assumed that if the fuel mass present at the take-off would be considered constant during the optimization process, some of the obtained design might be negatively affected by having to carry more fuel than necessary, resulting by a higher fuel burn due to the increased weight. The fuel state design variable was represented in the structural model by linking it to the concentrated mass elements representing the fuel tanks, as shown in the figure 8.5.

8.6. Constraints Model

Strength constraints served to assure structural safety of components undergoing change during the optimization. For this purpose a set of constraints spanning all el-

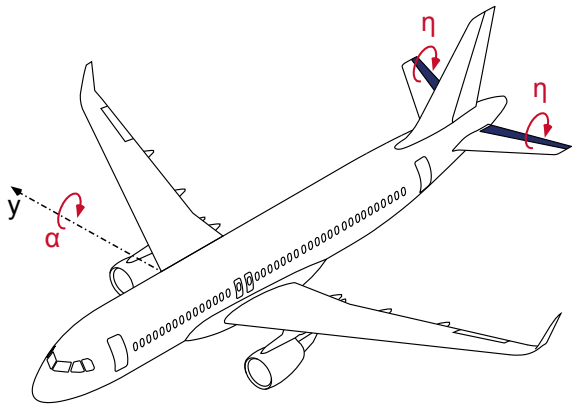

Figure 8.17: An identification of trimming variables in a demonstration model

Design Variable	#	**Lower Limit**	**Upper Limit**
Sizing			
Upper skin	10	$0.5mm$	$20.0mm$
Lower skin	10	$0.5mm$	$20.0mm$
Front spar	5	$0.5mm$	$20.0mm$
Back spar	5	$0.5mm$	$20.0mm$
Upper stringers	9	$160.5mm^2$	$481.5mm^2$
Lower stringers	9	$160.5mm^2$	$481.5mm^2$
Trimming			
Angle of attack	10	$-30.0°$	$30.0°$
Elevator deflection	10	$-30.0°$	$30.0°$
Mission			
Initial fuel level	1	$8953.5kg$	$18402.0kg$

Table 8.6: An overview of utilized design variables

ements that were linked to design variables has been established. Not applying these structural constraints for all elements of the used FEM model might have lead to a design with not allowable stresses on components not subject to an optimization, although this was deemed to be unobtrusive for the purposes of this demonstration. Von Mises Stress Criterion has been chosen for the strength constraints evaluation due to the homogeneous nature of the materials spanning the aircraft structure and to limit the total number of constraints. For the aluminium 7075-T6 used in the structural model, the maximum allowable stress had the value of 335.3 MPa, which already includes the safety factor of 1.5.

Buckling constraints were applied on the wingbox skin to avoid local loss of stability under the critical loads. It is one of the standard requirements for structural safety of slender elements. The buckling fields are limited by neighbouring stringers, ribs and spars which serve as supporting structures against the local loss of stability. An example of a few of the buckling fields is presented in the fig. 8.18. Similar constraints were applied for the stringer elements as well.

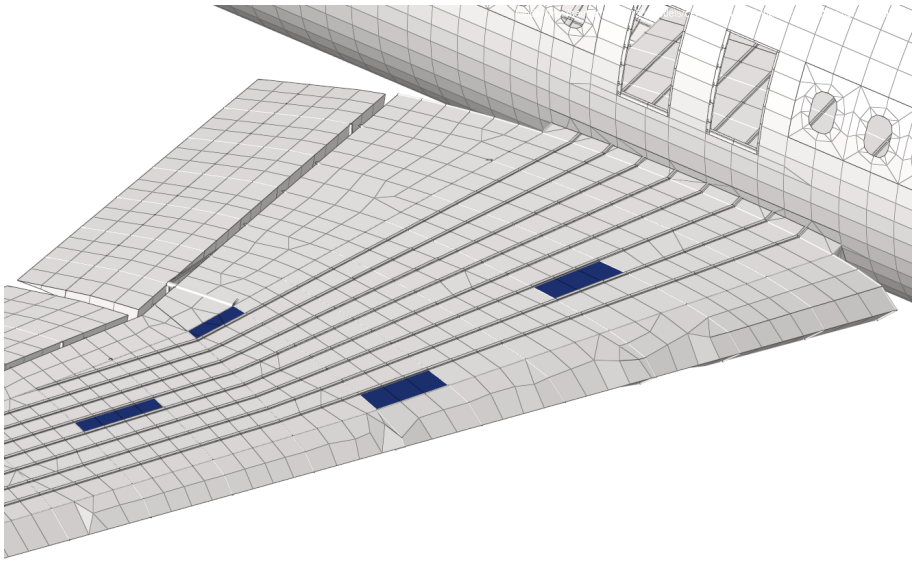

Figure 8.18: Examples of buckling fields on an upper skin on a wingbox

Trimming constraints were included in the criteria model to satisfy the condition that all critical loads are evaluated at flight states which are in equilibrium and as such represent viable operational conditions. These constraints compared the structural, the inertia and the aerodynamic forces and moments while considering the impact of elastic deformations. Both the load cases involving the v-N diagram points and the gust loads were assumed to be symmetrical, thus only the lift force and the pitching moment were being constrained. The target value for the resulting pitching moment is zero whereas the

required lift forces were computed from the inertia forces for various mass configurations and a loads factors.

Mission constraint was formulated as the amount of fuel remaining after finishing the mission. The take-off fuel for the investigated mission presented in table 8.4 was already calculated during the CeRAS project with specific reserve fuel requirements set by the regulation JAR-OPS 1.255 [105]. The fuel reserve estimation method prescribed in the regulation does result in the reserve fuel being about 23.6% of the trip fuel for the selected mission. Based on a preliminary mission evaluation using the aerodynamic data from the Euler simulations, which showed a worse aerodynamic performance than was the case for the reference CeRAS data, the reserve fuel required was reduced to 15.5% of the trip fuel, otherwise the the mission would not be achievable. This allowed for the initial design to have the same amount of take-off fuel as the reference. Even though the reserve fuel is prescribed in a different way that the regulation JAR-OPS 1.255 [105] requires, the important aspect of tying the absolute amount of the reserve fuel to be dependent on the flight performance of the aircraft is kept.

Type	**#**	**Condition**
Strength	91790	$\leq$ 335.3 MPa
Buckling	5790	$\geq$ 1.0
Trimming	20	$=$ 0.0
Remaining fuel	1	$\geq$ 15.5% of trip fuel

Table 8.7: An overview of conditions building up a criteria model

8.7. Objective Model

The study of M. Drela [19] has already shown the importance of a multi-point optimization in achieving a robust performance improvement. As such, it was important to consider few different objectives in this thesis to be able to determine the one leading to the best possible design for the aircraft configuration.

The first considered objective function was the structural mass represented by the equation 4.7. This is a basic objective function that is available even if no actual flight performance can be evaluated or is considered not to be relevant at a specific aircraft design phase. It is based on the consideration that a lighter aircraft will have an overall better range performance or that the amount of reduced structural mass can be directly translated to payload of fuel that an aircraft can carry, inherently extending the bounds of the payload-range diagram.

$$\Psi(x) = m_s(x) \approx m_{fem}(x) = \sum_{i=1}^{n_{elem}} m_{elem_i}(x) \qquad \text{(4.7 revisited)}$$

The more advantageous performance measures like the drag or lift to drag ratio [41, 46], which are commonly used as flight performance estimators in research and industrial applications, since they can be considered to be directly proportional to the fuel consumption. These estimators are especially useful if no engine data is available. Since the used demonstration model provided actual propulsion data, it was decided to directly compute the fuel consumption for each of the cruise segments of the investigated mission. This fuel consumption is computed analogously to the approaches that would be using the lift to drag ratios for the performance estimation. As such, few sample points from the cruise segments are chosen at which the required thrust, and hence the fuel flow, were simulated. The resulting discrete fuel flow values were weighted by the segment time according to the eq. (8.1), resulting in an overall estimation of the consumed fuel.

$$\Psi(x) = \sum_{i}^{N} \dot{m}_f(t_i) \cdot \Delta t_i \tag{8.1}$$

A possible drawback of the discretized point-wise evaluation is the lack of information about the actual fuel state at those points t_i, since no integrated mission analysis would be performed during the optimization steps. This might negatively influence the optimized design since the amount of fuel in the tanks is not updated in between the optimization steps. Hence the mass of the fuel might be higher than necessary, resulting in an increase in the required lift.

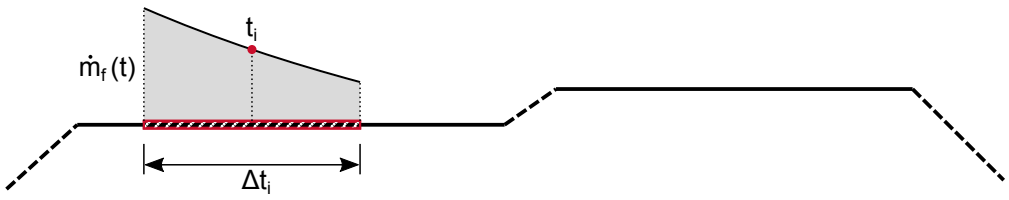

Figure 8.19: A point's influence segment length for purposes of weighting

Finally, a fully coupled mission performance analysis was integrated into an objective function in the form of a trip fuel. The equation 8.2 presents two equivalent ways to compute the trip fuel based on results from the mission analysis. In this demonstration, the trip fuel was defined as a difference between the initial and the terminal fuel mass, since the formulae to build up a corresponding gradient involves less terms and as such is less prone to error.

$$\Psi(x) = \int_{t_0}^{t_f} \dot{m}_f(t)\, dt = m_f(t_0) - m_f(t_f) \tag{8.2}$$

8.8. Used Aircraft Simulations Model

Before starting the optimization procedure it was necessary to compare the data provided by the reference CeRAS project [4] and those that were to be used for the demonstration, in order to check the validity of the newly generated data. The aerodynamics evaluation is summarized in the fig. 8.20, which shows polars comparison between the two considered aerodynamic solvers. The lift coefficient obtained from the AVL solver, which is based on potential flow theory, is linearly dependent on the angle of attack and at the same time underestimates the induced drag coefficient. The discrepancy between the lift estimated by the AVL and the Euler solver was deemed to be acceptable. This decision was based on the fact that the lift force is the major contributor to the overall stresses and strains generated on the aircraft structure, whereas the drag forces are in most cases a negligible contributor to deformations.

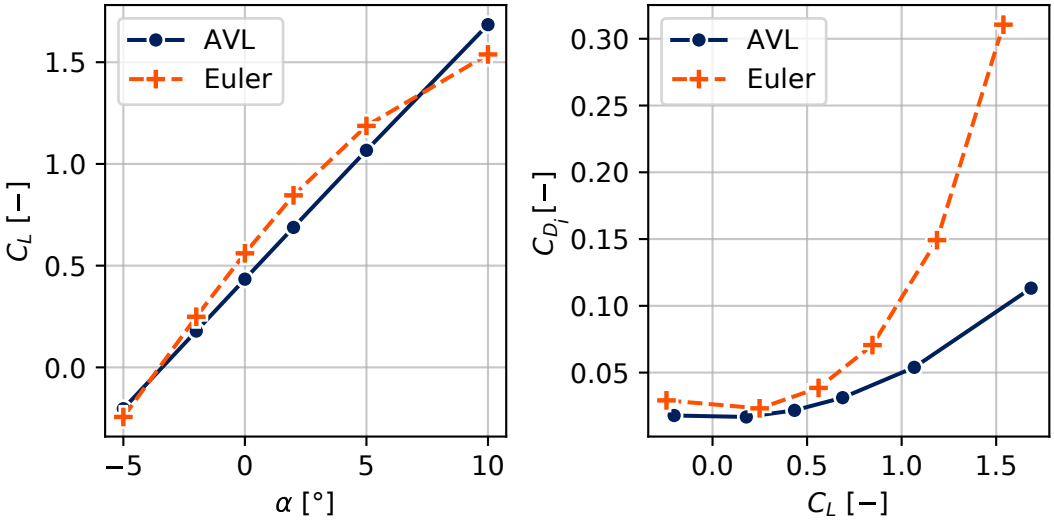

Figure 8.20: A comparison of non-trimmed polars for considered solvers

The CeRAS database included a set of trimmed aerodynamic polars for the CSR-01 configuration, which were generated using a low-fidelity model based on the Lifting Line theory with corrections. In the scope of the CeRAS project, those polars were utilized for the mission performance computation and a consequent costs assessment. To be able to perform a first step validation, similar polars for several Mach numbers were constructed using the AVL and the SU2 solver. The trimming was performed for a smaller subset of lift coefficients with the addition of zero pitch moment constraints, which was to be achieved by designating the angle of attack and the stabilizer deflection as trimming variables. The resulting polars were consequently used for an initial comparison of the reference data coming from the CeRAS database and the aerodynamic models of the demonstration model, with the fig. 8.21 summarizing the findings. Based on the obtained polars it was observed, that the AVL solver significantly underestimated the induced drag and as such was unsuitable for a use in the mission analysis, but was deemed satisfactory

for the computation of forces and moments for the critical load cases. On the other hand, the Euler based polars presented a seemingly viable match to data obtained from the CeRAS reference database, showing a more realistic induced drag estimation. Since the results coming from the reference database were originally obtained by corrected low-fidelity methods, it wasn't expected to see perfectly matching aerodynamic polars, but the overall aerodynamic performance showed that the Euler data could be well suited for the mission performance analysis. Additionally, the fig. 8.21 shows a comparison of a pure aerodynamic performance obtained on a jig shape and that simulated on an in-flight shape using an aerodynamic analysis coupled with a structural solver. For both the AVL and the SU2 aerodynamic data, the difference between rigid and elastic polars was around 0.9% on average. Even though the influence of elasticity seems negligible, it is important to note that this difference was computed based on the initial structural design, while the actual value is dependent on the stiffness distribution and thus was going to change during the optimization process.

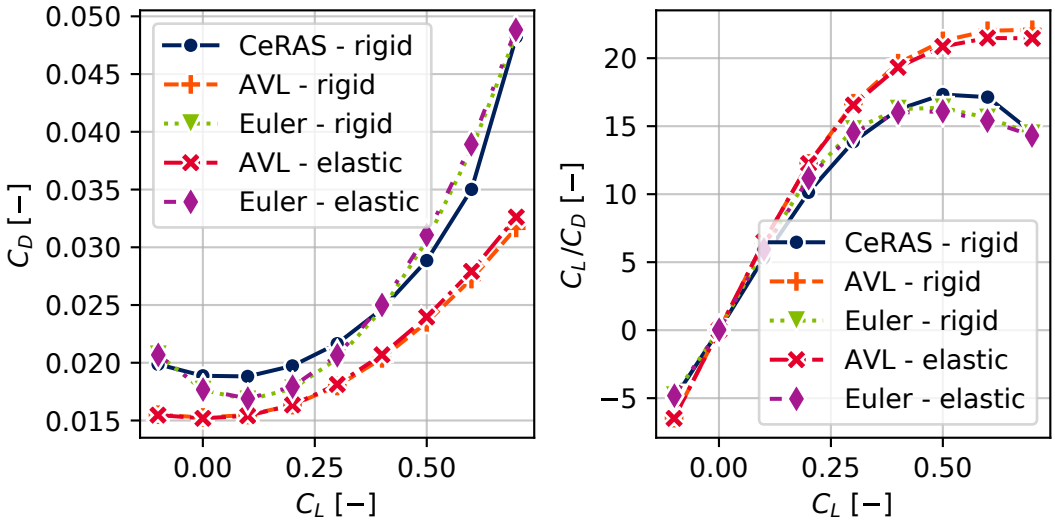

Figure 8.21: A comparison of trimmed polars for the considered solvers

To judge the viability of the developed framework utilized in this demonstration it was necessary to compare available mission analysis results provided in the CeRAS database and those generated by the implemented mission simulation. A first test was performed by simulating the reference mission using the CeRAS aerodynamic polar and the resulting flight profiles were compared with those in the original database. The corresponding results are shown in the figure 8.22, which presents the change of the fuel mass over time across simulated cruise and climb step segments. Comparing results of the mission analysis using the CeRAS aerodynamic data with reference fuel values coming from the CeRAS mission analysis showed a relative discrepancy of around 0.18%. Based on the negligible difference, it was assumed that the developed segment performance computation provided reliable results and could be utilized in the overall optimization

model. At the same time, the figure 8.22 shows results of mission analyses that were performed using trimmed aerodynamic polars obtained from the AVL and SU2 solvers. These profiles provided a first insight into the impact of higher fidelity solvers on the mission performance evaluation. The data based on the low-fidelity AVL solver resulted in an overestimation of the fuel mass left at the end of the final cruise segment by about 65.315% when compared to results based on the Euler simulation.

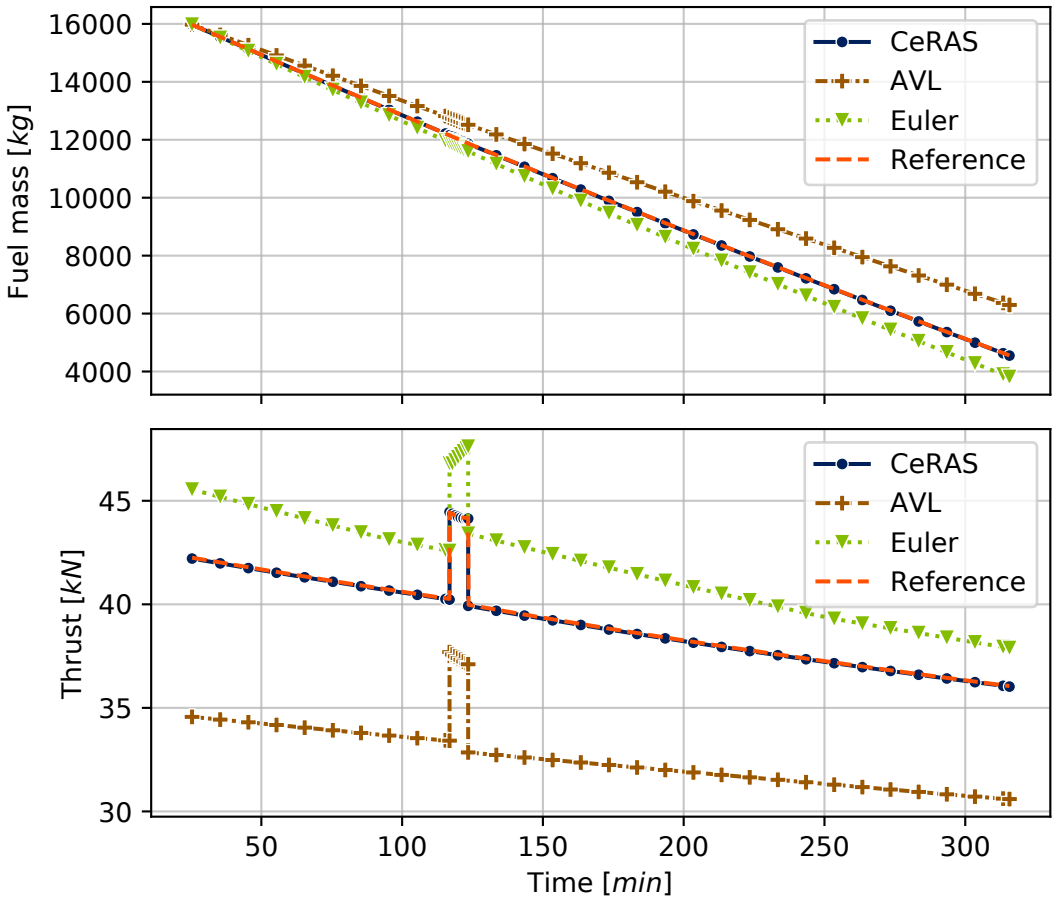

Figure 8.22: A comparison of a mission analysis using aerodynamic polars

The main aspect of the mission performance analysis that this demonstration sought to investigate was the impact of elasticity. Whereas the figure 8.21 presents an example of the elasticity's contribution on a sample-wise aerodynamic behaviour, it was deemed necessary to extend the investigation to an actual mission performance analysis. A sample output of the examination is presented in the figure 8.23, which quantifies the difference between fuel consumption obtained using an undeformed and an actual in-flight shape over time, for the two used aerodynamic solvers.

Even though the mission simulation using the polar based on the Euler data was using the same source for aerodynamic performance, the discrepancy in fuel mass remaining in

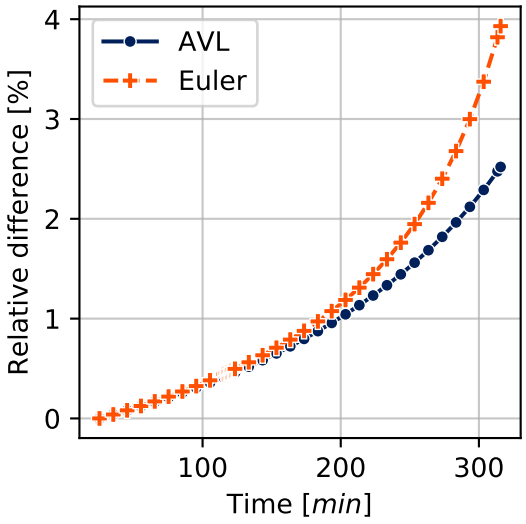

Figure 8.23: An influence of in-flight shape polars on a fuel consumption

the tanks has a mean of 1.74% when compared to the mission simulation which considered elastic deformations, as shown in the figure 8.24. The difference was attributed mainly to the inclusion of deformation, but other sources could have contributed as well. In the case of the fully coupled aeroelastic simulation the trimming included a contribution of the thrust force to the equilibrium in the lift direction and considered the angle of attack and the stabilizer deflection as the trimming variables. In contrast to the coupled analysis, those flight states computed using only the polar data have been evaluated by using only the angle of attack as the trimming variable, since the source polar was already pre-trimmed, while neglecting any contribution of the thrust force. Whereas the trimmed aeroelastic polars had been computed for an in-flight shape across a range of lift coefficients with an unchanging fuel amount, the fully coupled analysis evaluated each flight state while considering an updated fuel mass, resulting in a slightly different mass distribution across wings.

The figure 8.24 exposes a peculiar behaviour by showing an increase to the fuel consumption after performing the climb step, expressing a possible disadvantage of climbing to a higher altitude too early. The same behaviour was not detected when evaluating the specific mission profile using the AVL solver as the source of aerodynamic data. This aspect was already hinted at by the figure 8.21, which showed a steeper functional dependency of the drag on the lift coefficient when comparing Euler based data with those coming from other sources, at least in the c_l range between 0.2 and 0.7. Even though an uneconomical trade-off between a reduction of the dynamic pressure and an increase of $c_d(c_l)$ at the prescribed climb step position was detected, the climb step was not removed from the mission definition for reasons of consistency w.r.t. to the reference CeRAS database and that such a behaviour wouldn't impact the demonstrated workflow in any way.

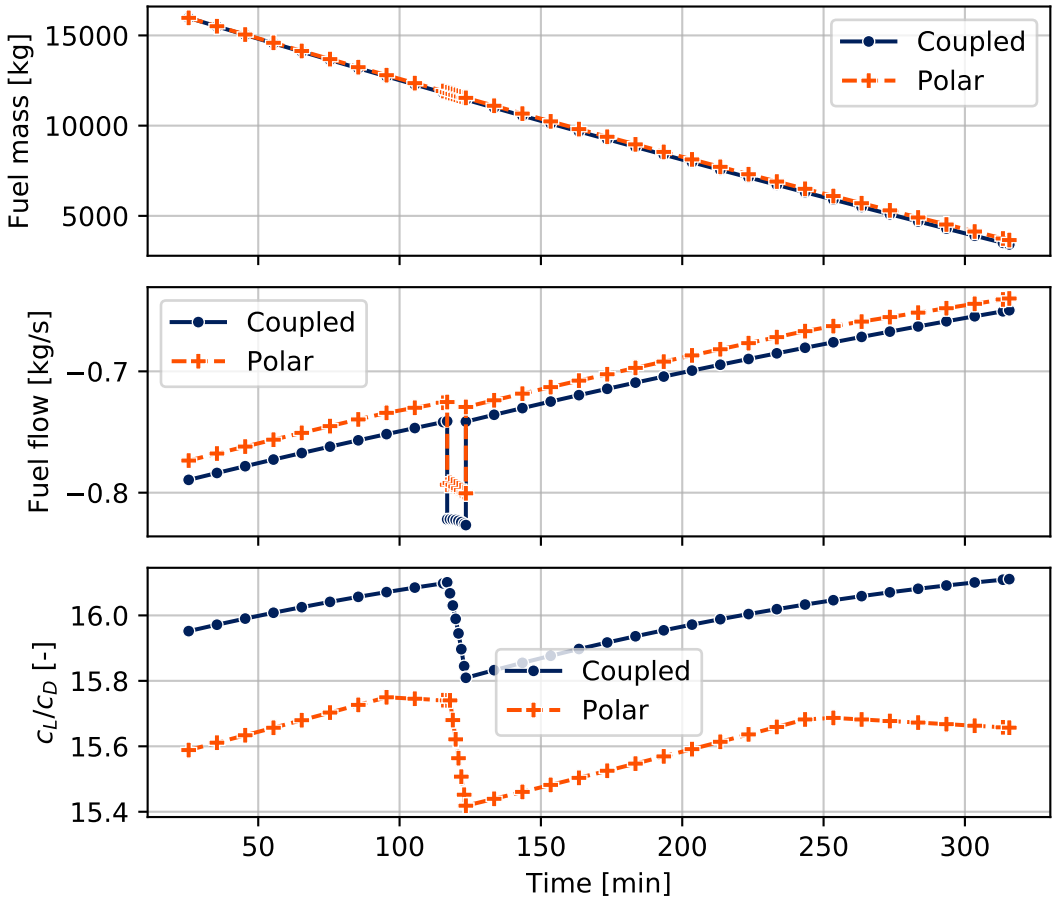

Figure 8.24: Results of a mission analysis using an initial design

During the validation process a question was raised in regard to the quality of the solution obtained from the fully coupled mission analysis. The figure 8.25 shows the results of a convergence study in the form of a dependency of the fuel mass, which was measured at the end of the last fully simulated cruise segment, on a number of steps used in the simulation. For estimating a relative error the reference value was taken from the mission analysis, which was computed using the smallest time step considered. Even though the fuel over time function was seemingly linear, as presented in the figure 8.24, the accuracy of its solution at the mission's terminal time is strongly dependent on the number of steps used. This is partially due to the use of the explicit Forward Euler Integration algorithm, that has been integrated into the mission simulation. A drawback of the chosen method is the fact that it uses only a current fuel mass value and a rate of change to estimate each consecutive step. Based on the results of the convergence investigation, a step size of 600 second has been chosen to be used in the optimization process, resulting in 38 simulated time steps. The use of this time discretization has generated a difference of around 1.4% in comparison to the reference value. This decision was done trying to balance targeted accuracy and potentially prohibitive computational efforts, that would arise from an excessive time discretization.

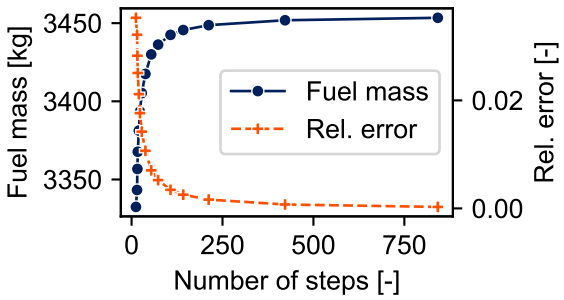

Figure 8.25: Accuracy vs number of time steps

The intention was to perform all of the planed optimization tasks using the NLPQL algorithm of Schittkowski [47], which required gradients of the objective function and constraints. For that reason it was important to evaluate the gradients obtained from the mission sensitivity analysis, which would allow to validate the gradients computation and to estimate its impact on the optimization performance. The figure 8.26 shows a sample of the investigation for the gradient of the fuel mass w.r.t. a single sizing design variable. Over the span of the mission, the relative error was continuously measured by comparing gradients obtained by a semi-analytical process and those computed by a purely numerical approach. The overall behaviour shown in the figure 8.26 points out an error accumulation. Since the error at the end of the final cruise segment stays below $1.e^{-4}$, the accuracy of the semi-analytical approach has been deemed satisfactory for its further use in optimization.

A slightly different behaviour is visible in the fig. 8.27, which presents time dependency of the fuel mass gradient w.r.t. a sample upper skin sizing variable. In comparison to the gradient obtained for the fuel design variable there is no visible consistent error

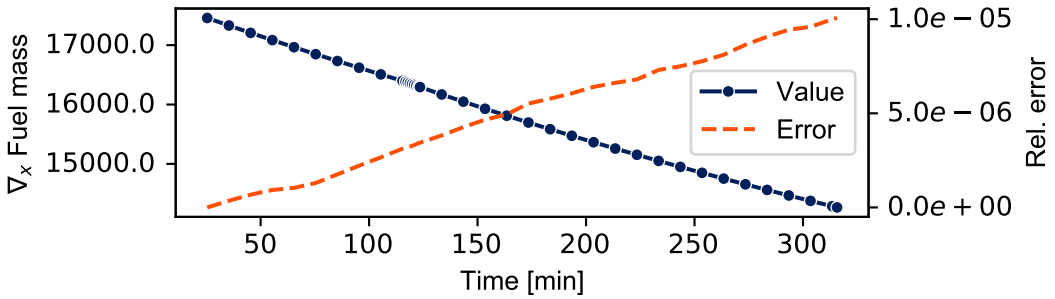

Figure 8.26: A gradient of a fuel mass w.r.t. a fuel variable during the mission analysis

accumulation between the semi-analytical and the numerical solution, but instead a fluctuating tendency has been observed, which remained below a 1.0% threshold. Similar but less pronounced fluctuations were observed in the case of the fuel design variable as well, but the mean value of the gradient was in the order of $1.e^4$ higher in comparison to the sizing variable. The fact that the error didn't show a consistent development over time was likely caused by the numerical sensitivity analysis itself, which has provided a noisy gradients curve over time when compared to the results from the semi-analytical computation.

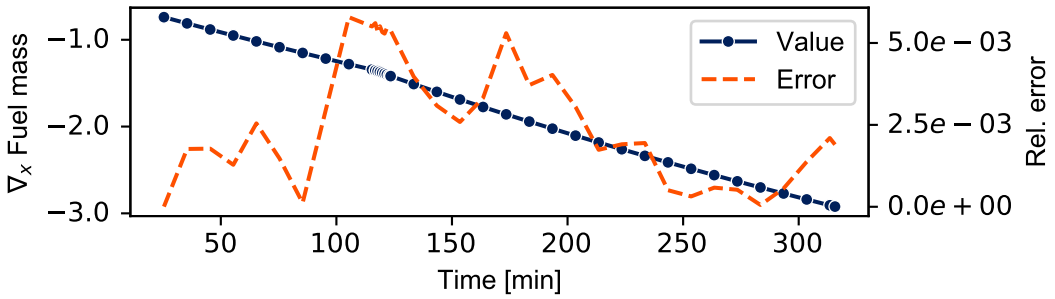

Figure 8.27: A gradient of a fuel mass w.r.t. a sizing variable during the mission analysis

To be able to better evaluate precision and consistency of the semi-analytical gradients, a convergence study has been carried out as well. Once again this was done for the sample sizing design variable and the fuel mass design variable with the results consequently compared side by side in the fig. 8.28. The previously chosen mission discretization with 38 time steps resulted in an error below 1.0% in the case of the sizing variable, which was deemed a worthy trade-off between the computational demands and the corresponding accuracy.

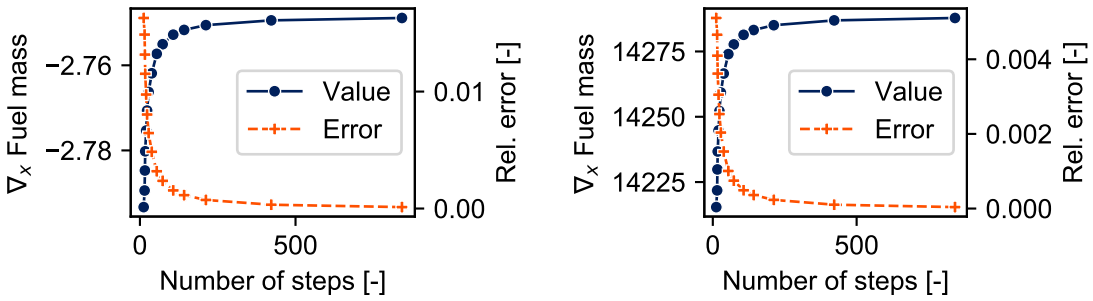

(a) Convergence for a sizing variable

(b) Convergence for a fuel mass variable

Figure 8.28: Sensitivity analysis convergence for various time step sizes

8.9. Optimization

Since one of the questions that this demonstration tried to answer was related to the choice of a suitable objective function applicable in the MDO process intended for an aircraft design in early stages, several different options were considered. The alternatives were based on the considerations made in the section 8.7 and are summarized in the table 8.8, which assigns each of them a concise reference code. This identification code is used in all intermediary and final results.

Objective	**DVs**	**Code**
Structural mass	Sizing	P-SM-S
Point wise drag	Sizing	P-D3-S
Point wise lift to drag	Sizing	P-L2D3-S
Point wise fuel consumption	Sizing	P-DM3-S
Initial mass with a fuel constraint	Sizing, Fuel	M-IM-SF
Trip fuel from a mission analysis	Sizing, Fuel	M-TP-SF

Table 8.8: Key characteristics of the demonstration model

The convergence behaviour of the considered objective functions is summarized in the fig. 8.29, where the plotted objective values were scaled with respect to their respective initial values. The task P-SM-S was identified as a baseline for further comparisons and represented a pure sizing optimization, which would be the first choice, especially if no reliable aerodynamic performance indicators would be available. The specific advantage of using the structural mass as the objective function was that it was linearly dependent on the sizing design variables, which resulted in a slightly better convergence compared to the other cases. The task P-DM3-S represented an intermediate step between the

pure structural mass and an inclusion of the full mission analysis, where the performance indicator was the amount of fuel burnt, approximated using a reduced number of mutually independent discrete sample points. Since no actual mission analysis was coupled directly in the P-DM3-S optimization problem, it was necessary to estimate the amount of fuel actually present in the fuel tanks at the considered time points. This was done by running a mission analysis for the initial design state and using the fuel level values obtained. A drawback common for all the discrete point-wise objective definitions was identified in the fact that the fuel states were not being updated between the optimization iterations, meaning that the point-wise flight performance values were obtained for mass configurations that would diverge slightly from those that would be obtained if the fully integrated mission simulation was utilized. Lastly, the actual mission analysis was integrated into the tasks M-IM-SF and M-TP-SF, which considered both the sizing and the initial fuel state design variables. Whereas both of these optimization problems included the reserve fuel constraint, only M-TP-SF used the results of the mission analysis to evaluate its objective function. The task M-IM-SF, which integrated the total initial aircraft mass as its performance measure showed convergence behaviour very similar to that of the task P-SM-S, which links only the structural mass as the performance indicator, without involving any mission analysis. The seemingly additional reduction of the performance measure value, when compared to the task P-SM-S, stems from the inclusion of the initial fuel mass as a design variable, and as such the optimization algorithm not only reduced the structural mass but the amount of fuel at the start of the considered mission as well. Finally, the task M-TP-SF integrated both the objective function and the fuel constraint, for which the values were obtained based on results of the fully integrated mission analysis. In comparison to the previously mentioned tasks, the trip fuel represented a non-linear function with respect to the considered design variables and thus it was assumed to be the reason for the slower optimization convergence presented in the figure 8.29.

The final design investigation was performed with the mission performance in mind, as this was the main target of this demonstration. Hence, additional mission analyses were performed for the single-point and multi-point optimization problems as to evaluate the performance benefits the resulting design have brought. Even so, this would not necessarily be an adequate comparison to the optimization problems that included the initial fuel state as a design variable. This is due to the fact that an aircraft will usually take only the amount of fuel on board, which is required for a planed specific mission. To consider this aspect, the actual amount of fuel needed for a mission was evaluated for each of the optimization problems that have neglected the initial fuel amount during the optimization process. This was done by defining an auxiliary optimization problem with a single design variable and a single constraint. These being the initial fuel mass and the reserve fuel respectively. The optimization was then done using a structural model with an already updated stiffness based on the proposed designs, resulting in the values shown in the fig. 8.30. All of compared mission profiles of the optimized designs satisfied the fuel constraint resulting in reserve fuel remaining being at the lower threshold of 15.56% of the trip fuel. After investigating the values resulting from the mission analysis, it

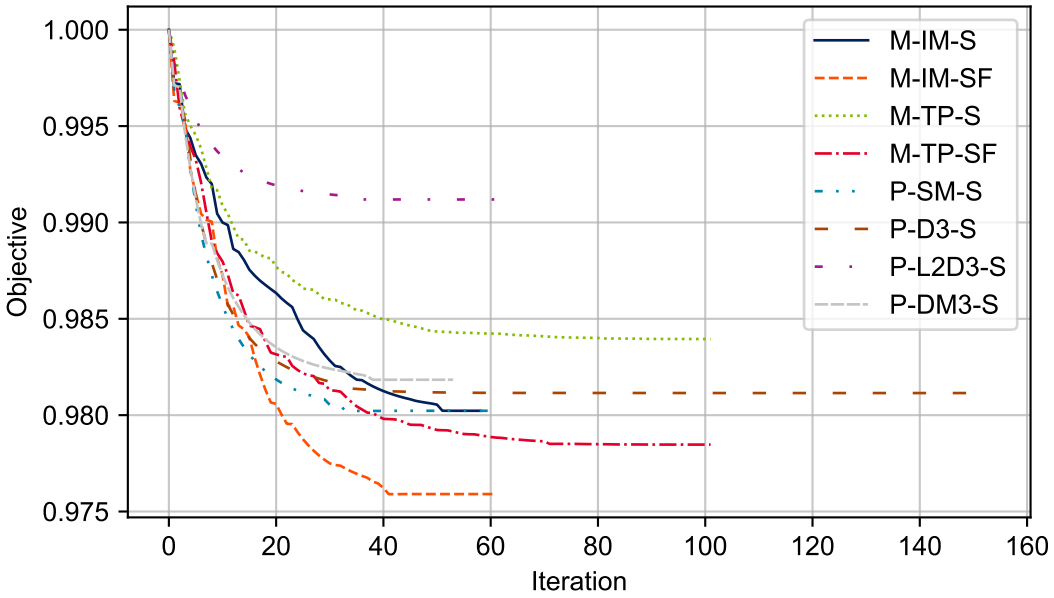

Figure 8.29: An optimization convergence for chosen objective functions

has to be stated that the obtained performance is close between all designs that were considering a flight performance as a part of their objective evaluation. In contrast to this the objective function taking only structural mass into account provides a diminished performance in comparison to the other designs, although still improving on the initial design.

Each of the final designs generated from their respective optimization problems was consequently evaluated based on their mission performance, which has been obtained by simulating the target mission for each of those designs. The main performance measure of interest in this demonstration was the amount of trip fuel required, which is presented in the figure 8.31 for each of the optimized designs. For the optimization problems that didn't involve concurrent initial fuel mass estimation, an additional optimization task was defined with the goal of computing the precise amount of start fuel needed to perform the considered mission, which was done in order to be able to correctly compare the obtained designs by estimating the amount of fuel that would be actually saved. The mission data obtained for each of the designs confirmed the benefits of the optimization based on the actual multi-disciplinary flight performance measure when compared to that of the single-discipline structural mass optimization. Even though purely reducing the total initial mass did result in a design, which provided a reduction of the consumed fuel by around 1.66%, the alternative objectives using the trip fuel evaluated by the coupled mission analysis or the point-wise estimated fuel burn resulted in an improvement of around 2.16%. The lack of any noticeable difference when comparing the results obtained by using the objective function which evaluated the amount of fuel consumed by the fully integrated mission analysis and its approximation using only the independent discrete

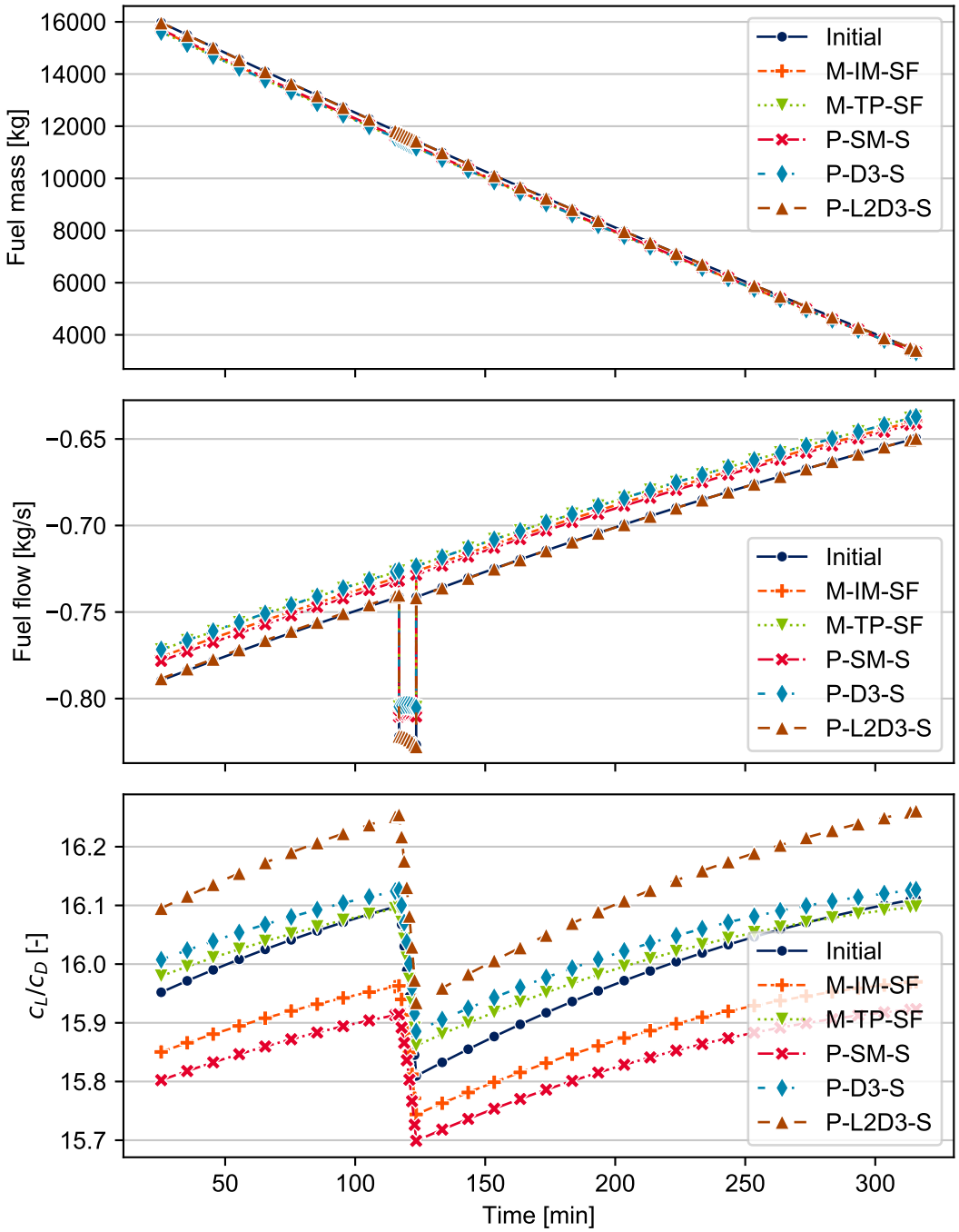

Figure 8.30: Resulting mission analysis from the various optimization tasks

points, at which the amount of fuel carried didn't change during the optimization process, was attributed to the linear dependency of fuel levels over time at the considered cruise segments. As such, using one or a few local points to approximate the overall trip fuel consumption provides comparable results for the aircraft configuration used in this demonstration. Since the actual fuel mass for these discrete points wasn't updated between optimization iterations, it served as an indicator that there was only a negligible design advantage in integrating the mission analysis in order to obtain correct fuel states at those points.

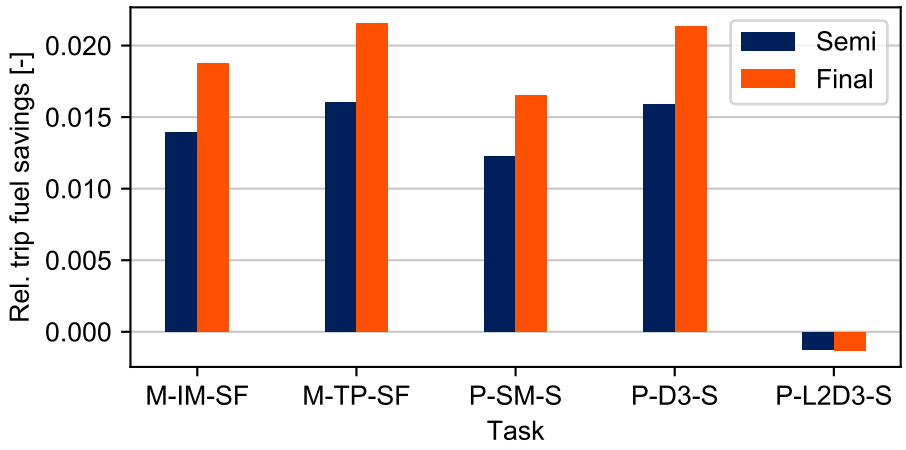

Figure 8.31: A trip fuel required by the obtained designs

The differences between the initial and the optimized designs were compared by investigated the changes in the structural mass and the required initial fuel as well. This information is presented in the figure 8.32. The savings of the initial fuel mass and the trip fuel mass are exactly the same when considering the point-wise performance optimization, but for the optimization with the fully coupled mission analysis there was a small difference detected. This discrepancy is assumed to have come from the ability of the coupled mission analysis to directly exploit the terminal fuel constraint, which has been defined using a percentage of the trip fuel burnt, and as such it was possible to achieve a reduction of the required initial fuel as well, since at the same time it did reduce the absolute amount of the requested reserve fuel.

An important aspect, visible in the figure 8.32, is the fact that the design optimized with the actual mission performance computation in mind did save more fuel even though the reduction of a structural mass was lower than in some other cases. The reason was interpreted based on the thickness distribution across the wings, whose example is shown in the fig. 8.33 for an upper skin. It was found out, that the optimization in the task P-SM-S, which was using the structural mass as the objective, has led to pure reduction of thickness everywhere, where it was not limited by the critical load cases. In comparison to this behaviour, the designs obtained by using an actual flight performance as an objective function showed a significantly different thickness distribution.

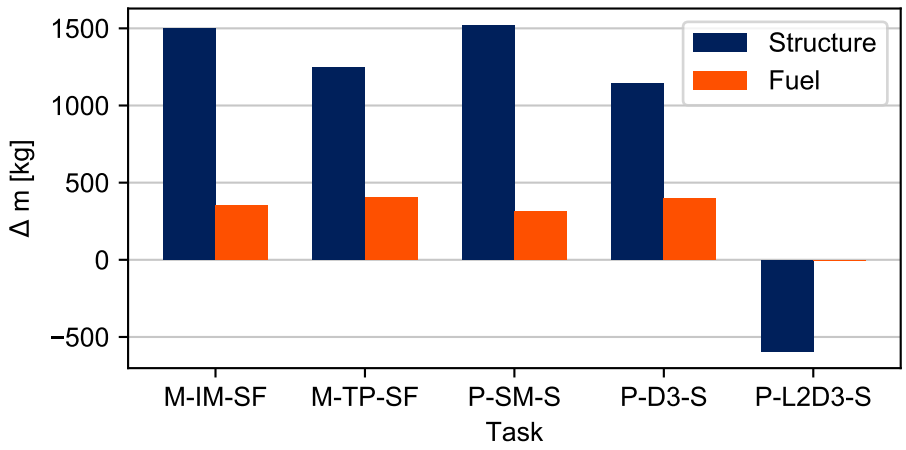

Figure 8.32: A saved structural and a fuel mass

The effects of different stiffness distributions were investigated by looking at the deformations that the wing was undergoing during structurally critical manoeuvres. The fig. 8.35 shows an example of the wing's bending for the critical loads case of the v-N diagram at the flight level of 378, the dive true airspeed of 518.0 knots and the acceleration vector of 2.5 g. The curves display a strong reduction of the twist ϕ_y deformation close to the wing tip, when comparing the performance based optimization with that of the pure structural mass minimization.

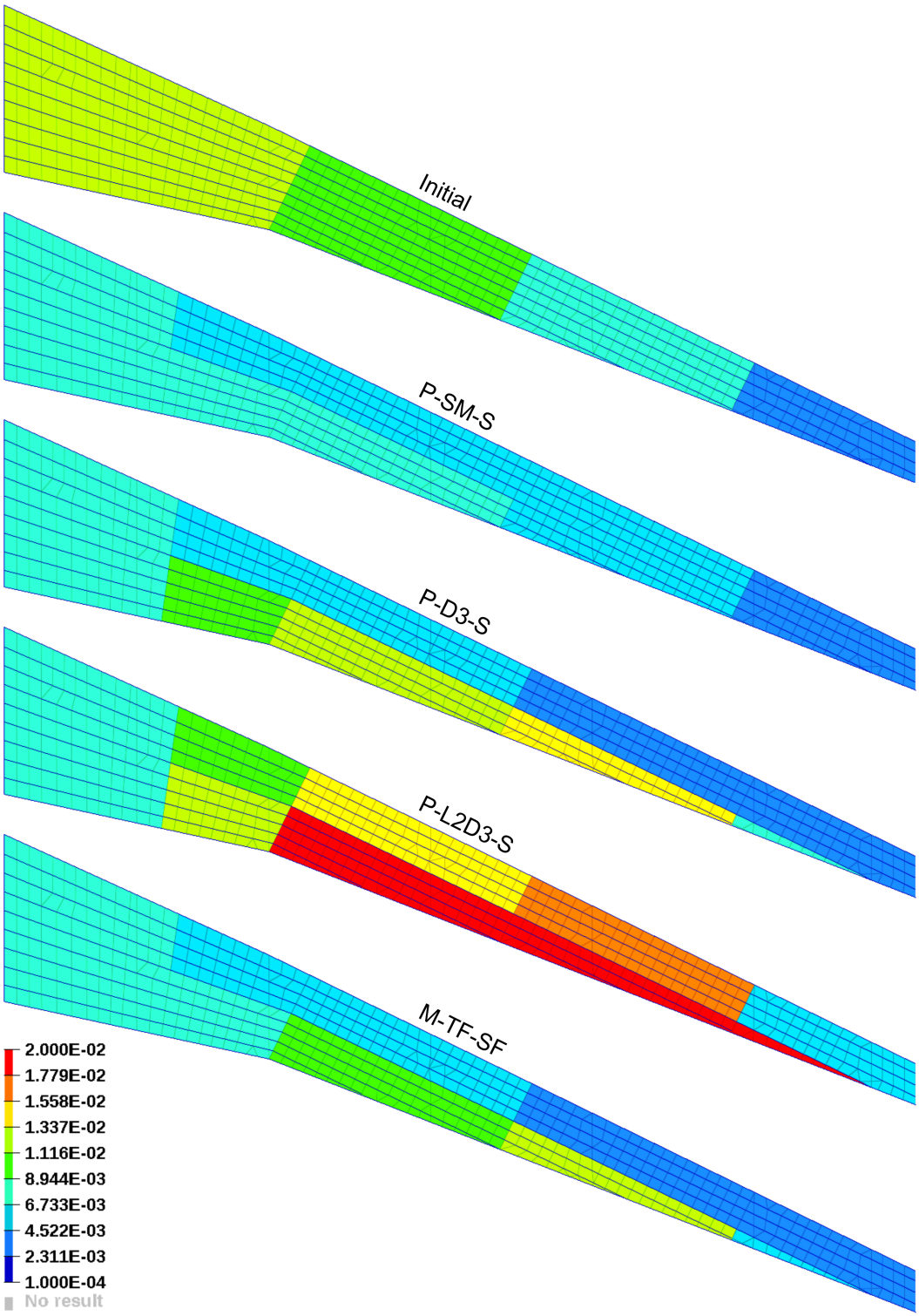

Figure 8.33: Upper skin thickness distribution for various designs

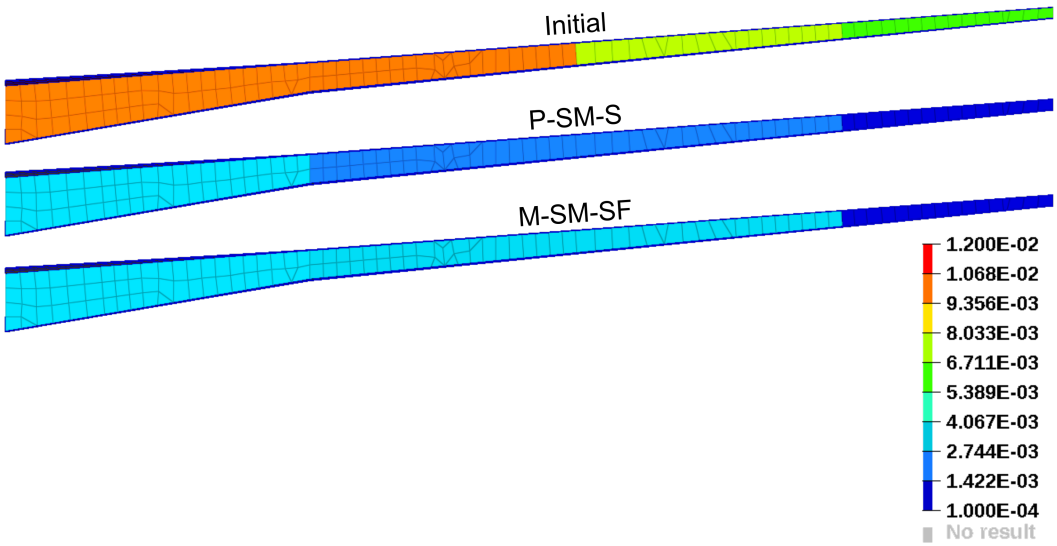

Figure 8.34: Back spar thickness distribution for various designs

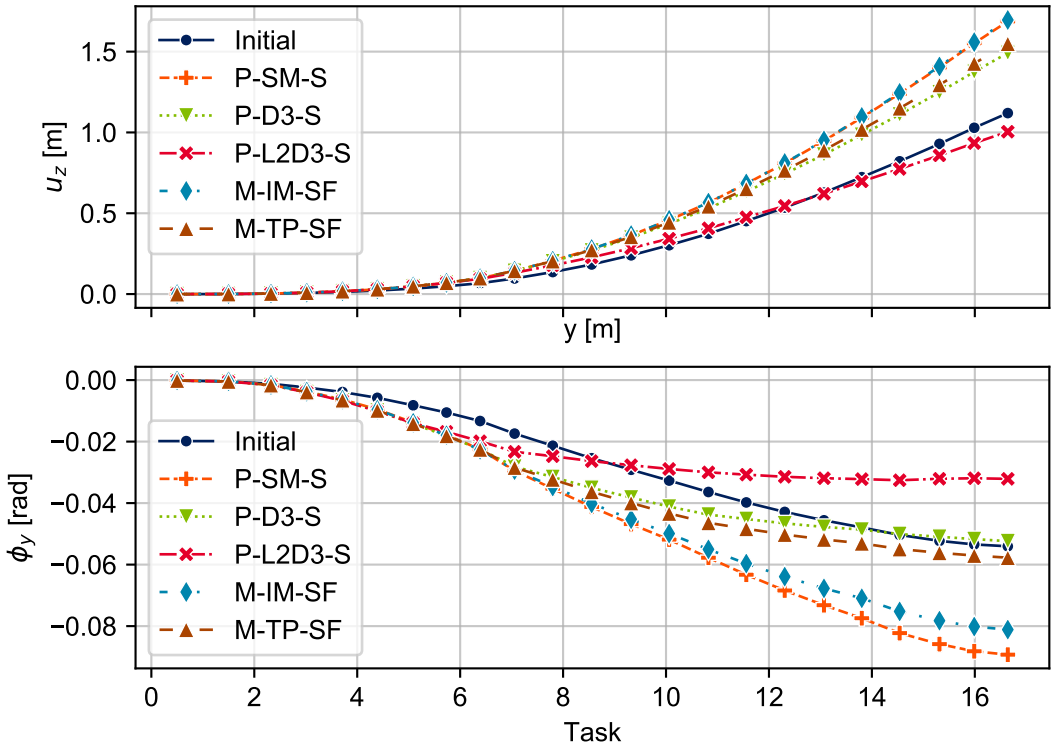

Figure 8.35: Displacement and twist along the span for various designs

Part IV.
Conclusion

9. Conclusion

The main focus of this thesis was to establish a framework to perform optimization tasks in for structural aircraft design in various development stages under the considered of aeroelastic behaviour and mission performance. Such a framework has to support large scale industrial problems where the flight performance is of utmost interest and strict feasibility criteria have to be applied. At the beginning, the requirements for such a framework were investigated. These would differ based on the design stage of the aircraft, in which such a framework should be deployed, and would include various subsystems or models which all together represent an optimization problem. Subsystems like parametrization models, objective functions, constraints model, optimization algorithm and underlying simulation models were at the centre of attention when defining the requirements.

It was concluded that the assembly of these components has to be considered to be an iterative process rather than a simple sequential one, mainly due to the models respective interactions with each other. For example starting from a parametrization model, which can be used to manipulate all sorts of variables connected to a geometry, a material distribution, structural elements or various mission definitions. The concrete choice of parameters has to be done with respect to the existing subsystems. A specific FEM model representation can limit the type of structural variables that are available for influencing elements or materials. At the same time such a limitation can be turned into a requirement for the involved subsystems, meaning that a more detailed structural sizing does necessitates a more detailed structural model in which the targeted variables are well represented. The same concept exemplified for an structural model applies for all the involved subsystems like aerodynamic, trimming, engine, mission model and others. Under considerations of the intended deployment design phase of the proposed framework, a parametrization model consisting of sizing variables and initial fuel state has been established.

The constraints model's main purpose was to assure a design feasibility, which is a necessary requirement for any structural optimization problem. The model has been built from strength and buckling constraints defined on areas of interest across the wing. These constraints were defined on a global FEM. Although this have increased computational costs by having to integrate a higher fidelity structural model, the risk of obtaining an infeasible design due to it not meeting safety regulations later on was deemed too costly.

Part of this thesis was a comparison between various definitions of an objective function. This was mainly due to the fact, that there is not a unique performance definition across all optimization tasks, since those are often defined together with the project requirements. Hence, the optimization framework was developed in such a manner that it can support an arbitrary objective function based on an underlying simulation model, providing its gradients w.r.t. design variables are made available. The investigation has concentrated on comparing point-wise objectives like structural mass, induced drag, lift to drag ratio, fuel burn estimation and a fully integrated mission values like trip fuel, which has been evaluated from a coupled mission analysis.

Range of algorithms that could be utilized to solve the optimization problem had to be considered as well. Both gradient based and stochastic based optimization algorithms are being currently utilized in research and industry. The framework presented in this thesis was developed for the use in a gradient based optimization algorithm, more specifically the NLPQL of Schittkowski [47]. This necessitated an development and implementation of sensitivity analysis to support the constraints model and the objective function. Since the sensitivities of the stress and buckling constraints w.r.t to the sizing variables have already been implemented before the start of the framework development, the main work was done on the sensitivities related to the mission performance analysis. The actual gradient computation presented a large endeavour when coupling the mission analysis into the framework on a theoretical and a practical level. Hence, a rigorous analytical derivation of the implemented mission analysis approach was necessary and presents an important part of the main contribution of this dissertation.

Finally, considerations were made for the choice of the simulation model serving as the main source of physical data in the overall optimization process. It was established that the selection of an adequate simulation model has to be done w.r.t. the design phase and the requirements set by the parametrization, constraints and objective model. This was projected by the various lower, medium and higher fidelity aerodynamic model which were considered. Similar examination was done for the structural and mission models.

The topic of a mission analysis has got an increased attention in the scope of this dissertation, since its inclusion was one of the requirements in the requested framework. After an initial investigation of already existing tools it was decided, that a specialized lightweight tool should be developed for the integration in the proposed framework. This allowed for an efficient implementation of a segment wise formulation of a mission profile definition, which is a closer to the industry's requirements for establishing flight plans. The use of the segments in the flight path definition necessitated an integration of terminal events, which establish boundary conditions for a segment termination. After completing the implementation for the mission flight state analysis, the developed toolbox was extended to allow for a direct mission sensitivity analysis to effectively couple it to a gradient based optimization algorithm. This proved to be more extensive aspect than was the case for the response mission analysis itself and had to correctly consider the terminal events as well. All these requirements for the mission analysis tools resulted in the theory established in the section 5, which was integrated in the developed tool and later utilized in a demonstration optimization process. When preparing the mission model to be utilized in the framework, further requirements on the involved sub-models had to be formulated. These consisted mainly of the need to integrate a suitable trimming analysis which is able to evaluate a flight equilibrium with a satisfactory accuracy, which in turn demands a reliable drag estimator.

The trimming analysis discussed extensively in the section 6 represents a critical component in the developed framework, as it is required to be able to provide feasible flight states for critical loads evaluation used by the constraints model. The trimming analysis was an integral part of the mission analysis as well. Two slightly different approaches were investigated and integrated in the optimization framework, both for distinct pur-

poses. The trimming approach that was already present in the existing Lagrange framework [53] that was implemented as an optimization problem itself, was utilized to trim out the critical load cases. This meant, that the trimming variables defined for this use were considered independent on all the other design variables. This provided to be an effective way to deal with the trimming problem inside of a larger optimization process by keeping the sensitivity analysis free of an unnecessary coupling of variables. This was allowed, since a gradient of these trimming variables w.r.t. any other design variable was not required for any objective or constraints. The second approach to the trimming problem was utilized inside of the mission analysis and for the point-wise performance objective definitions. The motivation behind this different methodology lied in the fact that the constraints and objectives based on the mission analysis required many trimming solutions whose results were used for the consequent time step evaluations. Dealing with the trimming analysis as a closed non-linear equation while reusing its Jacobian matrix for an adjoint sensitivity analysis allowed for an effective computation of gradients of the trimming variables w.r.t. any considered design variables.

A selection of aircraft simulation models, that could support all aspects of the intended framework, was explored. Especially in regards to computational speed, accuracy, sensitivity analysis and its flexibility in integration into the overall work flow. The various considerations, as presented in the section 7, have dealt mainly with an aerodynamics representation, as the requirement to include structural feasibility constraints involving buckling demanded a FEM model built using both 1D and 2D elements. Therefore smaller equivalent beam models couldn't be utilized. In regards to the possible sources to provide aerodynamic loads a trade-off between lower and higher fidelity models was evaluated. It was concluded, that although the suitability of the lower fidelity models is fairly limited due to the range of physical assumptions are necessary, the computational performance advantage outweighs the accuracy disadvantages in the early and mid design stages of an aircraft development. In the scope of this dissertation, the lower fidelity solver AVL based on the potential flow theory has been considered to be a suitable aerodynamic model for the needs of the critical loads analysis, where the drag plays a negligible role in inducing structural deformations. On the other hand, the flight performance evaluation demanded a more reliable drag estimation than a potential flow solver can provide. Though at the same time it had to provide a reasonable computational performance to keep the optimization process with a large number of evaluations feasible and requires and integrated sensitivity analysis to couple with an structural model. To achieve this goal, a concept commonly used in the industry for mission performance computations has been utilized. It consisted of exploiting a precomputed database holding concentrated aerodynamic force and moment coefficients at distributed integration points along the aircraft. The forces and moments at various flight conditions that are used to build up such a database, originate typically from departments responsible for aircraft aerodynamics and therefore come with a high level of quality assurance. Consequently, to allow for the inclusion of an aeroelastic behaviour, both the potential flow based solver and the precomputed database had to be coupled to the structural FEM model. The solver used in the coupled aeroelastic analysis was the fixed point iteration

scheme. A significant advantage of the proposed framework was that it allowed for a utilization of models of variable fidelity. Such a feature allows for a project dependent balancing between computational efforts and accuracy by exchanging the underlying simulation models for ones that better suit the task they serve.

The framework's performance was evaluated in the section 8 by performing an optimization of an civilian aircraft with passenger configuration similar to the Airbus A320. The existing CeRAS project [4] was used as the reference to achieve this task. The data pulled from the CeRAS database included outer surface geometry, sample missions definition, engine performance charts, aerodynamic polars, fuel tanks specifications and a mass breakdown. The missing internal wing, VTP and HTP structures were created inhouse. The structure was based on aircraft references of similar configurations in order to build up a viable stiffness model. The definition of structural elements like spars and ribs was done as to achieve reliable response of the model to changes it would undergo during an optimization process. Based on the demands coming from the parametrization and the constraints model, the FEM structural model was build by using two dimensional shell elements to model all surfaces, rib and spar webs, whereas one dimensional beam and rod elements represented stringers and caps. As a model simplification, all the load carrying structure and majority of the surface were assumed to be out of a single material, aluminium 7075. The only exception to this were the leading and trailing edges of the wing, HTP and VTP. They were build out of a honeycomb type sandwich structure to increase their buckling stiffness while keeping their contribution to the overall bending stiffness of the wing negligible. To allow for the consideration of the influence of deformation during the flight, the structural model was coupled to two different sources of aerodynamic forces. One for the critical loads computation and a different one for the mission analysis and the point-wise performance evaluation. These were the AVL solver and the precomputed database approach respectively. The data used to build up the aerodynamic database was coming from an Euler flow simulation provided by the software SU2. Both of the two aeroelastic simulations were enhanced by a trimming analysis. Additionally since both of these aerodynamic analyses were lacking the ability to provide the viscous drag component, a semi-empirical model for viscous drag estimation had to be coupled into the framework. More specifically this was achieved by using the flat plate skin friction tool FRICTION [107].

Two different approaches to trimming were integrated in the demonstration example to assure that all computed flight states remain feasible. First, the trimming analysis used during the critical loads evaluation inside of the constraints model was based on the assumption of a small angle of attack and was neglecting forces due to the thrust. This simplification was allowed as the angle of attack during the considered flight manoeuvre was expected to stay below 10° and the wing deformation contribution due to the drag component was considered negligible compared to forces due to the lift.. For the purposes of the constraints model, the trimming was considered as a part of the overall optimization problem, resulting in the trimming variables becoming design variables. The flight states experienced during the mission analysis and point performance evaluations were trimmed in a different manner. Mainly due to the need to include

the influence of the drag and thrust more precisely, a non-linear equation system was established to deal with the trimming. The results from this trimming analysis and the connected aeroelastic simulation were linked together with engine performance charts in order to build up a simulation model that could be used for performance evaluation.

The parametrization model consisted of 48 structural design variables that were connected to the thickness of wing surface patches and to the cross sectional properties of stringers. The feasibility of any optimized design was assured by integrating stress and buckling constraints across the structural elements inside of the criteria model. If the mission analysis was a part of a specific optimization problem, the terminal reserve fuel requirement was included in the constraints model as well. The optimization algorithm NLPQL was used in the optimization model for all the considered objective functions.

Before executing the optimization tasks, validation of the aircraft simulation model was performed, with the findings being presented in the section 8.8. Firstly, the behaviour of the utilized aerodynamic models was investigated by looking at the performance polars, both for rigid and elastic behaviour, while comparing the resulting curves with the ones provided by the CeRAS project. Conforming to a prediction, it was shown that the AVL based results provided a limited reliability in the area of an induced drag estimation when compared to the reference data. Still, it provided a viable pressure distribution for the use in the structural constraints model. The Euler based polars have provided significantly better match w.r.t. to the reference data, while showing a steeper tendency between drag and lift in the trimmed polars. The influence of elasticity on the aerodynamic polars for the initial aircraft design has been investigated as well, the difference was staying below 2.95% and 1.57% in the case of the AVL and Euler simulation respectively.

The fully coupled mission sensitivity analysis has been limited to two cruise segments and one climb step section in between. This allowed for less computation efforts, since it was not necessary to simulate the mission from the take-off till landing, while having the predominant part responsible for fuel consumption fully simulated. As a first step towards the validating the developed lightweight mission evaluation tool, the defined mission has been computed using the rigid and elastic aerodynamic polars and consequently compared with the reference mission data coming from the CeRAS database. Comparing the flight history resulting from a mission simulation, which had been run using aerodynamic polars provided by the original CeRAS database, against a reference mission history from the same database resulted in the fuel mass difference during the cruise segments staying below 0.18%. In an attempt to predict the impact of elasticity on the mission analysis, the reference aerodynamic polars were replaced with those specifically generated using the AVL and SU2 solvers, once assuming a rigid jig shape and once an in-flight shape. The difference has proven itself to be accumulative over time resulting of up to 4.0% relative difference of fuel mass at the end of the final simulated cruise segment. Next step was to replace the use of polars in the mission analysis with a fully coupled trimmed aeroelastic model. When tested, the fuel mass at the end of the last cruise segment differed by 7.36% in comparison to the results obtained by using the polars, even though the aerodynamic forces were coming from the same source. This large discrepancy was attributed to the difference in trimming models and the fact, that the

coupled aeroelastic analysis more accurately modeled the actual deformations together with updates to the fuel mass. The reliability of the mission analysis w.r.t. a chosen time step has come into question as well, which was followed upon by a convergence study. Even though the behaviour of the fuel mass over time seemed to be mostly linear during the cruise segments, the accuracy of the response values at the end of the simulated segments was strongly dependent on the number of time steps used to discretize them. This can be most like ascribed to the choice of a relatively simple time integration algorithm, this being the Forward Euler. For both mission state and sensitivity analysis 38 steps have been used to approximate the simulated segments, which has shown a difference of 1.07% in comparison to a solution obtained with 2102 steps. The same investigation has been performed for the mission sensitivity analysis, displaying an error up to 0.15% in the case of the fuel design variable. The maximum error across sampled sizing design variables came up to 0.77%.

Finally, using the established procedures several optimization problems have been defined, which have shared the structural constraints model and the sizing parametrization model. The target was to investigate the applicability end efficiency of the various objectives, ranging from a simple structural mass to a trip fuel computed by the coupled mission analysis. The main design variables considered across all the cases were the structural sizing variables which were linked to various components of the wing. Additionally, in the case of optimization with a coupled mission analysis, an extra design variable has been introduced to allow for a concurrent update of the amount of fuel present at the beginning of the mission. This was to keep the fuel on board to only the required amount as would be the case for an actual real case. At the same time the constraints model was enhanced by a constraint that assured that the amount of fuel remaining in the tanks at the end of the mission stayed at or above 15.56% of trip fuel consumed during the flight. All of the investigated optimization problems have managed to successfully converge to their relative optima. To be able to fairly compare the obtained designs when evaluating those coming from an analysis with integrated fuel constraint and those without it, an estimation of the fuel required for the design mission has been performed. Only the fuel at the beginning of a mission was used as a design variable, while the structural design was updated to represent the one obtained by previous optimization.

One of the observations made, was that some of the considered optimization problems have been redundant, since they led to identical designs as others. Such a redundancy was found in the case of an objective function using the total initial mass with and without the reserve fuel constraint while using only structural design variables. The resulting structural thickness distribution across the parts subject to the design optimization was identical in both of these cases. Most likely due to the equal objective functions and the fact, that the fuel constraint was always satisfied, since a reduction in the structural weight brought an improvement in fuel consumption during the mission. First noticeable difference was observed in the case which was using the same objective, but added the initial fuel as a design variable. The resulting designs were very similar, with the only difference being an increased stiffness of the back spar of the wing. This has led to an almost identical bending stiffness while strongly increasing the overall torsion stiffness

of the whole wing. When comparing these cases it was shown, that the model with the increased torsional stiffness conferred an improvement of 1.75% and 1.97% in saved fuel for the case without and with a fuel design variable respectively. The same behaviour wasn't observed when evaluating the influence of the initial fuel as a design variable together with the trip fuel as the objective function. In this case the addition of the fuel design variable didn't improve or degrade the performance and resulted in a design with only negligible design differences in comparison to the one coming from the optimization problem without the fuel design variable. As such, using trip fuel as the objective function resulted in saving 2.25% of the on-board fuel required before the take-off. The lack of any meaningful difference between the cases with and without the initial fuel being a design variable was probably the result of fully exploiting the available design space using an adequate objective function while applying only the sizing design variables. A similar result was achieved by using the induced drag as an objective function, where the specific value was estimated by using a weighted average from six uniformly distributed points across the two otherwise simulated cruise segments. This led to a design identical to the one using point-wise fuel burn estimation at those same six sample points, resulting in an 2.23% improvement in saved trip fuel. This presents the point-wise performance estimation as an adequate substitute for the fully coupled analysis for the investigated aircraft configuration. One outlier in the scope of the investigated objective functions was observed in the use of the lift to drag ratio as the objective function. In this case the amount of fuel saved was computed to be -0.03% even though the lift to drag ratio itself has been shown to be better at every point of the design mission than any of the alternative designs. This was likely the result of the increased structural stiffness, which was achieved by overall addition of thickness of almost all elements across the wingbox. Such an unrestricted increase in stiffness has come which an overall increase in weight, resulting in the observed increased fuel burn during the mission duration. These optimization results have been attributed to the fact, that an increase of the lift to drag ratio can be most easily achieved by a an increase of lift, rather then a decrease in induced drag. Due to the trimming solution being done for a non-fixed aircraft weight, the optimizer found it beneficial to increase the structural mass of the model and hence the lift. As such this objective function could not be recommended for a general use in performance optimization.

It was shown, that using the developed framework, a viable way to include a fully coupled mission analysis in an optimization problem is possible. The implemented framework was used to estimate an possible impact of a fully coupled mission analysis on an aircraft design process. In the presented form, the developed framework has utilized a lower fidelity aerodynamics model and a fixed aerodynamic database with medium fidelity data. At the same time, limiting the design space to only structural variables represented a industrial case where an outer shape of the aircraft had already been defined and fixed. These aspects place the demonstration example, which has been used to evaluate the established framework, somewhere around the beginning and mid of a preliminary design phase. Another viable application would be in the cases of a redesign of an existing aircraft with updated requirements. In that case, it represents a common

situation in which the outer jig shape of wings is required to stay the same to reduce the amount of re-tooling necessary and hence limit costs. This thesis has presented a design exploitation functionality by merging the flight performance optimization with the structural design into a single optimization problem. The included fully coupled mission analysis, although it presented non-negligible additional computational demands, did allow for a simultaneous structural design and a flight performance optimization, ensuring that one does not compromise the other. Such an optimization problem can reduce development costs by avoiding iterative sequential process across departments, saving time and resources.

The framework expanded upon in this thesis provided a viable way to merge the structural design and the mission performance analysis into a singular optimization task. During its development, the focus was on the inclusion of an aeroelastic behaviour during the flight and the applicability for optimization problems at early and mid preliminary stages of the aircraft design. As such, low and medium fidelity aerodynamic models were used to generate forces during flight manoeuvres. A promising avenue for improvement is represented by the potential utilization of higher fidelity aerodynamic models like those based on the RANS theory. As long as these models are able to provide sensitivities required for the trimming analysis and those related to the investigated design space, it is possible to fully integrate them into the current framework, providing increased accuracy. The main benefit of concentrating on the modeling fidelity lies in a consequent expansion of the applicability range of the presented framework to later aircraft design stages. A simple but valuable enhancement of the proposed approach for the mission performance optimization could be found in the inclusion of several mission profiles into one objective. In this thesis only a single mission was simulated to obtain the performance values, whereas for an actual design applicable in an industrial setting there would be a necessity to consider several various mission profiles during the optimization process. This observation was based on the fact that an aircraft has to complete various missions during its lifetime and a structural design optima for one mission profile isn't necessarily the same for an another. To accommodate for such a variability, a weighted combination of flight profiles could be integrated into a single objective function, either based on historical data for a given configuration type or coming from design requirements. Alternatively, a choice of a mission mix could be made with a target to expand the payload-range diagram, providing greater flexibility for a deployment by an airline. Following along the need to improve the computational performance, an adjoint methodology for the mission sensitivity analysis should be integrated. Due to the existing software capabilities of the tools utilized in the framework, the development was limited to the direct sensitivity method. Move to the adjoint based computation would provide a significant speed up, especially in optimization problems with a large number of design variables. Lastly, it has been shown that although a pure structural optimization can still provide a significant improvement by achieving an adequate in-flight shape, it provides only a limited room for design exploitation. Together with higher fidelity aerodynamic models, an inclusion of shape design variables is necessary to reach a global optima for the mission performance optimization.

Part V.
Appendix

A. Coordinate Systems

There are few coordinate systems that have to be considered throughout the whole process. The figure A.1 described the transformation between earth-fixed axis system (x_0, y_0, z_0) and body system (x, y, z).

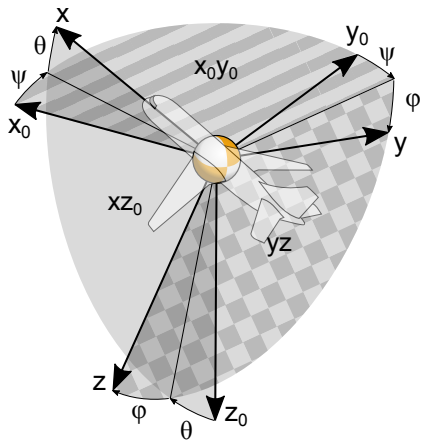

Figure A.1: Relation between aircraft-carried earth axis system and body axis system

Based on the yaw angle ψ, the pitch angle θ and the roll angle ϕ the following matrices are introduced

$$T_\psi(\psi) = \begin{bmatrix} \cos(\psi) & -\sin(\psi) & 0 \\ \sin(\psi) & \cos(\psi) & 0 \\ 0 & 0 & 1 \end{bmatrix} \tag{A.1}$$

$$T_\theta(\theta) = \begin{bmatrix} \cos(\theta) & 0 & \sin(\theta) \\ 0 & 1 & 0 \\ -\sin(\theta) & 0 & \cos(\theta) \end{bmatrix} \tag{A.2}$$

$$T_\phi(\phi) = \begin{bmatrix} 1 & 0 & 0 \\ 0 & \cos(\phi) & -\sin(\phi) \\ 0 & \sin(\phi) & \cos(\phi) \end{bmatrix} \tag{A.3}$$

using the final transformation matrix between the aircraft-carried earth axis system and the body system

$$^{0b}T(\psi,\theta,\phi) = T_\psi(\psi)\cdot T_\theta(\theta)\cdot T_\phi(\phi) \tag{A.4}$$

any arbitrary vector given in a body coordinate system $^b\mathbf{r}$ can be transformed into an aircraft-carried ground system using

$$^0\mathbf{r} = {}^{0b}T\cdot {}^b\mathbf{r} \tag{A.5}$$

and since all of the introduced transformation matrix are orthogonal a transformation of the coordinate system in the opposite direction is

$$^b\mathbf{r} = {}^{0b}T^T\cdot {}^0\mathbf{r} \tag{A.6}$$

Additionally there is the transformation between body system (x, y, z) and air-path system (x_a, y_a, z_a) as shown in the figure A.2.

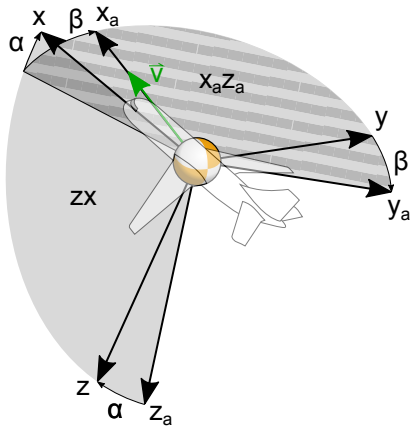

Figure A.2: Relation between body axis system and air-path axis system

The respective transformation matrices are

$$T_\alpha(\alpha) = \begin{bmatrix} \cos(\alpha) & 0 & -\sin(\alpha) \\ 0 & 1 & 0 \\ \sin(\alpha) & 0 & \cos(\alpha) \end{bmatrix} \tag{A.7}$$

$$T_\beta(\beta) = \begin{bmatrix} \cos(\beta) & -\sin(\beta) & 0 \\ \sin(\beta) & \cos(\beta) & 0 \\ 0 & 0 & 1 \end{bmatrix} \tag{A.8}$$

and the final transformation matrix can be expressed as

$$^{ba}T(\alpha, \beta) = T_\alpha(\alpha) \cdot T_\beta(\beta) \tag{A.9}$$

which can be used to transform an arbitrary vector in air-path coordinate system to a body coordinate system and vice versa using

$$^{b}\mathbf{r} = ^{ba}T \cdot ^{a}\mathbf{r} \tag{A.10}$$

$$^{a}\mathbf{r} = ^{ba}T^{T} \cdot ^{b}\mathbf{r} \tag{A.11}$$

last transformation necessary is between a body coordinate system (x, y, z) and structural coordinate system (x_s, y_s, z_s) in which the structural model of an aircraft is evaluated and loads are applied. The structural coordinate system can be obtained easily by rotating the body coordinate system around its y axis so that the longitudinal structural axis x_s is parallel to the longitudinal body axis x but points in the opposite direction from the tip of an aircraft to its tail. The relation of the coordinate systems is shown in the figure A.3.

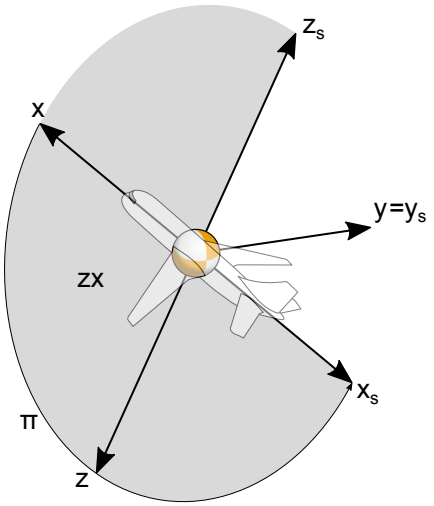

Figure A.3: Relation between body axis system and structural axis system

$$^{bs}T = \begin{bmatrix} -1 & 0 & 0 \\ 0 & 1 & 0 \\ 0 & 0 & -1 \end{bmatrix} \tag{A.12}$$

This matrix can be used to transform any arbitrary vector given in an structure coordinate frame $^{s}\mathbf{r}$ and vice versa.

$$ {}^{b}\mathbf{r} = {}^{bs}T \cdot {}^{s}\mathbf{r} \tag{A.13} $$

$$ {}^{s}\mathbf{r} = {}^{bs}T^{T} \cdot {}^{b}\mathbf{r} \tag{A.14} $$

The transformations can be compounded to allow for the coordinate transformations between the various systems. The ones of relevance later on are the transformation to the structural coordinate system. A transformation from an air-path coordinate frame to a structural frame is

$$ {}^{s}\mathbf{r} = {}^{bs}T^{T} \cdot {}^{b}\mathbf{r} = \underbrace{{}^{bs}T^{T} \cdot {}^{ba}T}_{{}^{sa}T} {}^{a}\mathbf{r} \tag{A.15} $$

and the transformation from a aircraft-carried ground frame to structural frame is

$$ {}^{s}\mathbf{r} = {}^{bs}T^{T} \cdot {}^{b}\mathbf{r} = \underbrace{{}^{bs}T^{T} \cdot {}^{0b}T^{T}}_{{}^{s0}T} {}^{0}\mathbf{r} \tag{A.16} $$

Part VI.
References

References

[1] IATA. Fact sheet 3: Tracking aviation efficiency. Technical report, IATA, 2019. iv, 2

[2] IATA. Airline Industry Economic Performance - 2016 End-year - Tables. Technical report, IATA, 2016. iv, 3

[3] IATA. Airline Industry Economic Performance - June 2020 - Data tables. Technical report, IATA, 2020. iv, 2, 3

[4] K. Risse, K. Schäfer, F. Schültke, and E. Stumpf. Ceras - central reference aircraft data system. Webpage, 2014. v, 72, 78, 81, 82, 83, 90, 109

[5] Kermit G. Pratt and Walter G. Walker. A revised gust-load formula and a re-evaluation of v-g data taken on civil transport airplanes from 1933 to 1950. Technical report, National Advisory Committee for Aeronautics. Langley Aeronautical Lab.; Langley Field, VA, United States, 1954. vi, 78, 80

[6] Airbus. Global Market Forcast: Cities, Airports & Aircraft 2019-2038. techreport, Airbus S.A.S., 2019. 2

[7] ICAO. ICAO Environmental Report. Technical report, ICAO, 2010. 2

[8] Daniel P Raymer. *Aircraft Design: A Conceptual Approach*, volume AIAA Education Series. Amer Inst of Aeronautics, 5 edition, 2012. 3, 52

[9] Dimitri Mavris and Daniel DeLaurentis. Methodology for examining the simultaneous impact of requirements, vehicle characteristics, and technologies on military aircraft design. 01 2000. 4

[10] Walter Tollmien, Hermann Schlichting, Henry Görtler, and F. W. Riegels. Über tragflügel kleinsten induzierten widerstandes. In *Ludwig Prandtl Gesammelte Abhandlungen*, pages 556–561. Springer Berlin Heidelberg, 1961. 5, 12

[11] R. T. Jones. The spanwise distribution of lift for minimum induced drag of wings having a given lift and a given bending moment. techreport 2249, Ames Aeronautical Laboratory, 1950. 5, 12

[12] Raphael T. Haftka and E. Carson Yates. Repetitive flutter calculations in structural design. *Journal of Aircraft*, 13(7):454–461, jul 1976. 5, 12

[13] Raphael T. Haftka. Optimization of flexible wing structures subject to strength and induced drag constraints. *AIAA Journal*, 15(8):1101–1106, aug 1977. 5, 12

[14] Jean-Francois M. Barthelemy and Fred D. Bergen. Shape Sensitivity Analysis of Wing Static Aeroelastic Characteristics. *Journal of Aircraft*, 26(8):712–717, 1988. 5

[15] Peter J. Roehl, Dimitri N. Mavris, and Daniel P. Schrage. Combined aerodynamic and structural optimization of a high-speed civil transport wing. In *36th Structures, Structural Dynamics and Materials Conference*. American Institute of Aeronautics and Astronautics, apr 1995. 5, 12, 21

[16] J. Reuther, A. Jameson, J. Farmer, L. Martinelli, and D. Saunders. Aerodynamic shape optimization of complex aircraft configurations via an adjoint formulation. In *34th Aerospace Sciences Meeting and Exhibit*. American Institute of Aeronautics and Astronautics, jan 1996. 6

[17] W.Kyle Anderson and V. Venkatakrishnan. Aerodynamic design optimization on unstructured grids with a continuous adjoint formulation. *Computers & Fluids*, 28(4-5):443–480, may 1999. 6

[18] Jamshid Samareh. Aerodynamic shape optimization based on free-form deformation. In *10th AIAA/ISSMO Multidisciplinary Analysis and Optimization Conference*. American Institute of Aeronautics and Astronautics, aug 2004. 6

[19] Mark Drela. Pros & Cons of Airfoil Optimization. In *Frontiers of Computational Fluid Dynamics 1998*, pages 363–381. WORLD SCIENTIFIC, nov 1998. 6, 12, 88

[20] Susan E. Cliff, James J. Reuther, David A. Saunders, and Raymond M. Hicks. Single-point and multipoint aerodynamic shape optimization of high-speed civil transport. *Journal of Aircraft*, 38(6):997–1005, nov 2001. 6

[21] Marian Nemec, David W. Zingg, and Thomas H. Pulliam. Multipoint and multi-objective aerodynamic shape optimization. *AIAA Journal*, 42(6):1057–1065, jun 2004. 6

[22] Howard P. Buckley, Beckett Y. Zhou, and David W. Zingg. Airfoil optimization using practical aerodynamic design requirements. *Journal of Aircraft*, 47(5):1707–1719, sep 2010. 6

[23] David J. J. Toal and Andy J. Keane. Efficient multipoint aerodynamic design optimization via cokriging. *Journal of Aircraft*, 48(5):1685–1695, sep 2011. 6

[24] K. Maute, M. Nikbay, and C. Farhat. Analytically Based Sensitivity Analysis and Optimization of Nonlinear Aeroelastic Systems. In *8th AIAA/USAF/NASA/ISSMO Symposium on Multidisciplinary Analysis and Optimization*, pages 1–10, 2000. 6, 12

[25] K. Schittkowski, C. Zillober, and R. Zotemantel. Numerical comparison of nonlinear programming algorithms for structural optimization. *Structural Optimization*, 7(1-2):1–19, feb 1994. 6

[26] John Frederick Gundlach. *Multi-disciplinary design optimization of subsonic fixed-wing unmanned aerial vehicles projected through 2025*. PhD thesis, 01 2004. 6

[27] E. Trefftz. Prandtlsche tragflächen- und propellertheorie. In *Vorträge aus dem Gebiete der Hydro- und Aerodynamik (Innsbruck 1922)*, pages 34–46. Springer Berlin Heidelberg, 1921. 6

[28] David L. Carroll. Chemical laser modeling with genetic algorithms. *AIAA Journal*, 34(2):338–346, feb 1996. 6

[29] Ruben Perez, Peter Jansen, and Joaquim Martins. Aero-Structural Optimization of Non-Planar Lifting Surface Configurations. In *12th AIAA/ISSMO Multidisciplinary Analysis and Optimization Conference*. American Institute of Aeronautics and Astronautics, sep 2008. 6, 12, 22

[30] G. J. Kennedy. Parallel Solution Methods for Aerostructural Analysis and Design Optimization. In *13th AIAA/ISSMO Multidisciplinary Analysis Optimization Conference*, number September, 2010. 7, 16

[31] Rhea Liem, Gaetan Kenway, and Joaquim R. R. A. Martins. Multi-point, multi-mission, high-fidelity aerostructural optimization of a long-range aircraft configuration. In *12th AIAA Aviation Technology, Integration, and Operations (ATIO) Conference and 14th AIAA/ISSMO Multidisciplinary Analysis and Optimization Conference*. American Institute of Aeronautics and Astronautics, sep 2012. 7, 12

[32] Philip E. Gill, Walter Murray, and Michael A. Saunders. SNOPT: An SQP algorithm for large-scale constrained optimization. *SIAM Review*, 47(1):99–131, jan 2005. 7

[33] G. A. Wrenn. An indirect method for numerical optimization using the Kreisselmeier-Steinhauser function. Technical report, NASA, 1989. 7

[34] Nicholas M. K. Poon and Joaquim R. R. A. Martins. An adaptive approach to constraint aggregation using adjoint sensitivity analysis. *Structural and Multidisciplinary Optimization*, 34(1):61–73, dec 2006. 7

[35] Joaquim R. R. A. Martins and John T. Hwang. Review and Unification of Methods for Computing Derivatives of Multidisciplinary Computational Models. *AIAA Journal*, 51(11):2582–2599, 2013. 8

[36] John Hwang, Dae Young Lee, James Cutler, and Joaquim R. R. A. Martins. Large-scale MDO of a small satellite using a novel framework for the solution of coupled systems and their derivatives. In *54th AIAA/ASME/ASCE/AHS/ASC Structures,*

Structural Dynamics, and Materials Conference. American Institute of Aeronautics and Astronautics, apr 2013. 8

[37] Joaquim R. R. A. Martins and Andrew B. Lambe. Multidisciplinary Design Optimization: A Survey of Architectures. *AIAA Journal*, 51(9):2049–2075, 2013. 8

[38] Tobias Wunderlich. *Multidisziplinäre Optimierung von Flügeln für Verkehrsflugzeuge mit Berücksichtigung der statischen Aeroelastizität*. PhD thesis, Technische Universität Braunschweig, 2013. 8, 12, 22

[39] T. H. Rowan. *Functional Stability Analysis of Numerical Algorithms*. PhD thesis, Department of Computer Sciences, University of Texas at Austin, USA, 1990. 8

[40] Gaetan K. W. Kenway and Joaquim R. R. A. Martins. Multipoint High-Fidelity Aerostructural Optimization of a Transport Aircraft Configuration. *Journal of Aircraft*, 51(1):144–160, jan 2014. 8, 12, 16, 22, 29, 55

[41] Francois Gallard. *Aircraft Shape Optimization for Mission Performance*. PhD thesis, IRT Saint Exupery, 2014. 8, 16, 19, 22, 35, 89

[42] Trent W. Lukaczyk, Andrew D. Wendorff, Michael Colonno, Thomas D. Economon, Juan J. Alonso, Tarik H. Orra, and Carlos Ilario. SUAVE: An open-source environment for multi-fidelity conceptual vehicle design. In *16th AIAA/ISSMO Multidisciplinary Analysis and Optimization Conference*. American Institute of Aeronautics and Astronautics, jun 2015. 9

[43] Emilio M. Botero, Andrew Wendorff, Timothy MacDonald, Anil Variyar, Julius M. Vegh, Trent W. Lukaczyk, Juan J. Alonso, Tarik H. Orra, and Carlos Ilario da Silva. SUAVE: An open-source environment for conceptual vehicle design and optimization. In *54th AIAA Aerospace Sciences Meeting*. American Institute of Aeronautics and Astronautics, jan 2016. 9

[44] Timothy MacDonald, Emilio Botero, Julius M. Vegh, Anil Variyar, Juan J. Alonso, Tarik H. Orra, and Carlos R. Ilario da Silva. SUAVE: An open-source environment enabling unconventional vehicle designs through higher fidelity. In *55th AIAA Aerospace Sciences Meeting*. American Institute of Aeronautics and Astronautics, jan 2017. 9

[45] Matthew Clarke, Jordan Smart, Emilio M. Botero, Walter Maier, and Juan J. Alonso. Strategies for posing a well-defined problem for urban air mobility vehicles. In *AIAA Scitech 2019 Forum*. American Institute of Aeronautics and Astronautics, jan 2019. 9

[46] Sebastian Moritz Deinert. *Shape and Sizing Optimization of Aircraft Structures with Aeroelastic and Induced Drag Requirements*. Doctoral, TU Munich, 2016. 9, 16, 19, 20, 22, 25, 29, 89

[47] K. Schittkowski. NLPQL: A fortran subroutine solving constrained nonlinear programming problems. *Annals of Operations Research*, 5(2):485–500, jun 1986. 9, 27, 95, 107

[48] Eric S. Hendricks, Robert D. Falck, and Justin S. Gray. Simultaneous propulsion system and trajectory optimization. In *18th AIAA/ISSMO Multidisciplinary Analysis and Optimization Conference*, 2017. 9

[49] Robert D. Falck, Jeffrey Chin, Sydney L. Schnulo, Jonathan M. Burt, and Justin S. Gray. Trajectory optimization of electric aircraft subject to subsystem thermal constraints. In *18th AIAA/ISSMO Multidisciplinary Analysis and Optimization Conference*. American Institute of Aeronautics and Astronautics, jun 2017. 9

[50] David A. Burdette, Gaetan K. Kenway, and Joaquim R. R. A. Martins. Performance evaluation of a morphing trailing edge using multipoint aerostructural design optimization. In *57th AIAA/ASCE/AHS/ASC Structures, Structural Dynamics, and Materials Conference*. American Institute of Aeronautics and Astronautics, jan 2016. 10

[51] John P. Jasa, John T. Hwang, and Joaquim R. R. A. Martins. Design and trajectory optimization of a morphing wing aircraft. In *2018 AIAA/ASCE/AHS/ASC Structures, Structural Dynamics, and Materials Conference*. American Institute of Aeronautics and Astronautics, jan 2018. 10, 12

[52] Eytan Adler and Joaquim R. Martins. Aerostructural wing design optimization considering full mission analysis. In *AIAA SCITECH 2022 Forum*. American Institute of Aeronautics and Astronautics, jan 2022. 10, 12

[53] G. Schuhmacher, F.Daoud, Ögmundur Petersson, and M.Wagner. Multidisciplinary Airframe Design Optimisation. In *28th International Congress of the Aeronautical Sciences*, 2012. 13, 23, 27, 108

[54] Dimitri Simos and Lloyd R. Jenkinson. Optimization of the conceptual design and mission profiles of short-haul aircraft. *Journal of Aircraft*, 25(7):618–624, jul 1988. 16, 19

[55] Giampietro Carpentieri. *An Adjoint-Based Shape-Optimization Method for Aerodynamic Design*. Prof, TU Delft, 2009. 16

[56] Takemiya Tetsushi. *Aerodynamics Design Applying Automatic Differentiation and Using Robust Variable Fidelity Optimization*. Phd, Georgie Institute of Technology, 2008. 16

[57] Tobias Wunderlich. Multidisziplinärer Entwurf und Optimierung von Flügeln für Verkehrsflugzeuge. 09 2009. 16

[58] Jordi Pons-prats, Gabriel Bugeda, and Eugenio Onate. Robust Shape Optimization in Aeronautics using stochastic analysis and evolutionary algorithms. In *Proceedings of the Institution of Mechanical Engineers Part G Journal of Aerospace Engineering*, number June 2016, 2010. 16

[59] Jeff Fike, Joaquim Martins, and Juan J. Alonso. Mathematical details of adjoint-based shape optimization for the Euler and Reynolds-Averaged Navier-Stokes equations. Technical report, 2011. 16

[60] Olivier Amoignon. *Adjoint-based aerodynamic shape optimization*. Dissertation, Uppsala University, 2003. 16

[61] K. Maute, M. Nikbay, and C. Farhat. Coupled Analytical Sensitivity Analysis and Optimization of Three-Dimensional Nonlinear Aeroelastic Systems. *AIAA Journal*, 39(11), 2001. 16, 21

[62] Karthik Mani and Dimitri J. Mavriplis. Adjoint-Based Sensitivity Formulation for Fully Coupled Unsteady Aeroelasticity Problems. *AIAA Journal*, 47(8), 2009. 16

[63] Jason Kao, John Hwang, Joaquim Martins, Justin S. Gray, and Kenneth T. Moore. A modular adjoint approach to aircraft mission analysis and optimization. In *56th AIAA/ASCE/AHS/ASC Structures, Structural Dynamics, and Materials Conference*. American Institute of Aeronautics and Astronautics, jan 2015. 16, 22, 55

[64] Rhea P. Liem, Gaetan K. W. Kenway, and Joaquim R. R. A. Martins. Multimission Aircraft Fuel-Burn Minimization via Multipoint Aerostructural Optimization. *AIAA Journal*, 53(1):104–122, jan 2014. 16

[65] H. Baier, C. Seeßelberg, and B. Specht. *Optimierung in der Struktur-mechanik*. LSS Verlag, 2006. 16, 26

[66] G. N. Vanderplaats. *Multidiscipline Design Optimization*. Vanderplaats Research & Development, Inc., 2007. 16, 26

[67] K. Maute and M. Allen. Conceptual design of aeroelastic structures by topology optimization. *Structural and Multidisciplinary Optimization*, 27(1-2):27–42, may 2004. 18

[68] Kai A. James, Graeme J. Kennedy, and Joaquim R.R.A. Martins. Concurrent aerostructural topology optimization of a wing box. *Computers & Structures*, 134:1–17, apr 2014. 18

[69] Antony Jameson. Transonic Flow Calculations. Technical report, Princeton University, 2014. 19

[70] Daniel Raymer. *Aircraft Design: A Conceptual Approach, Sixth Edition*. American Institute of Aeronautics and Astronautics, Inc., aug 2018. 20, 22, 83

[71] S. Iglesias and W. Mason. Optimum Spanloads Incorporating Wing Structural Weight. In *First AIAA Aircraft Technology, Integration, and Operations Forum*, 2001. 22

[72] Joseph Shigley. *Mechanical engineering design*. McGraw-Hill, New York, NY, 2004. 23

[73] Jack R. Vinson and Robert L. Sierakowski. *The Behavior of Structures Composed of Composite Materials*. Springer-Verlag GmbH, 2006. 23

[74] R. S. Sandhu. A survey of failure theories of isotropic and anisotropic materials. Technical report, Wright-Patterson Air Force Base, Ohio, 1972. 23

[75] E. F. Bruhn. *Analysis and design of flight vehicle structures*. S.R. Jacobs, Indianapolis, 1973. 23

[76] Rhea P. Liem, Charles A. Mader, and Joaquim R. R. A. Martins. Surrogate models and mixtures of experts in aerodynamic performance prediction for aircraft mission analysis. *Aerospace Science and Technology*, 43:126–151, jun 2015. 29, 55

[77] Hyunseok Lee, Hyungjoon Lee aand Einkeun Kwak, and Seungsoo Lee. Development of Aircraft Mission Performance Analysis Program. *International Journal of Aeronautical and Space Sciences*, 2013. 35, 55

[78] Andrew B. Lambe and Joaquim R. R. A. Martins. Extensions to the design structure matrix for the description of multidisciplinary design, analysis, and optimization processes. *Structural and Multidisciplinary Optimization*, 46(2):273–284, jan 2012. 45

[79] C. A. J. Fletcher. *Computational Techniques for Fluid Dynamics 2*. Springer-Verlag Berlin Heidelberg, 2 edition, 1996. 50

[80] Joseph Katz and Allen Plotkin. *Low-Speed Aerodynamics*. Cambridge University Press, 2 edition, 2001. 50, 52, 53, 54

[81] T. Cebeci, J. P. Shao, F. Laurendeau, and E. Kafyeke. *Computational Fluid Dynamics for Engineers: From Panel to Navier-Stokes Methods with Computer Programs*. Springer Berlin Heidelberg New York, 2005. 50, 52

[82] J. J. Bertin and R. M. Cummings. *Aerodynamics for Engineers*. Pearson Education Limited, 6 edition, 2014. 51

[83] Beer Gernot, Ian Smith, and Christian Duenser. *The Boundary Element Method with programming: For Engineers and Scientists*. Springer-Verlag Wien, 2008. 53

[84] F. W. Lanchester. Aerodynamics: Constituting the First Volume of a Complete Work on Aerial Flight. *Nature*, 78(2024):337–338, aug 1908. 53

[85] V. Falkner. The calculation of aerodynamic loading on surfaces of any shape. Technical report, Ministry of Aircraft Production, 08 1943. 53

[86] EDWARD ALBANO and WILLIAM P. RODDEN. A doublet-lattice method for calculating lift distributions on oscillating surfaces in subsonic flows. *AIAA Journal*, 7(2):279–285, feb 1969. 55

[87] Thiemo Kier and Gertjan Looye. Unifying manoeuvre and gust loads analysis. In *Conference: International Forum on Aroelasticity and Structural Dynamics*, 06 2009. 55

[88] D. S. Hague and H. L. Rozendaal. NSEG - A Segmented Mission Analysis Program for Low and High Speed Aircraft. Volume I - Theoretical Development. Technical report, NASA, 1977. 55

[89] Thomas D. Economon, Francisco Palacios, Sean R. Copeland, Trent W. Lukaczyk, and Juan J. Alonso. Su2: An open-source suite for multiphysics simulation and design. *AIAA Journal*, 54(3):828–846, 2016. 55, 77

[90] B. Barriety, O. Chandre-Vila J-P. Boin, and T. Mauermann. Fast fluid-structure computational method taking into account non-linear aerodynamic. In *AEROELASTICITY AND STRUCTURAL DYNAMICS. INTERNATIONAL FORUM. 2019. (IFASD 2019)*, 2019. 59

[91] D. Broomhead and D. Lowe. Multivariable functional interpolation and adaptive networks. *Complex Syst.*, 2, 1988. 60

[92] K.-J. Bathe and E. L. Wilson. *Numerical methods in finite element analysis.* Prentice-Hall, Englewood Cliffs, N.J, 1976. 61

[93] Kyung K. Choi and Nam H. Kim. *Structural Sensitivity Analysis and Optimization 1: Linear Systems.* Springer Science+Business Media, Inc., 1 edition, 2005. 61

[94] J E Marsden, L Sirovich, S S Antman, G Iooss, P Holmes, D Barkley, M Dellnitz, and P Newton. *Theoretical Numerical Analysis: A Functional Analysis Framework.* Springer-Verlag New York, 3 edition, 2009. 61

[95] Joel Chaskalovic. *Finite Element Methods for Engineering Sciences.* Springer Berlin Heidelberg, 2010. 61

[96] Carlos A. Felippa, K.-C. Park, and Charbel Farhat. Partitioned analysis of coupled systems. *Computer Methods in Applied Mechanics and Engineering*, 190(03):3249–3270, 2001. 63

[97] Hans Joach Bungartz. *Fluid-Structure Interaction: Modelling, Simulation, Optimisation* . Springer-Verlag GmbH, 2006. 63

[98] Ulrich Küttler and Wolfgang A. Wall. Fixed-point fluid–structure interaction solvers with dynamic relaxation. *Computational Mechanics*, 43(1):61–72, feb 2008. 63

[99] Joe Hoffman. *Numerical methods for engineers and scientists.* Marcel Dekker, New York, 2001. 64

[100] J. Douglas Faires Annette M. Burden. *Numerical Analysis.* BROOKS COLE PUB CO, 2015. 64

[101] Manfred Bischoff. *Theorie und Numerik einer dreidimensionalen Schalenformulierung.* PhD thesis, 1999. 73

[102] European Union Aviation Safety Agency. Certification specifications and acceptable means of compliance for large aeroplanes, cs-25, amendment 22, 2018. 78, 81

[103] GasTurb GmbH. Gasturb. 81

[104] Pauli Virtanen, Ralf Gommers, Travis E. Oliphant, Matt Haberland, Tyler Reddy, David Cournapeau, Evgeni Burovski, Pearu Peterson, Warren Weckesser, Jonathan Bright, Stéfan J. van der Walt, Matthew Brett, Joshua Wilson, K. Jarrod Millman, Nikolay Mayorov, Andrew R. J. Nelson, Eric Jones, Robert Kern, Eric Larson, CJ Carey, İlhan Polat, Yu Feng, Eric W. Moore, Jake Vand erPlas, Denis Laxalde, Josef Perktold, Robert Cimrman, Ian Henriksen, E. A. Quintero, Charles R Harris, Anne M. Archibald, Antônio H. Ribeiro, Fabian Pedregosa, Paul van Mulbregt, and SciPy 1. 0 Contributors. SciPy 1.0: Fundamental Algorithms for Scientific Computing in Python. *Nature Methods*, 17:261–272, 2020. 81

[105] Joint Aviation Authorities. *JAR-OPS 1 deutsch - Gewerbsmäßige Beförderung von Personen und Sachen in Flugzeugen*, 2006. 88

[106] European Commission. *Commission Regulation (EU) No 965/2012.* Official Journal of the European Union, 2012.

[107] W. Mason. Friction v3. 109